National Transportation Safety Board
Office of Railroad, Pipeline and Hazardous Materials Investigations
Washington, DC 20594

Edwardsville, Illinois
March 11, 2022

PLD22FR002

PIPELINE OPERATIONS/INTEGRITY MANAGEMENT

Group Chair's Factual Report

Report Date: October 19, 2023

A. ACCIDENT

Location:	Edwardsville, Illinois
Date:	March 11, 2022
Time:	8:15 a.m. CST
Operator:	Marathon Pipe Line, LLC
System Type:	Hazardous Liquid
Commodity:	Wyoming Asphaltic Sour Crude Oil

B. PIPELINE OPERATIONS/INTEGRITY MANAGEMENT

Group Chair	Ashley Horton/Kim West[1] National Transportation Safety Board Oklahoma City, Oklahoma
Group Member	Wesley Mathews Pipeline and Hazardous Materials Safety Administration Oklahoma City, Oklahoma
Group Member	Joshua Stufft Marathon Pipe Line, LLC Findlay, Ohio

[1] Each serving for a portion of the investigation.

TABLE OF CONTENTS

C. SUMMARY

For a summary of the accident, refer to the *Accident Summary* report within the docket.

D. FACTUAL INFORMATION

1.0 Operational Overview

Pipeline operations and integrity management depend on the pipeline operator, existing infrastructure, and the environment in which the pipeline operates, as described below. Some aspects are required by regulation (See Section 6.0).

1.1 Description of the Operator

Marathon Pipe Line, LLC (Marathon) is headquartered in Findlay, Ohio, and is an indirect subsidiary of MPLX LP (MPLX), a limited partnership formed and indirectly majority owned by Marathon Petroleum Corporation (MPC). Figure 1 displays a map of all the pipeline assets Marathon operates, including the Woodpat pipeline system involved in this accident.

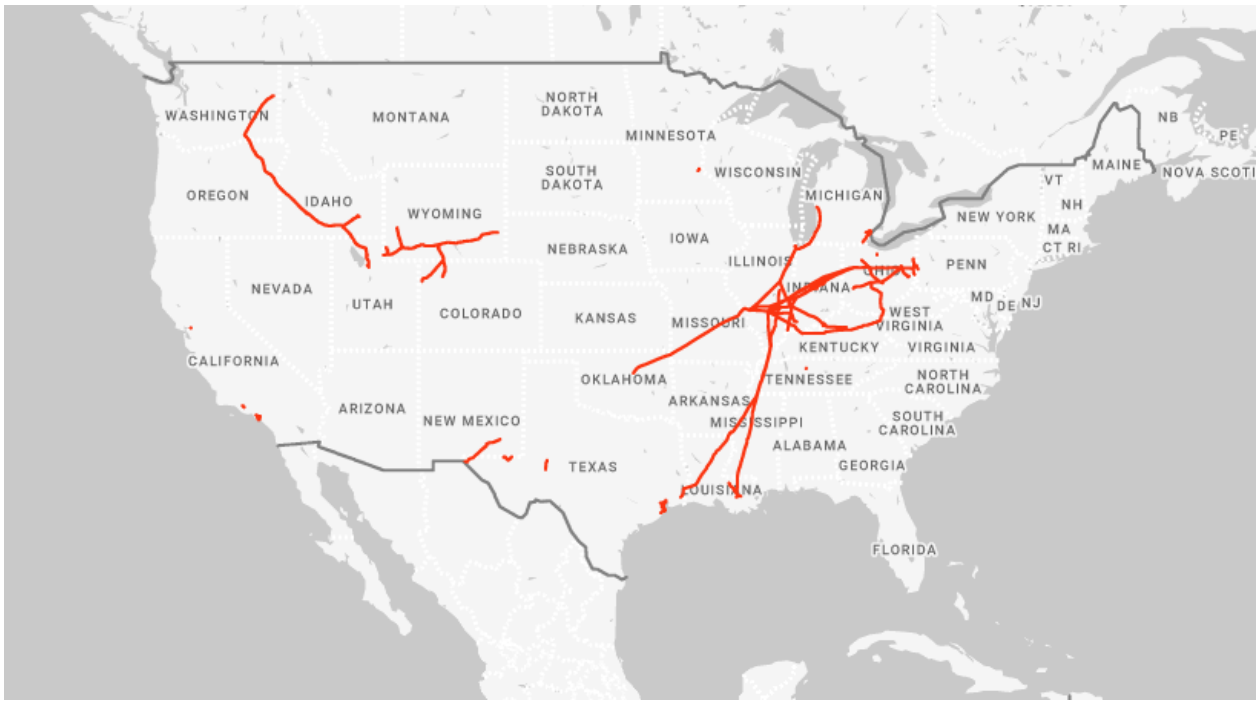

Figure 1. Map of the United States showing Marathon's natural gas transmission and hazardous liquid pipeline assets. (Source: Marathon).

MPLX's assets consist of a network of crude oil and refined products pipelines with supporting assets, including storage facilities (tank farms) located in the Midwest and Gulf Coast regions of the United States. There are 62 light-product terminals with

approximately 24 million barrels (bbl.) of storage capacity, an inland marine business, storage caverns with approximately 2.8 million bbl. of storage capacity, and a barge dock facility with approximately 78,000 barrels per day (bpd) of crude oil and refined product throughput capacity. MPLX also has gathering and processing assets that include approximately 5.9 billion cubic feet per day of gathering capacity, 8.7 billion cubic feet per day of natural gas processing capacity and 610,000 bpd of fractionation capacity. In addition, MPLX provides fuel distribution services to MPC and owns refining logistics assets consisting of tanks with storage capacity of approximately 56 million bbl., as well as refinery docks, loading racks, and associated piping. Marathon operates approximately 7,900 miles of hazardous liquid pipelines.[2]

1.2 Description of the Pipeline System

Texaco built the Woodpat pipeline in 1949, and Marathon purchased the pipeline in 1968. The Woodpat pipeline system is 57-miles long, consisting primarily of 22-inch nominal diameter pipe (Figure 2). It can transport approximately 360,000 bpd of crude oil. Woodpat has two pump stations and a receipt station, located in Wood River, Illinois, Roxana, Illinois, and Patoka, Illinois, respectively. The pump stations are known as Wood River Station and Roxana Station. This accident occurred on the Woodpat pipeline, about 6.2 miles downstream of the Roxana Station.

There is an approximate two-mile long segment that runs from the Wood River Station to Roxana Station, which consists primarily of 24-inch diameter pipe, with a small portion of 20-inch diameter pipe. The remaining 55 miles of the Woodpat system, from Roxana Station to Patoka Station, consists of a 22-inch diameter pipe.[3]

The Woodpat pipeline is a common carrier pipeline that runs in batches 24 hours a day, seven days a week, 365 days a year. The system starts where the Ozark 22-inch diameter pipeline system delivers into the Roxana Station. Crude oil flows north to south on the Wood River Station to Roxana Station pipeline segment, and west to east on the Roxana Station to Patoka Station segment. See Figure 2.

[2]PHMSA Data Mart for Operator ID 32147 Marathon Pipe Line LLC for Report Year 2022.
[3] Alignment Sheet Roxana - Patoka Woodpat 22" Liquid Mainline.

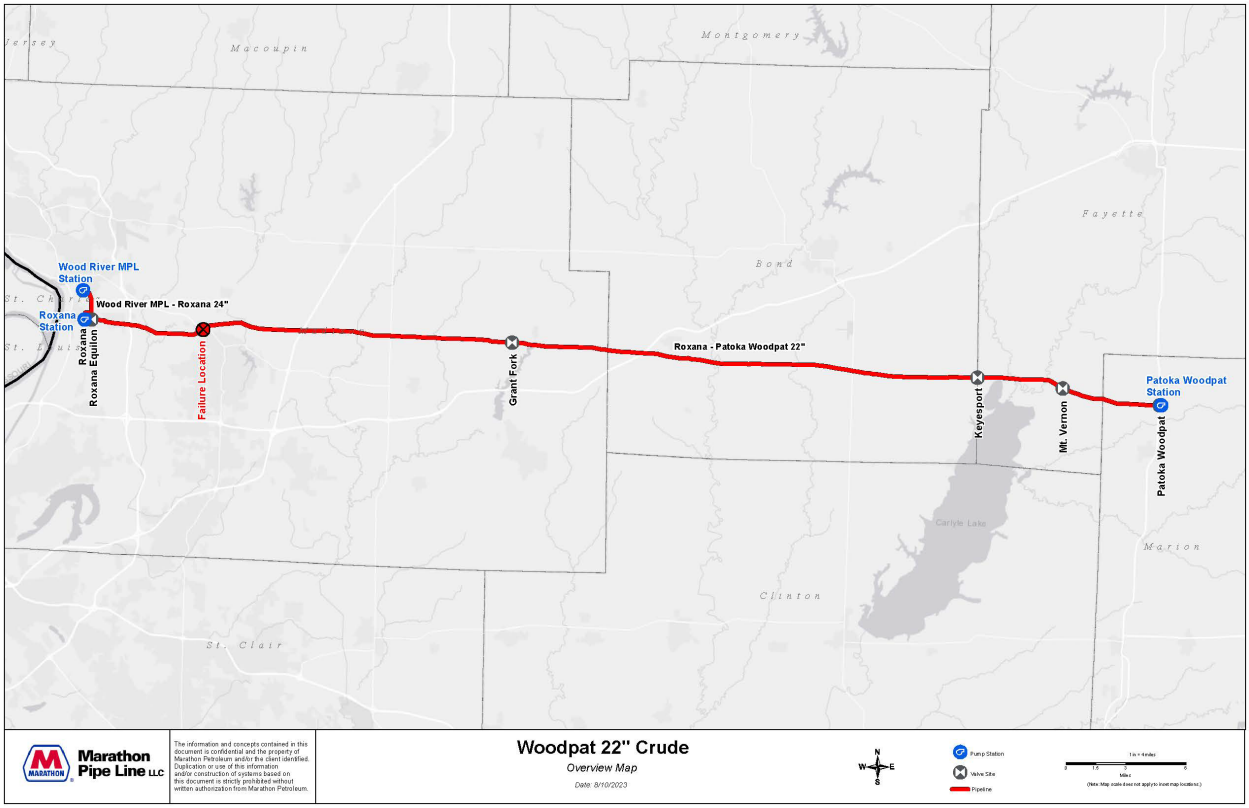

Figure 2. Map of the Woodpat pipeline system showing the pump station and mainline block valves. (Source: Marathon.)

There are five mainline block valves (BV) on the Woodpat pipeline system:

- Roxana Equilon BV
- Grant Fork BV
- Keyesport BV
- Mt. Vernon BV
- Patoka Woodpat BV

At the time of the accident, the Woodpat pipeline was operating at a pressure of 479 pounds per square inch gauge (psig).[4] There were no excursions over the maximum operating pressure (MOP) of 881 psig between Roxana Station and Patoka Station.[5] At the time of release, Woodpat was delivering Wyoming Asphaltic Sour (WAS) crude oil from the Platt Pipe Line system. WAS is considered a medium grade

[4] Time and Pressure Data for Roxana Station Discharge Pressure by Hour.
[5] MOP Excursions Prior 5 Years.

crude oil with an API gravity of 21.6 °[6] The specifications for the pipeline are shown in Table 1.

Table 1. Pipeline specifications.[7]

Diameter	22 inches
Material	Steel
Grade/Specified Minimum Yield Strength (SMYS)[8]	API-5L-X46
Long Seam Weld	Low Frequency - Electric Resistance Welded (LF-ERW)
Manufacturer	Youngstown Sheet & Tube
Year Installed	January 1, 1949
Wall Thickness	0.344 inch
Flow Direction	West to East
MOP	881 psig
Operating Pressure (at time of failure)	479 psig
External Coating Type	Coal Tar Enamel
Cathodic Protection Method	Impressed Current

Woodpat is operated out of Marathon's Pipeline Operations Center (POC), in Findlay, Ohio, where the POC Manager oversees a varying number of staff members. At the time of the accident, there were 63 individuals on staff. The Woodpat pipeline is monitored and controlled by a supervisory control and data acquisition (SCADA) system. The SCADA system allows the pipeline controller to monitor pipe pressures and crude oil flow rate from one point to another along the system. The system also

[6] Heavy crude oil has been defined as any liquid petroleum with an API gravity less than 20°. Extra heavy oil is defined with API gravity below 10.0° API (API gravity, is a measure of how heavy or light a petroleum liquid is compared to water).
[7] Accident Report - Hazardous Liquid Pipeline Systems Form 7000-1 No. 20220077-36598.
[8] API 5LX defines specific grades of carbon steel pipeline, each with a minimum yield strength. The higher the grade of the pipe, the higher the strength of the steel used to manufacture that pipe.

provides the pipeline operator the capability of manipulating the remotely controlled pipeline valves, monitoring leak detection of the pipeline, reviewing safety-related conditions, monitoring, acting on alarms, and receiving direct reports of any detected anomalies to the controls.

Each console is assigned to a single pipeline controller during the work shift, who had decision making authority for pipeline operations on selected pipeline systems. Each pipeline system is designated to a specific console. Each console is the physical area containing SCADA equipment, leak detection equipment, console phone, console cell phone, a personal computer, and other resources needed to operate a pre-determined, but not permanently fixed, selection of pipeline systems. The POC in Findlay is in a secure facility with limited access that is tracked. The POC has nine active operational consoles, two active specialist consoles, and an additional nine consoles with SCADA access to be used for project work, spare consoles, shelter in place workstations, social distancing provisions, and allowances for future expansion. Each console is staffed 24 hours a day, seven days a week, 365 days a year by controllers on 12-hour shifts (day and night). The POC is staffed with controllers, shift specialists, or backup specialists.

The On-Duty Pipeline Controller, who operated and monitored pipeline system movements on the Woodpat system, was working out of Console 8. The responsibility for monitoring pipeline systems is tied to the console so any controller that sits at a particular console must be qualified on that console. The On-Duty Pipeline Controller and the Prior Controller, who monitored Console 8 prior to the release, were both qualified on Console 8.[9]

1.3 Description of the Accident Site

The crude oil release occurred at milepost 6.2 on the Woodpat pipeline ROW, in a rural area near the town of Edwardsville (Madison County), Illinois. Marathon found crude oil flowing into the Cahokia Creek bank, emanating from the ridge overlooking the creek. The pipeline failed approximately 40 feet from the creek edge. The Cahokia Creek flows westward and joins the Mississippi River, approximately 9.8 miles downstream of the spill area. The site is bordered to the north by the intersection of IL Route 143 (Edwardsville Road) and Old Alton Edwardsville Road, with the Cahokia Creek and agricultural properties beyond. To the east and south, it is bordered by Old Alton Edwardsville Road, with a Norfolk Southern railroad track, and residential and commercial properties beyond. To the west, there is forested land, with residential properties further on.

Three parallel pipelines share the ROW in the area where the accident occurred on the Woodpat pipeline, the failed pipeline, was the northernmost of three parallel

[9] Interview with the On-Duty Controller (April 5, 2022), Prior Controller (April 6, 2022), and OQ Documentation and Training Records for On-Duty Controller.

pipelines that shared the ROW, and the closest to the creek. The failed pipeline is a 22-inch diameter crude oil interstate transmission pipeline, operated by Marathon. They also operate the center pipeline, Roxana to Patoka. The middle pipeline is a 12-inch diameter crude oil interstate transmission pipeline, which is also part of the Marathon Roxana to Patoka pipeline system. The Keystone is the southernmost pipeline is a 30-inch diameter crude oil interstate transmission pipeline which is operated by TC Oil Pipeline Operations, Inc. (Figure 3).

Figure 3. The Woodpat 22-inch pipeline, Roxana to Patoka 12-inch pipeline, and Keystone 30-inch pipeline, are shown north to south, in a shared ROW adjacent to the Cahokia Creek, the purple diamond shows the failure location. (Source: National Pipeline Mapping System.)

The area where the accident occurred is an "Unusually Sensitive Area" drinking water resource per 49 CFR 195.6, and an "Other Populated Area" per 49 CFR 195.450. This area is a High Consequence Area (HCA), according to federal regulations, subject to the pipeline integrity management requirements in 49 CFR 195.452. Cahokia Creek runs adjacent to the accident site and is part of the Indian-Cahokia Creek watershed.[10] At the point of failure, the approximate depth of cover was 48 inches.

[10] https://heartlandsconservancy.org/water/indian-cahokia-creek-watershed/.

2.0 Accident Sequence

2.1 Events Leading up to the Accident

Marathon took several actions to address slope stability issues near the accident site prior to the failure. For example, Submar mats[11] were installed at the accident location in 2014 as a preventative and mitigative measure (P&MM) to stabilize the bank and cover and protect the pipeline from erosion that occurred in 2012. In 2017, the existing matting was repaired, and additional mats and riprap were installed to address a 2016 ROW observation.[12]

Since 2012, Marathon had completed several integrity assessments of the affected pipeline with in-line inspections (ILI). On August 21, 2012, a GE combination caliper and circumferential magnetic flux leakage MFL-C ILI assessment was completed to detect for seam weld defects, metal loss defects, mechanical damage, and geometric anomalies. The survey found a total of 5,477 seam weld defects, 11,527 metal loss defects, 50 ferrous metal objects, one dent, and 32 shell repairs. Of the seam weld defects, five had characteristics associated with crack-like defects and 63 had some characteristics associated with crack-like defects. Of the metal loss defects, 2,074 were classified as seam weld metal loss and 9453 were classified as general metal loss.[13] This tool run resulted in the installation of four sleeves over girth welds in the area of the slippage.

Rosen performed an inertial measuring unit (IMU)/electromagnetic acoustic transducer (EMAT) assessment for Marathon on Marathon's 22-inch diameter Woodpat pipeline on January 5, 2018. Rosen indicated that the IMU data was of acceptable quality, performed bending strain analysis by analyzing curvature patterns, and identified areas of total bending strain greater than 0.125% for further review. Their report identified 18 areas with total bending strains exceeding 0.125%. The highest bending strain on this system (0.34%) occurred near the accident failure location (Table 2 and Table 3)[14]. However, the failed weld was about five feet upstream of the start of the strain event identified by Rosen. Rosen reported that the acceptance of bending strain values was dependent on numerous factors (e.g., cause, pipe diameter to wall thickness ratio, and material properties) and no single bending strain limit was applicable. Rosen further noted that any acceptable value should consider the age of the pipeline, the quality of the welds, the cause of the bending strain, and any interacting anomalies. Rosen indicated that mitigation may include finite element assessments, in-situ strain monitoring, stress relief, additional IMU runs accompanied by a pipe movement assessment, or pipeline replacement.

---

[11] *Submar mats* consist of flexible concrete that is connected by fiber rope, commonly used for erosion control.
[12] Soil Stabilization Documentation for 2014 & 2017.
[13] Excerpt 2012 GE CMFL Final Report Results.
[14] Rosen Bending Strain Report.

In 2019, Marathon evaluated the risk of the affected segment, finding that this segment had an above average likelihood of failure and a below average consequence of failure relative to other Marathon assets. Threats driving the above average likelihood of failure included: external corrosion, internal corrosion, manufacturing defects associated with the manufacturing process used for the long seam (LF-ERW), construction and fabrication defects (buried flanges), and weather/natural forces. This risk assessment also noted that the Submar matting at Highway 143 near Edwardsville is visually inspected after flooding events. The matting was installed in 2014 due to the waterway encroaching on Marathon's ROW. Marathon considered the mats to be stable.[15]

Marathon explained that the strain anomaly from the 2018 IMU dataset (Item 765 in Table 3) was determined to be a "Priority 1 Feature" and a project was created for site investigation.[16] Marathon contracted GeoMorphic Solutions, LLC (GeoMorphic) to perform a strain investigation of this feature. On June 15, 2021, GeoMorphic completed a field inspection, and on July 7, 2021, they completed a desktop review. GeoMorphic reported that "Historic and current aerial imagery indicates that the left bank of Cahokia Creek is prone to ongoing erosion and failures. Concrete matting has been installed on the left bank (first visible in imagery October 2014) but appears to cover only a portion of the top of bank. Ongoing bank erosion and failures are still notable after matting installation. The left bank was badly eroded with evidence of instability including recent failures, scarps, and cracking. This bank instability could be resulting in the observed pipeline bending. The data collected suggests that the pipeline is bending both horizontally and vertically in the direction of the bank failures here." GeoMorphic ranked the severity of the geohazard at 7 of 10 (10 being the most severe) due to the proximity of ongoing bank instability and recommended "increased monitoring of bank stability and repeat depth of cover surveys. Consider additional armoring of left bank to decrease ongoing bank instability." The report did not quantify the resulting pipeline strain demand, nor did it discuss the expected strain capacity.[17] A bending strain and pipe movement analysis was planned for 2022, but it was not completed prior to the accident.

In response to the Geomorphic report, in October 2021, Marathon also completed a girth weld strain capacity analysis of two girth welds on the Woodpat pipeline to compare to Item 765. The girth welds analyzed yielded strain capacities of 0.73% and 1.5% respectively. Item 765 was reported as having strain of 0.344%, that showed the strain capacity of both of the girth welds to be more than twice the strain measured.

[15] Mainline Risk Assessment Report for Martinsville Region 2019.
[16] Summary of Marathon's Response to Geomorphic Report.
[17] 2021 GeoMorphic Report.

On August 31, 2021, Rosen completed an IMU/caliper survey for Marathon. As of the date of the accident (more than 6 months later), the strain report had not been requested and no further evaluation of the strain had been completed.

On September 17, 2021, Marathon issued the Mainline Risk Assessment Report for the Martinsville Region. This report evaluated risk by area and segment groups. The affected pipeline was in the Wood River Area and in the segment group Roxana – Patoka Woodpat 22". This report noted P&MMs implemented in 2018 which included additional ILI tool runs (ultrasonic circumferential crack detection [UTCCD], EMAT, and MFL-C) to mitigate the threat of manufacturing defects. It was noted that this line has been observed for environmentally assisted cracking due to hydrogen embrittlement and Marathon was running crack tools. The failure location had an overall risk of failure score of 26.6. This is relative to Marathon's overall average 12.91 (range is 2.6-42.2). The failure location was in the 95th percentile, driven by manufacturing defects associated with the manufacturing process used for the long seam (LF-ERW), environmentally assisted cracking, and consequence of failure (higher end of moderate).[18]

NDT Global performed a UTCCD survey for Marathon on Marathon's Woodpat pipeline on September 20-21, 2021, utilizing a 22-inch Evo 1.0 inspection tool. NDT Global classified the run as technically successful and analyzed the data for linear, circumferential anomalies that were at least 0.039 inches deep and 0.98 inches in length. NDT Global's analysis report, version 1 was completed on December 17, 2021. NDT Global detected crack-like anomalies (189), manufacturing indications at girth welds (5,246), notch-like anomalies (9), laminations (218), and geometric anomalies such as dents (4). Two manufacturing indications were found on the failed girth weld.

The complete list of integrity assessments Marathon has completed since acquiring this pipeline, along with the year and vendor, can be found in Table 4.

Table 2. 2018 IMU Strain Report Summary results in vicinity of the failure location.

Bending Strain Anomaly No.	Start Distance (ft.)	End Distance (ft.)	Height (ft.)	Max Bending Strain (%)	Length of Strain Area (ft.)	Comment
BSTR #003	32604	32800	440.697	0.34	196.00	bending strain, combined with sleeve and sleeved bend

[18] Mainline Risk Assessment Report for Martinsville Region 2021.

Table 3. 2018 IMU Strain Report results in vicinity of the failure location.

ItemNo	PipeFeature	CalcStation[19]	DefectJointNo	JointMapId	TotalStrain
760	WELD	256468.58	7470	29782	
761	Strain - Start		7470	29782	0.0034
762	WELD	256428.52	7480	29783	
763	WELD	256388.4	7490	29784	
764	WELD	256348.43	7500	29785	
765	Strain - Bending		7500	29785	0.0034
766	WELD	256308.49	7510	29786	
767	WELD	256268.24	7520	29787	
768	Strain - End		7520	29787	0.0034
769	WELD	256228.28	7530	29788	

Table 4. Complete list of integrity assessments Marathon has completed since aquiring the pipeline.

Year	Technology	Vendor
1991	Hydrotest	N/A
2002	CAL	Enduro
2003	UTWM	Pii
2004	Hydrotest	N/A
2007	MFL/CAL	CPIG
2009	Hydrotest	N/A
2012	UTWM/CMFL/CAL	GE
2013	Hydrotest	N/A
2013	UTCD	GE
2017	IMU/UTWM/CMFL/CAL • KMAP analysis	GE
2018	UTCD (pre and post hydrotest)	GE
2018	IMU/EMAT	Rosen
2018	Hydrotest	N/A
2019	UTCD (Eclipse)	NDT
2019	Bending Strain Analysis	Rosen
2020	UTCD (Eclipse)	NDT
2021	IMU/MFL/CMFL/CAL/RoMAT PGS	Rosen
2021	UTCCD	NDT

[19] Station numbers begin at Patoka.

2.2 System Isolation

The initial indication of a release occurred at 8:15 a.m., when a rate-of-change alarm showed low suction (inlet) pressure on mainline pump Unit 3, the only mainline pump running at the time of the crude oil delivery shut down without action from the controller. Low suction pressure alarms, that were audible and visible, populated the console desk screen to the On-Duty Controller. During the crude oil delivery into Patoka Station, the pipeline was in a steady state (meaning no changes were occurring at Wood River). The On-Duty Controller told NTSB investigators that he initially thought the pressure changes within the pump had to do with an issue with the booster pump. He observed that the booster had stopped putting out pressure for a split second then returned. He thought that was just enough to cause the pump to shut down. If the booster pump does not supply enough pressure to the mainline pumps, an alarm will automatically be sent to the SCADA indicating a loss of suction pressure on the mainline pump. He also thought the problem with the booster pump was just a quick issue that might explain the loss of suction on the mainline pump. At this point he realized it was not the booster, but "something didn't look right."[20]

The On-Duty Controller stated to the NTSB that he shut down Woodpat and then called the maintenance crews who were conducting welding work for Marathon about mid-way through the pipeline segment, to notify them the line was shut down. Once Woodpat was secured, the On-Duty Controller informed the Operations Specialist that pump Unit 3 had shut down uncommanded. The Operations Specialist assisted initiating the investigation, by reviewing the pressures, and the leak detection system. The On-Duty Controller called the Wood River Station field operator to see if there was any field work or activity that may have caused an issue with the pump unit, but learned there was no work occurring on the pipeline. After further discussions with the Operations Specialist, he telephoned the area operators at Wood River Station to have them inspect the manifold (above ground piping at the station). They later reported no issues at Wood River and Roxana Stations. The On-Duty Controller then reported back to the shift specialist's desk to assist further. This was around the time when the Operations Specialist began the stop-help-start process. At this point, the On-Duty Controller returned to Console 8 to continue operating the other pipelines.[21]

The Operations Specialist and his Operations Center Supervisor continued with the investigation by examining the SCADA pressure trends at the Roxana and Patoka Stations and reviewing pump unit specific pressures and the booster pressures at Wood River for anomalies that could explain what they had observed.

At this time, field operations personnel were actively traversing the ROW to find a potential leak. Once the source was found at approximately 9:50 a.m., field personnel proceeded to reduce the length of the isolated pipeline segment by

[20] Interview with the On-Duty Controller (April 5, 2022).
[21] Interviews with On-Duty Controller and Operations Specialist (April 5, 2022).

manually closing two additional valves: Equilon BV (9:51 a.m.) and Grant Fork BV (10:07 a.m.) about 17 minutes after the discovery of the release and approximately two hours after the rupture. This reduced the size of the isolated pipeline segment from 55 miles to 27 miles.

The following timeline (Table 5) indicates the actions taken by Marathon employees and contractors to address the loss of a main pipeline unit and to put the pipeline in safe mode. Isolation was complete at approximately 8:23:18 a.m.

Table 5. Marathon timeline of events after the release.[22]

8:15:21	**Roxana – Discharge Pressure Value – Rate of Change - Low**
8:15:21	Roxana Unit 3 – Change to State Off - Low Suction Shut Down
8:15:58	Roxana Unit 2 – Issue Command to Start
8:17:18	Roxana Unit 2 – Change of State On
8:19:25	Roxana Unit 2 – Issue Command Stop
8:19:27	Roxana Unit 2 – Change state to Off
8:19:57	Wood River Unit 9 – Issue Command Stop
8:19:59	Wood River Unit 9 – Change State to Off
8:20:07	Wood River Booster 8 – Issue Command Stop
8:20:11	Wood River Booster 8 – Change State to Off
8:20:35	Roxana Valve IN1 – Issue Command Closed
8:21:26	Patoka Valve HG1 – Issue command Closed
8:22:00	Roxana Valve IN1 - Closed
8:22:15	Meter Counts Stop
8:23:18	Patoka Valve HG1 – Closed
9:35	Field personnel were dispatched to close Equilon BV and Grant Fork BV valves

[22] Marathon Timeline of Events After Release.

9:51	Equilon BV – Closed
10:07	Grand Fork BV - Closed

2.3 Notifications

On March 11, 2022, at 10:15 a.m., Marathon made the initial National Response Center (NRC) notification (Report No.330806) of a 3,000-bbl. release of materials from an underground pipeline due to equipment failure.

On March 13, 2022, Marathon made a 48-hour follow up to the NRC (Report No. 1330949) increasing the reported release volume to 3,900 bbl. of crude oil.

On April 22, 2022, Marathon submitted Accident Report - Hazardous Liquid Pipeline Systems Form 7000-1 No. 20220077-36598, with an updated release volume of 3,500 bbl.

2.4 Post-Accident Drug and Alcohol Test

On March 11th, shortly after the crude oil release was confirmed, the On-Duty Controller left the console and was escorted for the required post-accident drug testing at approximately 11:30 a.m., and then driven home. [23] Once the test results were confirmed negative, the On-Duty Controller returned to work a few days later. The field personnel responsible for surveying the ROW to identify the crude oil release, were not required to submit a drug and alcohol test because Marathon believed their actions were not a contributing factor to the accident.

3.0 On-Scene Examination

Several emergency response activities occurred following the accident on March 11, 2022, including establishment of an on-site incident command system structure, the placement of additional boom strings, resource mobilization, and infrastructure development.[24] An engineering service performed a GPS survey of the pipeline for about 500 feet on March 12, 2022, while most of the pipeline was still covered. The pipeline was surveyed again on the morning of March 13, 2022, after about 300-feet had been exposed. Figure 4 shows a comparison of the results from the GPS in-situ survey, 2021 IMU data, 2018 IMU data, and the accident location. Also on March 12th, the day shift field crews installed a Modu-tap near the upstream girth

[23] Federal regulations require that Marathon perform a post-accident drug test, no later than 32 hours after an accident of a covered employee whose performance of a covered function either contributed to the accident or cannot be completely discounted as a contributing factor to the accident. (See: 49 CFR 199.105 and 199.223)

[24] See the *NTSB Environmental Response Group Factual Report* contained in the docket for this investigation for further details about the oil spill response.

weld to support drain-up of the pipeline and isolation. The evening shift cold cut the pipeline and removed the failed section. The following day, field crews excavated the soil around the pipe to relieve pipe stress and the pipe was prepared for the required hot work to isolate the pipe section and install the new piping. Figures 5 and 6 show the point of failure that caused the release.

Figure 4. GPS survey locations compared to 2018 and 2021 IMU data with a red dot indicating the accident location.

Figure 5. Woodpat pipeline point of failure. (March 12, 2022, 7:26 p.m.)

Figure 6. Close up of the Woodpat pipeline separated at the girth weld. (March 12, 2022, 7:00 p.m.)

The following evidence was retained by the NTSB:

- 4-foot 4-inch section of pipe on the upstream side of the failed girth weld, including the upstream fracture face (joint ID MAPL 29781/29782)

- 4-foot 4-inch section of pipe on the downstream side of the failed girth weld, including the downstream fracture face (joint ID MAPL 29782)
- 53.5-inch section of pipe encompassing the next upstream girth weld, as an exemplar sample (joint ID MAPL 29780/29781)

Each section was placed in a separate crate. On March 15, 2022, the crates were shipped to the NTSB Materials Laboratory in Washington, D.C., for metallurgical testing and analysis (See Figure 7). See the *NTSB Materials Laboratory Factual Report* contained in the docket for this investigation for further details.[25]

Figure 7. Woodpat pipeline section preparing for shipment to the NTSB Materials Laboratory. (March 14, 2022, 9:19 p.m.)

[25] The external pipe surfaces of the fractured girth welds were visually examined and had six arc strikes, eight undercuts, one low cap, and one repair. The coating was consistent with coal tar asbestos-based coating applied during installation. The chemical and mechanical compositions were consistent with requirements for API-5L-X46 pipe. The fracture features were reported to be consistent with overstress fracturing.

4.0 Procedures

Marathon's applicable Emergency Response Plan in Edwardsville, Illinois, was the Martinsville Response Zone Plan, which had last been revised on March 2, 2021. The plan provided guidance on how to respond to a spill in the Martinsville Response Zone, in a quick, safe, and effective manner. The plan had specific procedures for Marathon personnel on how to mitigate and/or prevent discharge resulting from in-facility operations. The plan was written to comply with 49 CFR 194 and 49 CFR 195.402.[26]

Marathon's Control Room Management (CRM) Plan, that was in effect at the time of the accident, Marathon POC CRM Plan, had an effective date of February 1, 2022, and had last been updated on February 14, 2022. The plan outlined the departmental policies, standards, governing documents, procedures, and guidelines that are to be incorporated to comply with federal regulations under 49 CFR 195.446. The CRM plan also incorporated Marathon's Alarm Management Plan and Fatigue Risk Management System.

Marathon's Alarm Management Plan that was in place during the accident, Marathon-DOT-01382-PRS), had an effective date of March 2, 2022. The purpose of the plan was to aid the pipeline controllers in surveillance of the pipeline operations and to maintain compliance with 49 CFR 195.446. The plan addressed the following items related to alarms: roles and responsibilities, alarm criteria, alarm summary display characteristics and usage, handling methods, rationalization, system design, system performance, related training, system maintenance, management of change, maintenance of tools that support the system, and controller workload. The Fatigue Risk Management System in use at the time of the accident was effective as of February 1, 2021, and had last been reviewed by Marathon on February 9, 2022. The purpose of this document was to mitigate and manage controller fatigue, as well as comply with 49 CFR 195.446.

Marathon's Integrity Management Program (IMP) Plan that was in effect at the time of the accident, Marathon-DOT-01167-POL, Revision 6, was dated January 13, 2022.[27] The purpose of the IMP Plan was to help ensure compliance with 49 CFR 195.452, *Pipeline Integrity Management in High Consequence Areas*, and applicable state requirements. The IMP Plan included sections on HCA identification, data integration, risk identification and analysis, integrity assessment intervals and method selection, integrity assessments and remedial actions, P&MMs, process effectiveness and metrics, continual process improvement, and IMP role qualifications.

Marathon also utilized their stop-help-start process during the response to this accident. The process aimed to enhance decision making for pipeline events that fall

[26] Excerpt Martinsville Emergency Response Plan.
[27] Excerpt Marathon Integrity Management Program.

outside of normal operations but have not yet reached a level requiring emergency response. Marathon procedures indicated that once a system has been placed in safe mode, it cannot be restarted until all provisions of the stop-help-start process have been completed; this includes agreement to restart from all stakeholders including the On-Duty Controller.

Marathon provided the NTSB a narrative outlining their geohazard management program and included supporting documentation.[28] Marathon explained that their geohazard program is led by a Geohazard Integrity Engineer who uses company procedures to guide implementation (Marathon-MNT-01422-PRS and Marathon-MNT-01568-PRS). Marathon uses IMU data to calculate bending strain. Features with strains greater than or equal to 0.35% total strain or 0.15% horizontal strain screen in for further assessment, which is prioritized based on the likelihood that a geohazard is affecting the feature. The program defines a "Priority 1 Feature" as likely affected by geohazards and requires a desktop study and site assessment to confirm if the geohazard is active and affecting the pipeline. Systems that are determined to be susceptible to geohazards will be assessed via an ILI tool with GPS every five years at a minimum. Pipe movement between ILI tool runs are to be analyzed and strain changes greater than 0.04% are to be flagged for prioritization and investigation.

5.0 Industry Guidance and Consensus Standards

The Woodpat pipeline was constructed in 1949, with limited records available. It was built prior to the regulatory requirements for construction required by the U.S. Department of Transportation, Office of Pipeline Safety. The Hazardous Liquid Code (Part 195) was implemented in 1979.[29]

The following industry guidance is applicable to this accident:

- Pipeline and Hazardous Materials Safety Administration Advisory ADB 2019-02: *Pipeline Safety: Potential for Damage to Pipeline Facilities Caused by Earth Movement and Other Geological Hazards*
- API Recommended Practice 1160, *Managing System Integrity for Hazardous Liquid Pipelines*
- Canadian Standards Association, Z662, *Oil and gas pipeline systems,* includes non-mandatory Annex C, *Limit states design.* This Annex provides guidance for the design of oil and gas industry steel pipelines based on the limit states design method.[30] To apply this method, all permanent, operational,

[28]Summary of Marathon's Geohazard Program.
[29] Title 49 Code of Federal Regulations Part 195 Transportation of Hazardous Liquids by Pipeline.
[30] *Limit states design* means a reliability-based design method that uses factored loads (nominal of specified loads multiplied by a load factor) and factored resistances (calculated strength, based on nominal dimensions and specified material properties multiplied by a resistance factor).

environmental, and accidental loads that significantly affect the strength, fatigue life, stability, or serviceability of the pipeline system must be considered.

- The "Guidelines for Management of Landslide Hazards for Pipelines," Version 1, was published by Interstate Natural Gas Association of America on August 17, 2020. The report noted that most bending strain features reported by ILI vendors are not associated with geohazards, but the following are indications that a strain feature is associated with geohazards:
    - Pipeline deflection has a sinusoidal shape (or "W-shape"), with on dominant side.
    - Intersection of proximity of bending strain feature to known landslide hazards.
    - High overall strain magnitude. The report noted that a 50% correlation for reported bending strain magnitudes over 0.35%; over 90% correlation when it exceeds 0.42%.
    - High horizontal strain magnitude. The report indicated a 50% correlation for reported horizontal component of bending strain exceeds 0.14%; 100% correlation when it exceeds 0.36%.

6.0 Regulatory Requirements

Federal pipeline safety regulations are found in 49 CFR Parts 190-199. Pipeline and Hazardous Materials Safety Administration (PHMSA) regulations in 49 CFR Part 195, Transportation of Hazardous Liquids by Pipeline: Minimum Federal Safety Standards, include several requirements that are applicable to the affected pipeline, such as:

- Subpart B - Annual, Accident, and Safety-Related Condition Reporting
    - 195.50, Reporting accidents.
    - 195.54, Accident reports.
    - 195.52, Immediate notice of certain accidents.
- Subpart E – Pressure Testing
    - 195.302, General requirements.
    - 195.310, Records.
- Subpart F – Operation and Maintenance
    - 195.401, General requirements.
    - 195.402, Procedural manual for operations, maintenance, and emergencies.
    - 195.422, Pipeline repairs.
    - 195.444, Leak detection.
    - 195.446, Control room management.
    - 195.450, High Consequence Area.
    - 195.452, Pipeline integrity management in high consequence areas.

Other applicable pipeline regulations to the accident are below:

- 49 CFR Part 191, Transportation of Natural and Other Gas by Pipeline; Annual, Incident, and Other Reporting
- 49 CFR Part 199, Drug and Alcohol Testing
- 49 CFR Part 194, Response Plans for Onshore Oil Pipelines

7.0 Historical Records

7.1 Leak and Failure History

In the ten years prior to this accident, Marathon has had seven accidents on the Woodpat system. Five failures were related to threaded and non-threaded connections, one incorrect installation, and one internal corrosion. As a result, a cumulative total of 687.3 bbl. of crude oil spilled. The largest spill volume was 646 bbl. and occurred on June 29, 2014, in Vernon, Illinois. Below are the accident summaries and the failure causes determined by Marathon on the accident reports required by 49 CFR 195.54:

- On December 2, 2016, in Hartford, Illinois, Marathon found approximately 4 ounces of crude oil leaked from between the yoke tube and valve bonnet due to a valve packing failure.
- On July 28, 2016, a 0.2 bbl. spill occurred at Vernon, Illinois. The failure cause of was due to a threaded connection failure.
- On May 15, 2015, a 0.8-barrel spill occurred at Vernon, Illinois. The cause of failure was determined to be a broken pipe nipple threaded into the valve flange, which is the discharge line of the differential thermal relief system.
- On April 27, 2015, a 4 bbl. crude oil spill at Vernon, Illinois. A leak was discovered on the flange connection at the gasket.
- On June 29, 2014, a 646 bbl. crude oil spill occurred at Vernon, Illinois, due to internal corrosion.
- On August 22, 2012, a 25 bbl. crude oil spill occurred at Wood River, Illinois, due to an incorrect installation. The cause of the failure was determined to be a lack of fusion of the weld due to ineffective inspection procedures.
- On March 26, 2012, a 1.6 bbl. crude oil spill occurred at Patoka, Illinois, due to non-threaded connection failure. There was a valve packing O-ring issue related to old age of the valve.

7.2 Operator Qualifications

The On-Duty Controller was a fully qualified on consoles 1, 5, and 8. His training consisted of a six-week period in a classroom setting. He completed his qualifications on July 26, 2019.[31] Covering qualifications included:

- Monitor line pressure,

[31] OQ Documentation and Training Records for On-Duty Controller.

- Operate valves remotely (field),
- Use real-time computational pipeline monitoring,
- Monitor metering,
- Monitor hazardous atmosphere detectors,
- Monitor sumps,
- Select meter factor,
- Set analog values,
- Monitor relief systems,
- Monitor tanks,
- Perform remote pipeline start-up,
- Verify communications,
- Prove meters remotely,
- Remotely operate control valve,
- Perform remote pipeline shutdown.

The welder that manually closed Grant Fork BV had had been working for Marathon for about two years. On February 10, 2020, he was trained and qualified to operate valves, and to manually or remotely open or close valves or other equipment (field). At the time of the accident, his qualifications were set to expire on May 10, 2023.

The operations technician that manually closed the Equilon BV had been working for Marathon for 14 years. On May 7, 2019, he was qualified to operate valves remotely on a liquid pipeline system and operate valves remotely (from the control room). At the time of the accident, his qualifications were set to expire on August 7, 2022.[32]

8.0 Post-Accident Actions

8.1 Pipeline and Hazardous Materials Safety Administration

In response to the Edwardsville failure, Marathon provided PHMSA a commitment letter on March 14, 2022, that included specific actions they would take in response to the failure. Marathon committed to performing API RP 579 Fitness for Service calculations for remaining strength of the unearthed girth welds, completing reinforcing repairs to vintage girth welds which were exposed during the failure response, performing a geotechnical analysis of the Cahokia Creek banks, complete site evaluations at the 17 locations on the pipeline where increased strain had been identified, summarize the events which may trigger mitigative actions, and complete a strain data analysis from the 2021 ILI and compare the data to the 2019 ILI analysis. PHMSA oversaw Marathon's implementation of their planned activities. Marathon also enhanced their geohazard susceptibility criteria and applied that plan to all Marathon pipelines. PHMSA approved Marathon's restart plan prior to Marathon bringing the

[32] OQ Documentation for Welder and Operations Technician.

pipeline back into service, the pipeline was restarted on March 15, 2022, 7:31 a.m. PHSMA developed and published within the Federal Register an Advisory Bulletin to remind the pipeline industry of the threat of earth movement and the expectation for operators to monitor and mitigate threats that affect pipeline integrity[33]. In December 2022, PHMSA held a public meeting that also highlighted the lessons learned from recent geohazard failures and emphasized the need for operators to evaluate and take mitigative actions to prevent future geohazard failures.

8.2 Marathon

Following the accident, Marathon initiated numerous repairs and remediation activities. Figure 8 is a simplified process flow diagram showing the area of the rupture, from several girth welds upstream of the failed girth weld to several girth welds downstream. As part of the activities to repair and restart the pipeline, Marathon exposed from joint identification (ID) 29779 to 10 feet downstream of Joint ID 29787. Aside from the girth welds removed from Joint IDs 29781 and 29782 for metallurgical testing, all girth welds were non-destructively examined using ultrasonic phased arrays.[34]

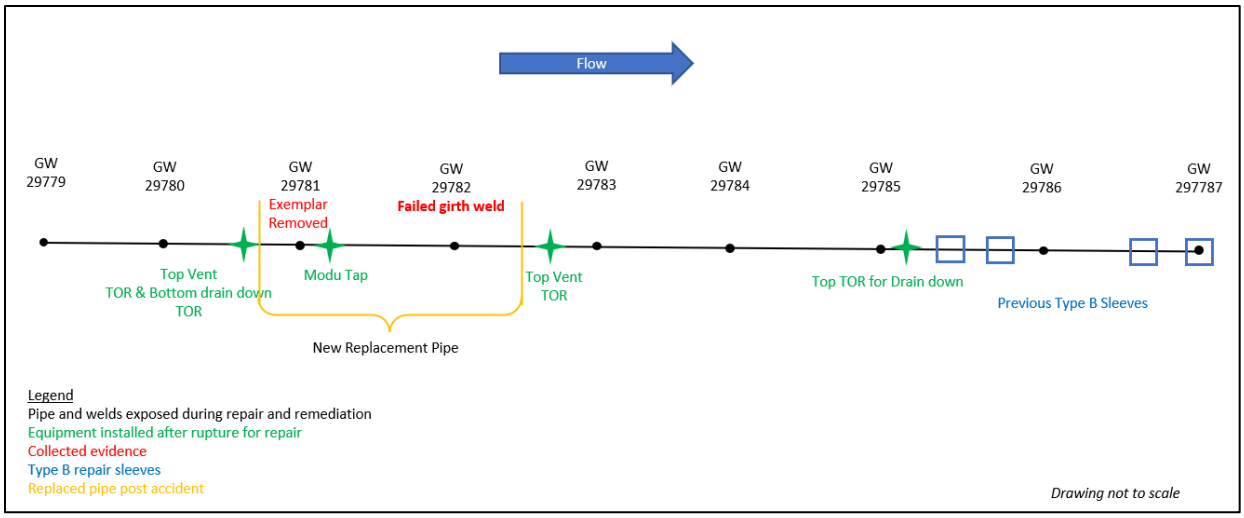

Figure 8. Simplified flow diagram showing the girth welds upstream and downstream of the failure. (Source: PHMSA.)

After removing joint ID MAPL 29781, and approximately 10 feet of joints MAPL 29782 and 29780, Marathon installed approximately 60 feet of new pipe. This new

[33] PHMSA-2022-0063, Pipeline Safety: Potential for Damage to Pipeline Facilities Caused by Earth Movement and Other Geological Hazards (June 2, 2022).
[34] Ultrasonic Phased Arrays (PAUT) are arrays of ultrasound transducers that fire individual elements on the array in a specific sequence to direct the sound wave in a specific direction. PAUT transducer uses multiple elements during a scan.

section was installed on March 15, 2022. The pipeline was restarted March 15, 2022, at 07:31 a.m.

ADV Integrity was contracted by Marathon to perform a failure examination on the failed girth weld (Attachment 1). A comparison of the 2012, 2018, and 2021 IMU analyses was completed (Figure 9), as well as a numerical analysis using calibrated models established by the 2018 and 2021 IMU data, and data collected after the accident to determine the total strain near the girth weld.

The data from the 2012 IMU examination had out-of-straightness profiles that ADV reported it considered inaccurate because the geospatial data was inconsistent with the 2018 and 2021 data outside the area of interest.[35] ADV determined the bending strain profiles from 2012 were consistent with the other two data sets, though. Figure 9 compares the IMU results.

The 2018 IMU data showed a maximum overall combined bending strain of 0.33% with 5.7 feet horizontal deviation from straight, 2021 IMU data exhibited an increased bending strain of 0.41% with 8 feet horizontal deviation from straight, and after the accident the horizontal deviation had increased to 8.2 feet. The bending strain near the girth weld increased from 0.02% in 2018 to 0.25% in 2021, and the as-found condition was estimated at 0.42%, a 68% increase from 2021 to the time of failure. Figure 10 represents the out-of-straightness profiles of the IMU results from 2012 ,2018, 2021, and the in-situ information collected after the accident.

[35] *Out-of-straightness profiles* represent curves or bends that were not present when the pipeline was manufactured.

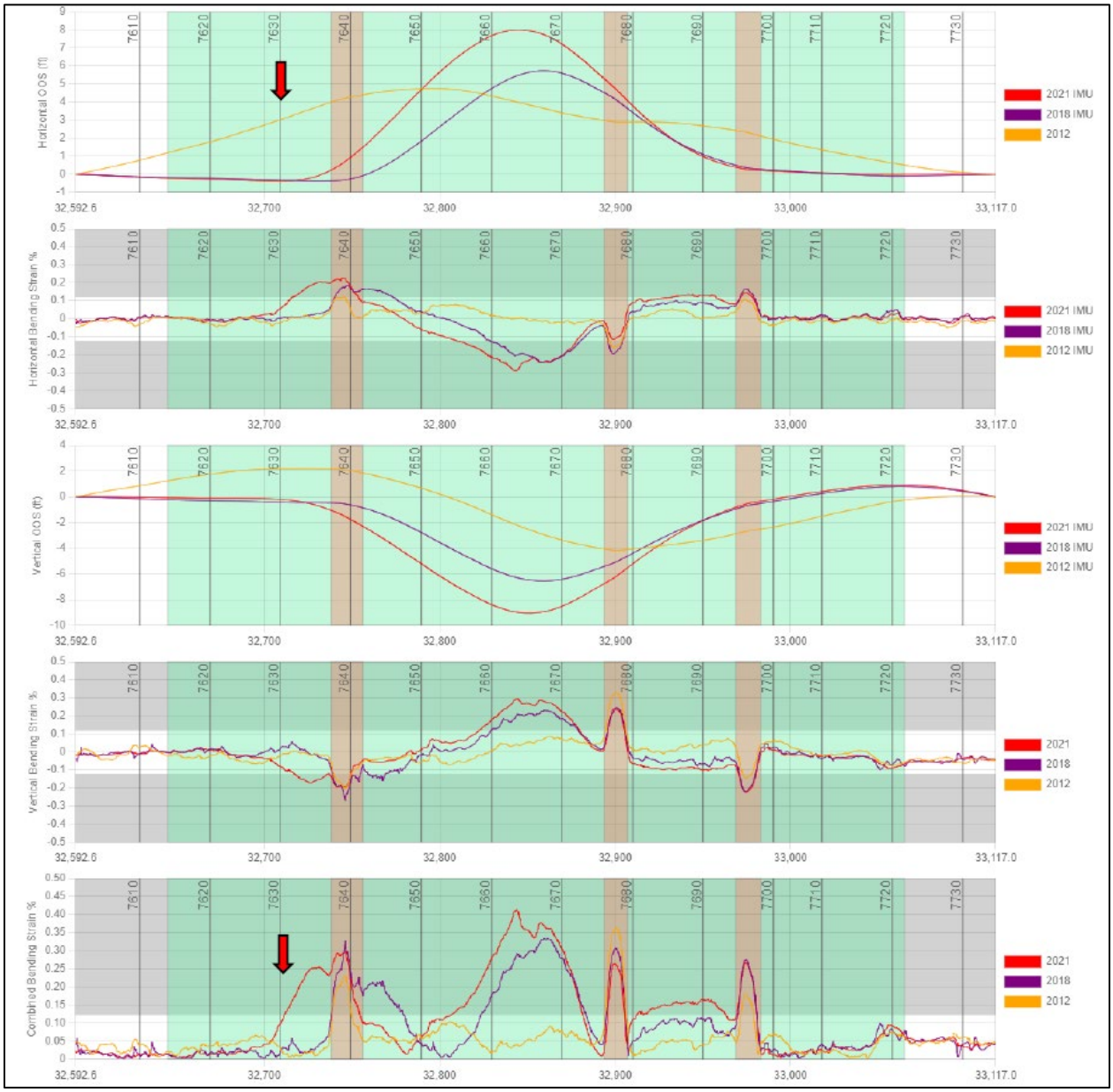

Figure 9. IMU data comparisons for 2012, 2018, and 2021. The red arrow indicates the failed girth weld #7630. (Source: ADV Integrity.)

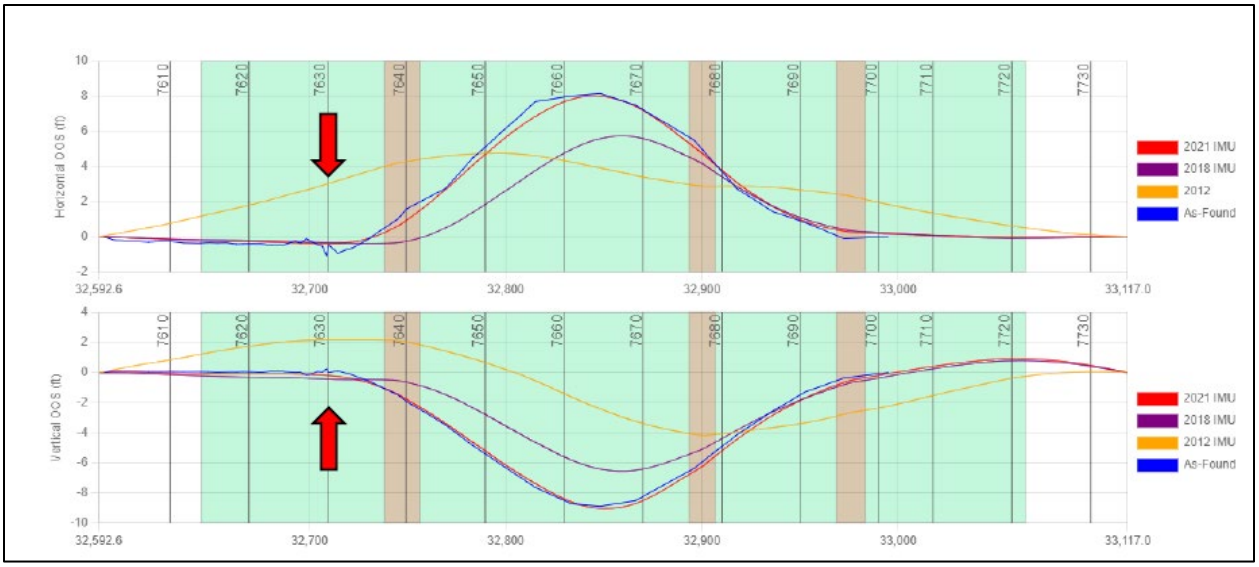

Figure 10. Comparison of out-of-straightness from data collected 2012, 2018, 2021, and post-accident. (Source: ADV Integrity.)

Boreholes were taken on either side of the pipeline to determine soil characteristics. The borehole north of the pipeline showed soft to medium stiff clays at pipeline depth, and south of the pipeline the soil was soft clay at pipeline depth. The numerical analysis addressed load cases based on different soil types and properties, the load case descriptions are:

- Load Case 1 – Upper Bound Undrained Clay,
- Load Case 2 – Lower Bound Undrained Clay,
- Load Case 3 – Lower Bound Drained Sand,
- Load Case 4 – Upper Bound Drained Sand.

The numerical analysis results indicated all load cases had a sharp increase in strain approximately 10 feet from the failure location. Table 6 summarizes the results of analysis for load cases 1-3, load case 4 data was considered inaccurate. In the table, total strain at girth weld 7630 represents the total strain (membrane and combined bending strain) from the node representing the girth weld's location. Bending strain is calculated based on curvature and membrane strains demonstrate how the pipe has stretched of compressed due to axial loading. The maximum total strain in the table is the maximum membrane strain in the area near the girth weld, which is typically within 10-feet of the girth weld plus the maximum bending strain. The results showed that the maximum total strains near the girth weld were between 0.61% and 0.83%. ADV indicated the sharp change in strain near the girth weld is indicative that the girth weld was experiencing higher strains than predicted at the girth weld (0.17-21%).

Table 6. Summary of numerical analyses for load cases 1-3. (Source: ADV Integrity.)

	LC1	LC2	LC3
Total Strain at Girth Weld 7630	0.18%	0.21%	0.17%
Max Bending Strain Near Girth Weld 7630	0.42%	0.30%	0.35%
Max Membrane Strain Near Girth Weld 7630	0.41%	0.31%	0.29%
Max Total Strain Near Girth Weld 7630	0.83%	0.61%	0.64%
Simulated Displacement After Failure (As-Found 7.3 inches)	4.8 inches	6.5 inches	6.6 inches

Also following the accident, Marathon reevaluated its Integrity Management Program and improved its processes. Specifically, Marathon 1) improved and standardized its method of identifying geohazard threats, 2) enhanced usage of in-line inspection to locate pipeline segments at risk from geohazards, 3) used lessons learned from the Edwardsville release to expand training and provide advanced tools to identify geohazards, and 4) reviewed and contributed to PHMSA and industry research projects related to geohazards.

To standardize its evaluation of geohazards, Marathon updated its Strain Feature Prioritization Flow Chart (Figure 10). The updated Flow Chart includes improvements such as using an integrated approach with light detection and ranging (LiDAR) for threat identification and revised total bending strain action limits. Marathon expanded its LiDAR usage for geohazard susceptibility to survey the entire Woodpat pipeline. It has completed an additional 4500 miles of LiDAR surveys across all our assets to enhance geohazard threat identification. The LiDAR data for the entire Woodpat pipeline system was analyzed, and no new locations of land movement were identified.

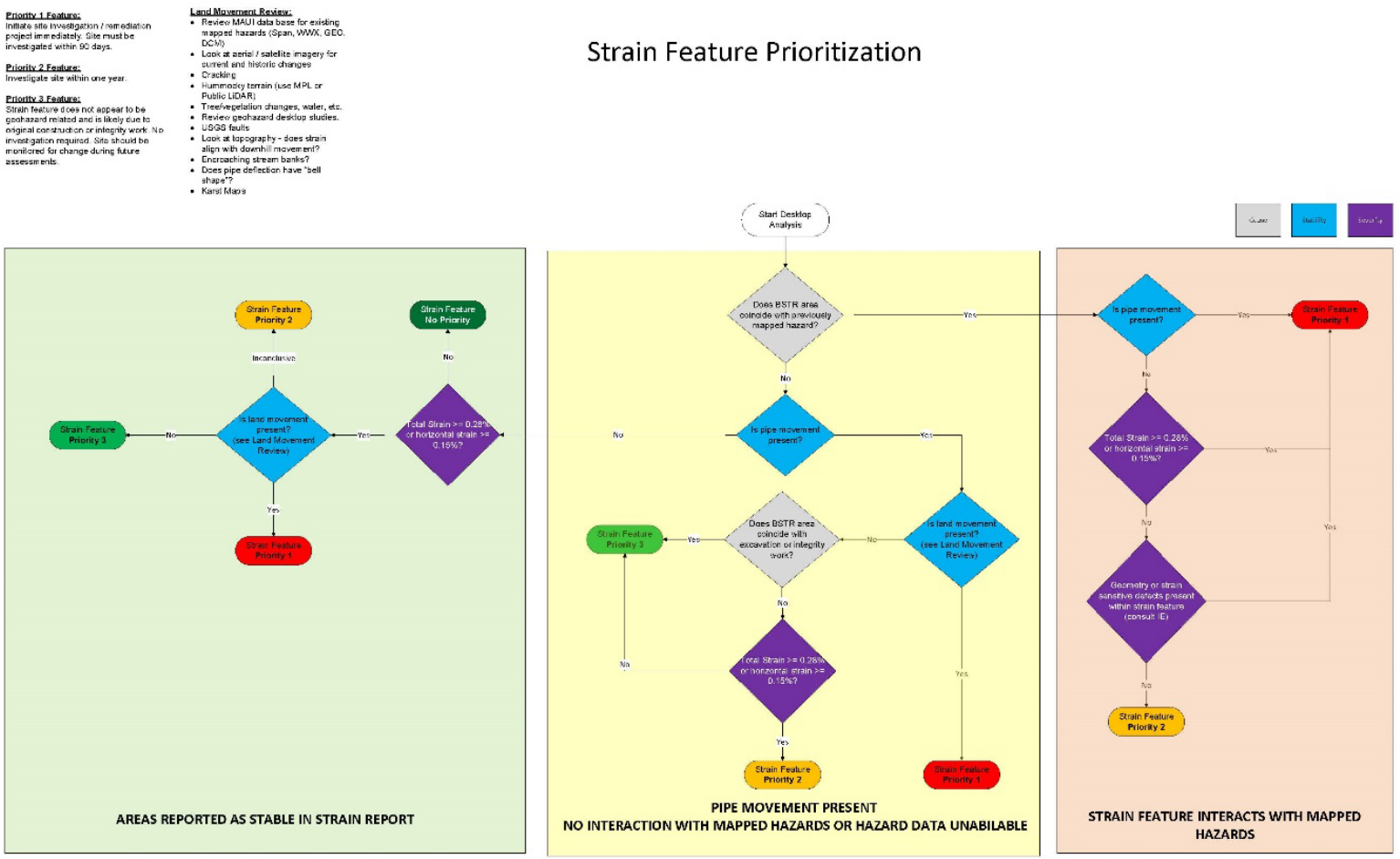

Figure 10. Marathons updated strain feature prioritization flow chart. (Source: Marathon.)

To provide an outside review of its geohazard program, Marathon hired third-party geotechnical and engineering consultants to review the program's identification of geohazard threat protocols, strain analysis protocols, and to identify gaps. The consultants found that the matting and riprap placed in 2014 and 2017, to control the erosion occurring along the Cahokia Creek streambank, had little to no impact on preventing or slowing the ground movement. The hydrotechnical analysis determined the cause of the ground movement was due to scouring in the river and large woody debris, which creates localized areas of scouring. Slope stability was also analyzed and Geosyntec reported that in combination with the scouring occurring, there was a reduction of shear strength in the soil. Based on the final report, Marathon's prioritization for immediate action was lowered to 0.28% total bending strain from 0.35%. The lower prioritization level will result in additional site investigations and remediation projects for locations that could be at risk of geohazard-related damage. Marathon also started collecting deviation from straight values during bending strain analysis to be included in the analysis of bending strain features which assists with analysis of baseline IMU runs. Based on the report, Marathon has also expanded the use of LiDAR to proactively identify geohazards threats and formalized the protocol to calculate total strain demand on pipelines from strain features.

Based on the PHMSA Advisory Bulletin addressing the potential of geohazard damage, Marathon reviewed its pipelines for geohazard susceptibility under improved susceptibility criteria, including lessons learned from the Edwardsville incident. This review included waterways running parallel to the pipeline right-of-way, erosion, and increased flood potential. Marathon initiated a susceptibility assessment of all their rights-of-way for geohazard threats with a geotechnical engineering consultant. This work is expected to be completed later in 2023. Marathon also revised its geohazard assessment frequency based on system susceptibility. Pipeline movement between multiple IMU ILI runs is also analyzed in our integrated approach.

Between March 11, 2022, and September 1, 2023, Marathon conducted 41 IMU ILI runs to complete baseline bending strain assessments. In addition, 35 bending strain reports were completed from previously completed IMU ILI runs. To date, they have completed baseline bending strain assessments for 6,385 of 6,561 miles susceptible to earth movement (97%). The Pipeline Research Council International (PRCI) strain capacity estimation tool was utilized to calculate the Tensile Strain Capacity (TSC) of the pipeline at the strain feature. The TSC and total strain demand values were compared to determine the necessary mitigation for the strain feature. Extensive analysis of all bending strain reports resulted in 242 geotechnical site assessments, 22 new sites being monitored with strain gauges and inclinometers, and 23 mitigation projects initiated.

Marathon has improved the content of its formal geohazard training program based on lessons learned and incorporating the threats identified by the PHMSA

Bulletin.[36] Marathon expanded groups being trained for holistic threat recognition to aerial patrol, and additional field resources to improve geohazard identification. They have revised their right-of-way inspection program and training. Through its Right-of-Way Management Program, Marathon identifies the indications of potential geohazard threats and reviews the findings with the Integrity and Corrosion Engineering Department to identify potential threats. Marathon's process and training packet for its right-of-way inspection patrollers incorporates examples and indications of slope stability and erosion. These visual indications and examples of potential threats have been reinforced with right-of-way Inspection patrollers. In addition, Marathon has added new functionality to right-of-way inspection tablets to allow patrollers to view images of previously reported sites and report if any observable change has occurred between inspections.

Marathon has begun piloting and developing an advanced right-of-way inspection program, leveraging aerial imagery and Artificial Intelligence (AI) models to help automate and improve the effectiveness of inspections. Natural force threats remain a top focus of the program's roadmap for AI model development. Marathon works with a third party to collect aerial imagery during quarterly flights. The technology is being tested to validate 100% right-of-way coverage during inspection, automated AI detection for mechanical equipment and encumbrances, and supplemental passive leak detection. In addition, AI models are currently in development to identify visual indications of pipe exposures, deep tilling, and geohazards within the collected imagery. This technology is being evaluated to incorporate with routine aerial patrols.

In 2022, due to the Edwardsville release, Marathon added content to its existing leak detection training to include scenarios like those at Edwardsville to help controllers recognize a release event. The new material helps operators on systems that do not have booster stations. Marathon also modified its existing leak detection training for new controllers to include horsepower values as another data point to detect when and where a release could occur. In addition. Marathon added language to the Computational Pipeline Monitoring (CPM) leak alarm response to reference horsepower and how it will react in a leak scenario. Marathon created a lesson-learned training detailing the events of the release that was shared with all the controllers. The lessons-learned training focused on the different ways to recognize a release, especially when there are not any booster stations on the system. It also focused on using all resources to gather data as controllers evaluate abnormal events.

To improve the knowledge of geohazards, Marathon has participated in projects related to geohazards and applied lessons learned to geohazard management practices. These geohazard projects include:

[36] PHMSA-2022-0063, Pipeline Safety: Potential for Damage to Pipeline Facilities Caused by Earth Movement and Other Geological Hazards (June 2, 2022).

- PHMSA/Gas Technology Institute (GTI) Development and Validation of a Probabilistic Method for Estimating Accumulated Strain and Assessing Strain Demand and Capacity on Existing Pipelines project (2023)
- INGAA Phase II project to develop a Recommended Practice for Pipeline Integrity Management of Landslide Hazards (2022-2023)
- American Petroleum Institute (API) development of Recommended Practice 1187 for pipeline geohazards (2022-2023)

Marathon also led an operator-to-operator information sharing webinar within 3.5 weeks of this incident. The industry sharing event had approximately 900 attendees on the webinar. Marathon shared with the industry the details of the incident, initial learnings, and the steps they were taking in response.

E. LIST OF ATTACHMENTS

ATTACHMENT 1 – ADV Integrity Edwardsville Failure Analysis Final Report

Submitted by:

Ashley Horton

Group Chair

ADVINTEGRITY

ADVANCING INDUSTRY TOGETHER

Edwardsville Failure Analysis

Final Report

Prepared for

Marathon Pipe Line LLC

100440-RP01-Rev1-071723

July 2023

WHEN TECHNOLOGY WORKS, TREMENDOUS THINGS ARE POSSIBLE.

Edwardsville Failure Analysis

Final Report

Prepared for

Marathon Pipe Line LLC

Findlay, OH

July 2023

Reviewed by:

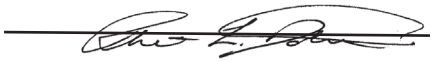

Rhett Dotson, PE

[redacted]

Reviewed by:

Chris Alexander, PhD, PE

[redacted]

ADVINTEGRITY

ADVANCING INDUSTRY TOGETHER

100440-RP01-Rev1-071723

Rev	Date	Description	Prepared	Reviewed
0	07.17.2023	Issued for Use	RLD	CRA
1	07.17.2023	Issued for Use with Minor Revisions	RLD	CRA

EXECUTIVE SUMMARY

On March 11, 2022, an incident occurred involving a 22-inch diameter crude oil pipeline operated by Marathon Pipeline, LLC (MPL) near Edwardsville, IL adjacent to Cahokia Creek. At the time of the accident, the pipeline was transporting Wyoming Asphaltic Sour Crude. The failed pipeline was the northernmost of three parallel pipelines that shared the right-of-way, and the closest to the creek. Soil stabilization had been previously completed in 2014 in the area where the failure occurred. The affected pipeline was constructed from API 5L Grade X46 pipe with a 0.344-inch wall thickness and installed in 1949.

Numerical analysis was performed using calibrated models based on information collected from previous IMU inspections in 2018 and 2021 in addition to information collected after the incident. The numerical models considered representative soils and operating conditions at the time of failure. The following conclusions were made based on the results of the numerical analysis.

1. The area near the failure had a maximum combined bending strain of 0.33% based on the 2018 bending strain results with a 5.7-ft horizontal deviation from straight. The same area exhibited change between 2018 and 2021 with the combined bending strain increasing to 0.41% and the horizontal deviation increasing to 8-ft. The data collected at the time of failure showed a marginal increase in horizontal deviation to 8.2 feet.

2. Calibrated numerical models were developed representing both undrained (clay) and drained (sand) soil conditions; however, the models were easier to calibrate for the undrained conditions indicating that the soil behavior is more likely representative of undrained conditions at the time of failure, which is consistent with the soil conditions observed near the incident.

3. Both the drained and undrained models showed that the pipeline developed a fully yielded cross section (i.e., a plastic hinge) near the failed girth weld between the 2021 IMU inspection and the time of failure. The strains rapidly increased at this location as the membrane and bending strains accumulated at the location of the plastic hinge.

4. The numerical models showed that the location and magnitude of the strains at the plastic hinge depend on soil properties and the extents of the movement profile. However, interaction of the plastic hinge with the failed girth weld is considered likely.

5. The maximum total strain within the plastic hinge ranged from 0.61% to 0.83% in the numerical models. The bending strains and membrane strains contributed almost equally to the total strain at this location.

6. As a result of the plastic hinge forming, the strains near the critical location were changing more rapidly between 2021 and the time of the failure than the strains near the peak pipeline displacement or the location of maximum bending strain.

7. The dimensions of the feature in the girth weld exceeded the size limitations of the PRCI SIA-1-7 strain capacity calculator. However, a feature was assessed with a size approximating the identified girth weld feature with respect to the peak depth. The assessed feature had a length of 3.27 inches with a depth of 80% NWT. This assessed feature is shorter than the actual feature, but with a depth near the measured peak depth. The tensile strain capacity (TSC) based on this feature was 0.29%. The calculated tensile strains from the numerical model were greater than this TSC, indicating that the girth weld failed because the increased demand from soil movement exceeded the TSC of the girth weld.

CONTENTS

1.0 BACKGROUND

On March 11, 2022, an incident occurred on a 22-inch diameter crude oil pipeline operated by Marathon Pipeline, LLC (MPL) near Edwardsville, IL adjacent to Cahokia Creek. At the time of the incident, the pipeline was transporting Wyoming Asphaltic Sour Crude. The failed pipeline was the northernmost of three parallel pipelines that shared the right-of-way, and the closest to the creek. Soil stabilization had been previously completed in the area where the failure occurred. The affected pipeline was constructed in 1949 from API-5L Grade X-46 material with a 0.344-inch nominal wall thickness.

The failed pipeline transports refined products from Wood River, IL to Patoka, IL and is referred to as the "WoodPat" system. The incident and subsequent product release occurred because a girth weld failed during operations. Images taken during the remediation of the girth weld failure are shown in Figure 1.1. The image on the left is taken looking upstream across the incident site toward the failed girth weld with Cahokia creek on the right-hand side of the image. The image shows that the WoodPat pipeline experienced both horizontal and vertical displacements. The image on the right-hand side of Figure 1.1 shows an image of the failed girth weld. The pipeline separated both laterally and axially at the failure location. An aerial image of the remediation site is shown in Figure 1.2.

Figure 1.1: Failed Girth Weld During Excavation

Figure 1.2: Aerial Image of Failure Location

2.0 OBJECTIVE

MPL requested that ADV Integrity, Inc. (ADV) help identify the causal factors that resulted in the accident. Specifically, ADV was asked to develop numerical models simulating the condition of the pipeline prior to the incident. The models were expected to account for the as-laid condition of the pipeline and the influence of ground movement near Cahokia Creek. The objective of the numerical analysis is to provide information on the strain demand near the failed girth weld at the time of the incident. Furthermore, the strain demand from the models will be compared to representative strain capacities determined through material testing and the methodology from the Pipeline Research Council International (PRCI) project SIA-1-7 (Wang, 2019).

To achieve these objectives, the scope of work proposed by ADV included the following tasks:

- Task 1: Review historical data, including inspection information, operating conditions, and prior stabilization efforts.
- Task 2: Determine initial as-laid condition based on a review of as-built drawings and historical IMU information.
- Task 3: Construct an FEA model and calibrate the model to measured conditions.
- Task 4: Use the model to investigate variations in soil properties and movement.
- Task 5: Estimate strains near the failed girth weld at the time of failure and compare strain capacities based on metallurgical evaluation and material testing.

3.0 SUPPORTING INFORMATION

This section presents a summary of the information provided to ADV and reviewed as part of Task 1. A summary of the documents is included in Table 3-1.

Table 3-1: Documents Reviewed

Document	Description
22in_Woopat Pipeline_Wood River to Patoka_2021_IMU Data	2021 High Resolution IMU Data
22in_Woopat Pipeline_Wood River to Patoka_2021_Weld Log	2021 Girth Weld Listing
Rosen 2021 Pipeline Movement and Bending Strain Assessment Report 3-30	Strain Comparison Report
22in_Woopat Pipeline_Wood River to Patoka_2018_IMU Data	2018 High Resolution IMU Data
22in_Woopat Pipeline_Wood River to Patoka_2018_Weld Log	2018 Girth Weld Listing
2012 Roxana - Patoka Woodpat (120265_22A) IMU Raw Data	2012 High Resolution IMU Data
2012 GE Pii CAL CMFL	2012 Feature Listing
IR#14 - Alignment Sheet with stationing of Release location	Alignment Sheet
TXG0258_Marathon_Edwardsville Geotech Site Assessment	Geohazard Assessment
TXG0258-MPL Edwardsville-Borehole Logs-Final	Borehole Results
MPL - Cahokia Canal DOC Exhibit	Post-Incident Survey Locations
3-0220457 - Original 03-12-22 Adjusted with LatLong	Post-Incident Geospatial Locations
Post-Accident Excavation Notes -PRELIMINARY	Field Notes

3.1 IMU Data Review

The bending strains based on the inspection from October 28, 2021 are reproduced in Figure 3.1. The maximum combined bending strain at this location is 0.41%. The girth weld that failed is #7630, located at odometer 32709.3 ft, and is annotated in the image with the red arrow. The IMU data indicates approximately 8-ft of horizontal deviation from a straight line across the impacted area and 9.3 feet of vertical deviation from a straight line across the impacted area.

ADV aligned and compared all the available IMU data sets as shown in Figure 3.2. ADV observed that the out-of-straightness (OOS) profiles from the 2012 IMU data do not appear plausible. When the IMU data was examined outside of the area of interest in stable locations, the horizontal and vertical geospatial information from 2012 often showed deviations that were inconsistent with the information from the inspections in 2018 and 2021. However, the bending strain profiles calculated from the pitch and azimuth did appear consistent with the other two data sets. These types of issues with geospatial accuracy are

more common in older IMU data sets. While they do not restrict the ability to compare calculated strains between the data sets, the OOS profiles often cannot be compared.

When comparing the strains in Figure 3.2, a clear progression in the horizontal, vertical, and combined strains is evident from 2012 to 2018 and from 2018 to 2021. This data confirms that the pipeline was experiencing external loads and being subjected to both horizontal and vertical movement in the time between 2012 and 2021.

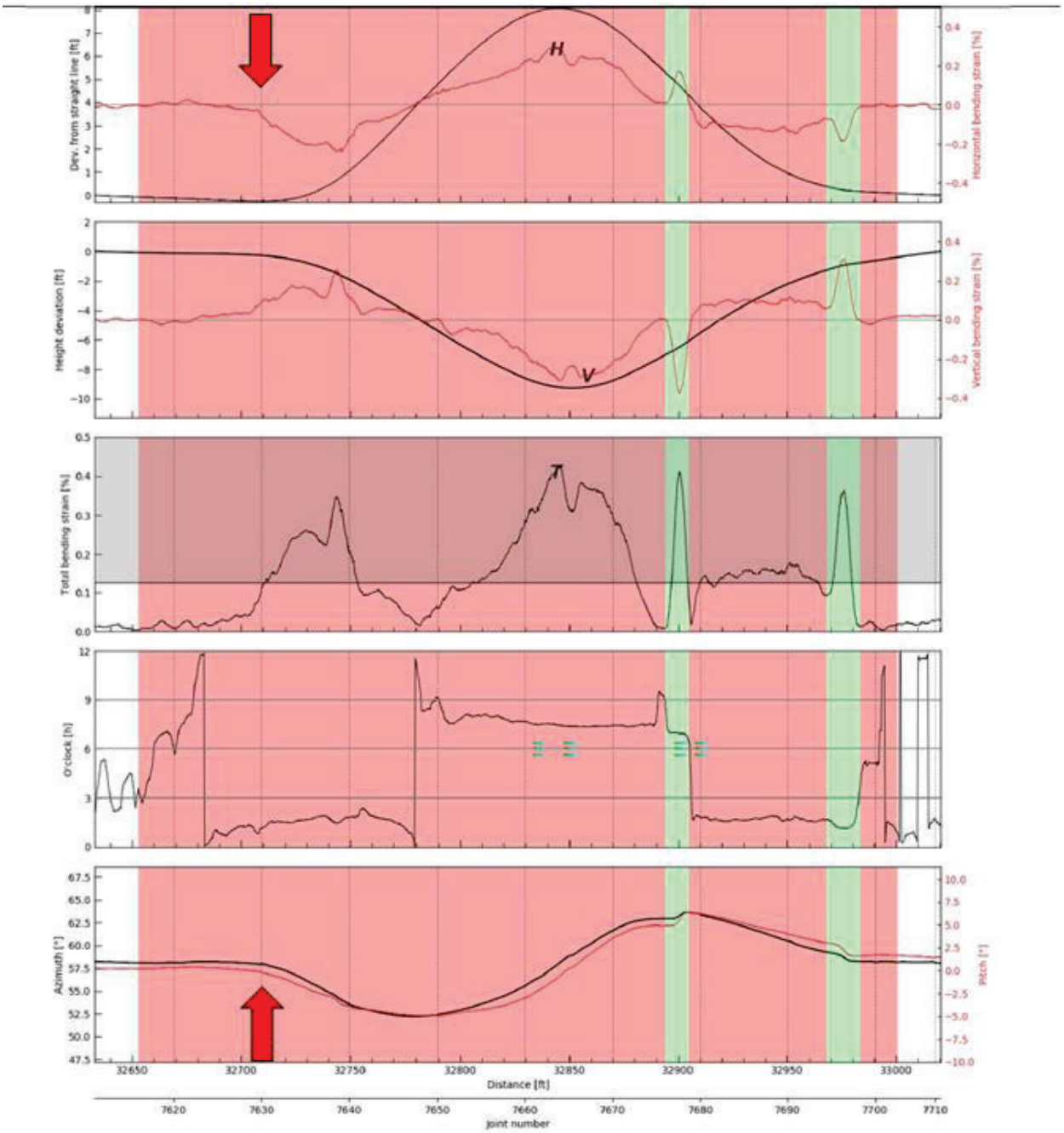

Figure 3.1: Bending Strain Site #7610 (ref: Strain Comparison Report)

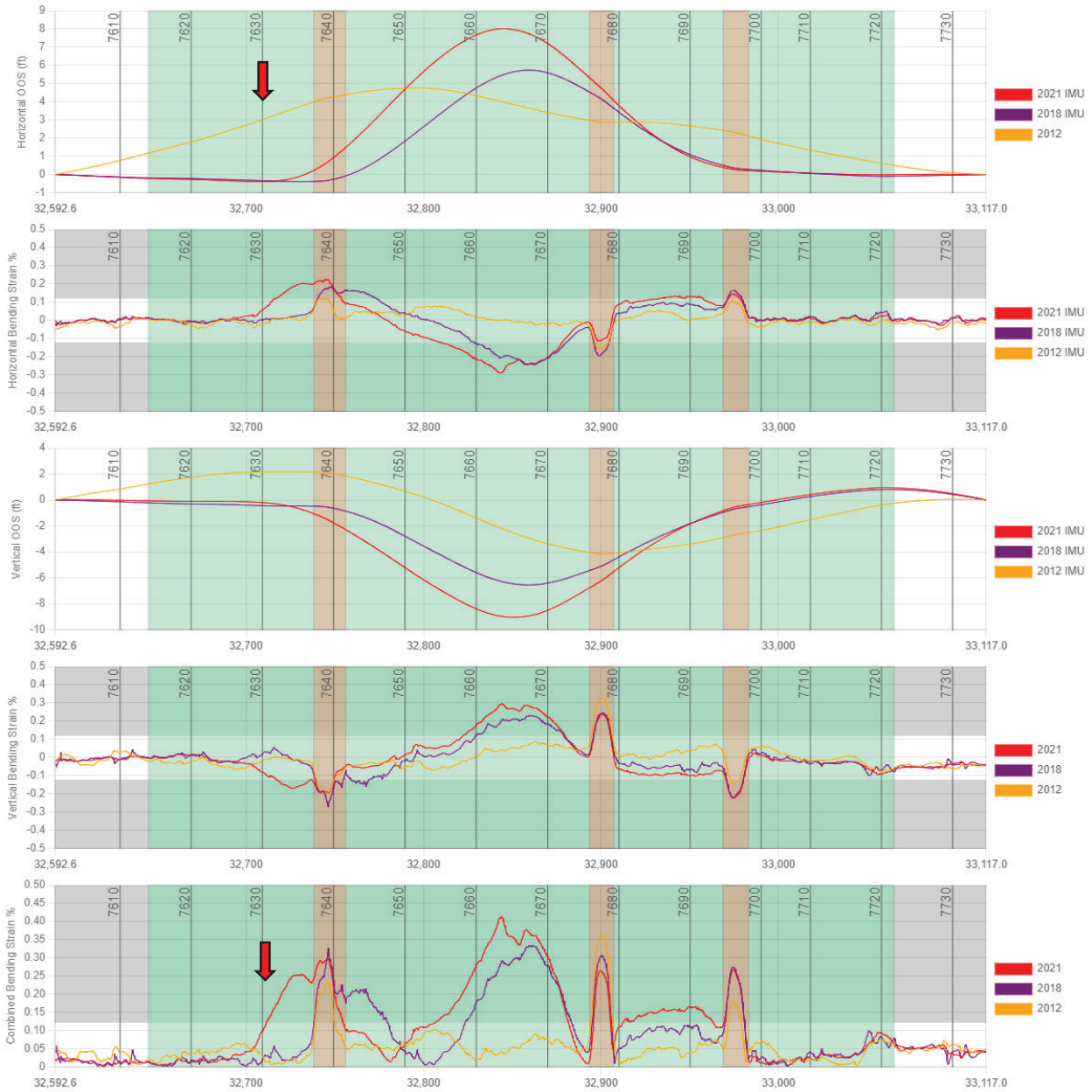

Figure 3.2: IMU Comparison for 2012, 2018, and 2021

3.2 Alignment Sheet Information

Information showing the original pipeline construction location from 1949 was not available. Marathon provided alignment sheets with information on the surface elevation, top of pipe elevation, and depth of cover. The information from the alignment sheet near the failure is enlarged in Figure 3.3. This information does not reflect as-built conditions but was collected prior to the incident (the alignment sheet was dated February 18, 2022). The information shows that the ground elevation near the failure was characteristic of a depression with the low-point approximately 4-6 feet lower than the surrounding area. This

information was confirmed by satellite imagery showing a drainage channel crossed over the pipeline near the failure location. The alignment sheet also confirmed the depth of cover near the failure varies from 22 to 57 inches.

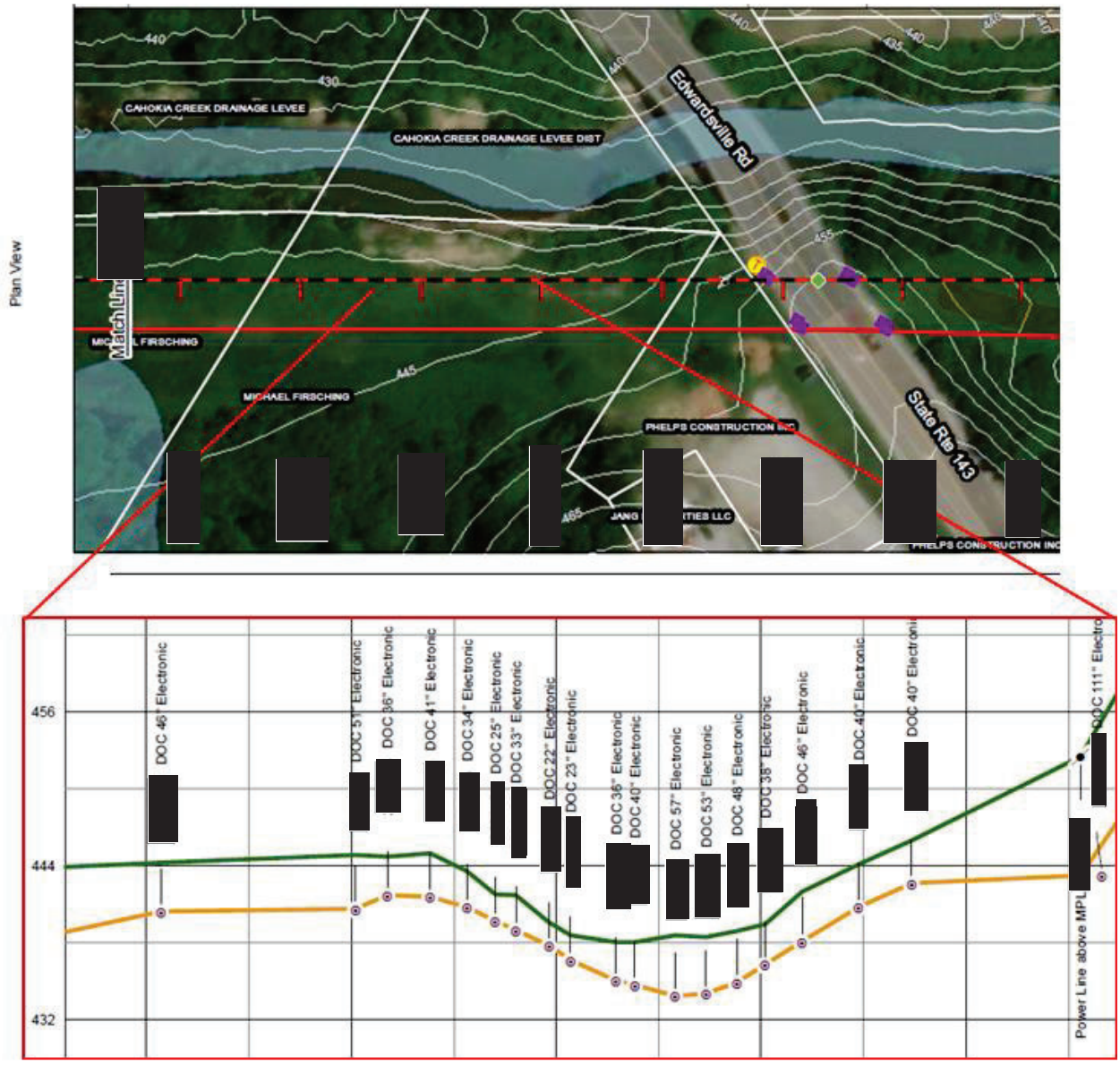

Figure 3.3: Alignment Sheet Information

3.3 Soil Data

Soil characteristics were collected from two boreholes located near the failure as shown in Figure 3.4. Based on the depth of cover survey, the soils of interest would occur between 3 and 8 feet deep. An image of the data from the IN/PZ1 borehole is provided in Figure 3.5. The IN/PZ1 borehole shows soft to medium stiff clays at the pipeline depth. The information from the IN/PZ2 borehole is provided in Figure 3.6,

showing soft clay at the pipeline depth. The pocket penetration values for unconfined compressive strength varied from 0.5 to 1 ton per square foot between the two boreholes. The lab results indicated a dry unit weight of 100.3 pcf and a moist unit weight of 125.8 pcf.

Figure 3.4: Borehole Locations

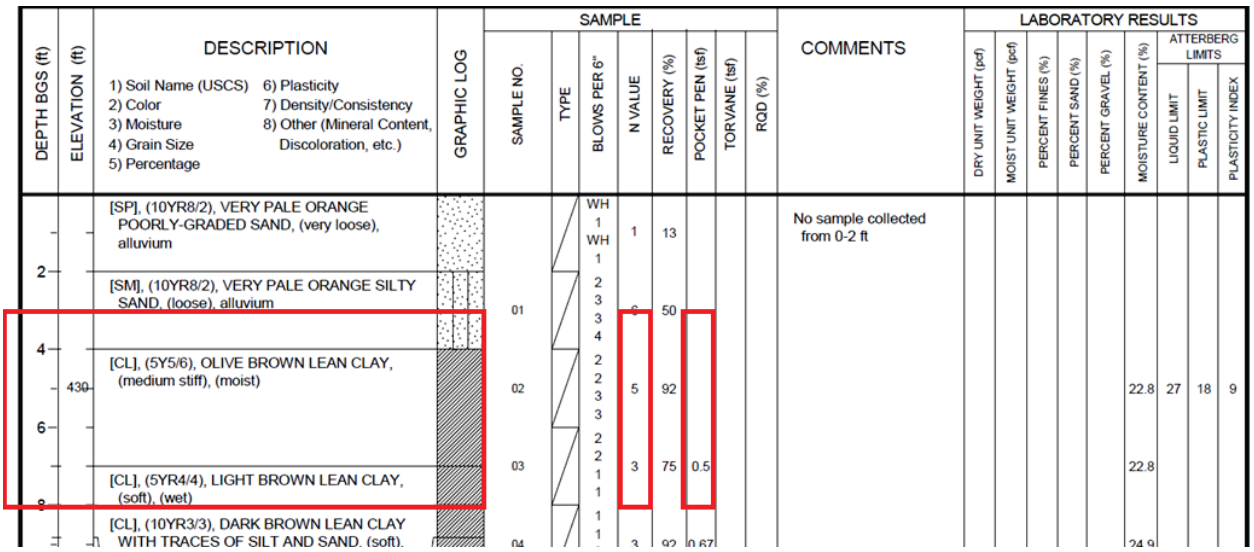

Figure 3.5: IN/PZ1 Borehole Information

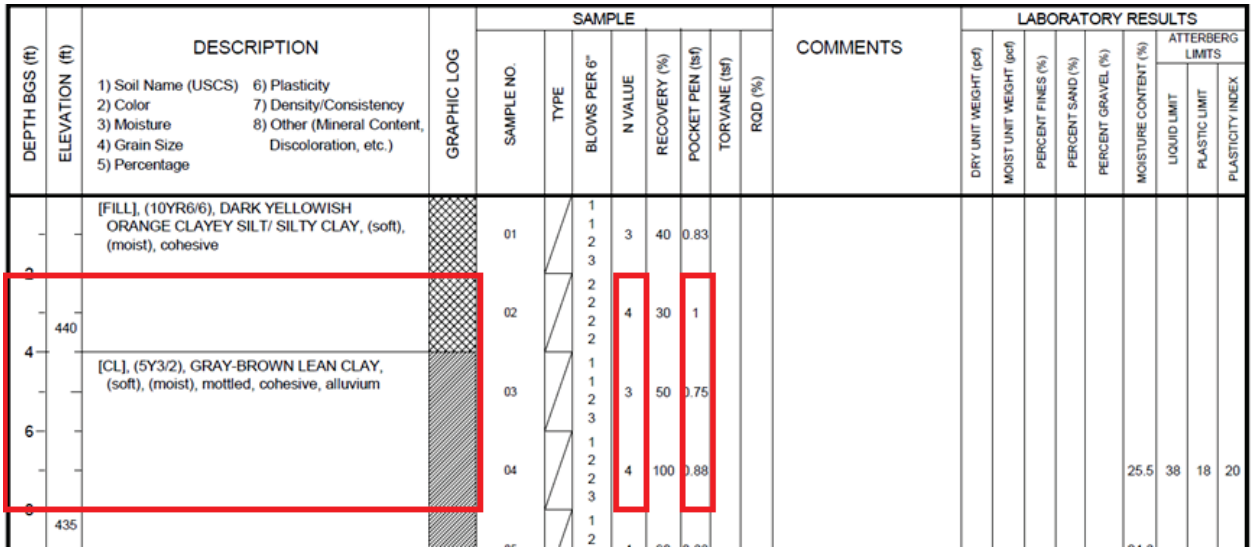

Figure 3.6: IN/PZ2 Borehole Information

3.4 In-Situ Information

ADV received information describing the geospatial location (latitude, longitude, and elevation) of the pipeline post-failure at select locations. Additionally, field notes taken during the remediation captured information pertaining to the pipe "separation" at the failed girth weld. The information is reproduced in Table 3-2.

Table 3-2: Pipe Separation Measurements

Orientation	Separation Distance
12 o'clock (TDC)	7 ½ inches
3 o'clock (south)	8 inches
6 o'clock (bottom)	7 inches
9 o'clock (north)	6 ¾ inches
Lateral (12 o'clock)	4 ¼ inches
Lateral (6 o'clock)	7 ¾ inches

The information from the as-found survey was aligned and overlaid with the available IMU data sets. The comparison for the horizontal and vertical out-of-straightness profiles are shown in Figure 3.7. The survey information shows that the Woodpat pipeline exhibited slight additional movement after the 2021 survey with a total horizontal out-of-straightness of 8.2 feet. The vertical out-of-straightness did not show a measurable difference when compared to the 2021 IMU data set with a total vertical deviation of 9-feet.

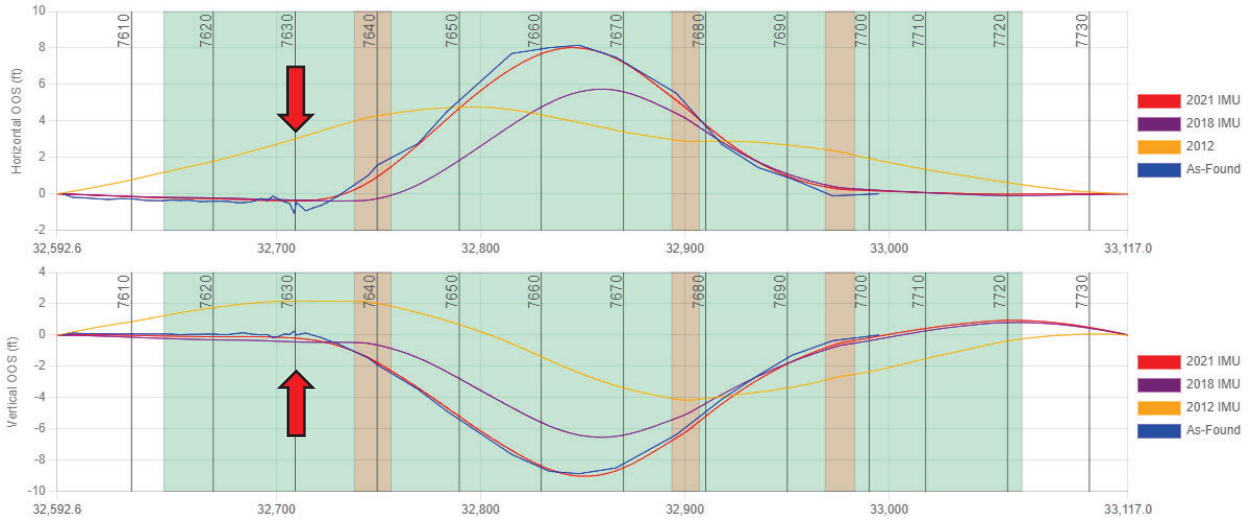

Figure 3.7: As-Found Survey

3.5 Operating Conditions

The WoodPat system is composed of 22-inch Diameter, 0.344 NWT, API 5L Grade X46 pipe material at the location of the incident. At the time of the failure, the Woodpat system was transporting crude oil with an API Gravity of 21.6°. The pressure at the Roxana discharge station was recorded as 476 psi at 8:15 AM.

4.0 NUMERICAL MODEL

4.1 Structural Properties

The numerical model was evaluated using the Abaqus general-purpose finite element code and utilized beam elements (type PIPE31) to represent the pipeline. The beam elements were modeled as 22-inch outer diameter with a nominal wall thickness of 0.344-inches. The effective weight of the elements was modeled as 1,370 lb/in^3 accounting for the weight of the steel pipe and internal contents. Elastic-plastic material properties were specified for the pipe material based on the specified minimum properties for API 5L Grade X46 pipe material. A Ramberg-Osgood formulation was used to generate the true stress – true strain curve based on a yield strength of 46,400 psi and an ultimate tensile strength of 63,100 psi. The resulting material curve is shown in Figure 4.1.

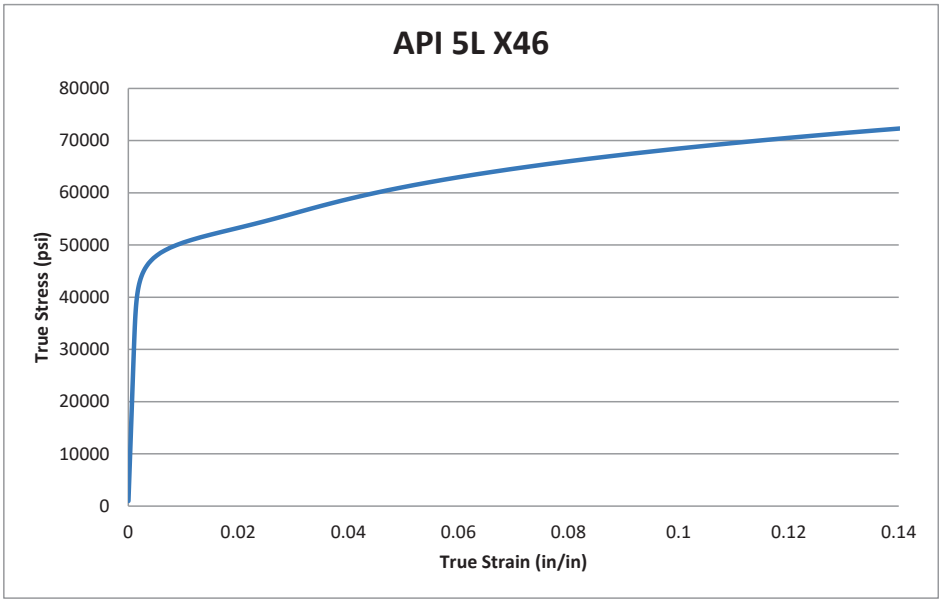

Figure 4.1: API 5L Grade X46 Elastic Plastic Material Properties

4.2 As-Laid Configuration

Identifying the as-laid condition of the pipeline consisted of three tasks. First, the heading angles (pitch and azimuth) recorded by the IMU during inspections were reviewed to identify which components of the pipeline within the bending strain area are consistent with manufactured bends. Second, the heading angles were reviewed to identify a plausible as-laid trajectory, and then the heading angles were reconstructed to fit this as-laid trajectory. Finally, the reconstructed heading angles were used to generate an as-laid centerline for the pipeline.

Figure 4.2 provides a comparison of the horizontal out-of-straightness profiles and azimuth angles from the 2018 and the 2021 inspections. The 2012 data was not included in the comparison as the heading

angles and out-of-straightness profile were not considered accurate as discussed in the previous section. Both inspections show similar behavior in the azimuth angle consistent with external loads acting on the pipeline. The azimuth angle is approximately 58-degrees near the beginning and end of the bending strain and movement area in both inspections. Two minor 2-degree horizontal manufactured bends appear in the data near odometer 32,900 feet and 39,990 feet. This information suggests that the pipeline was initially laid nearly straight throughout this area with minor deviations. This pattern is typical of most pipelines. Within the displaced area, the azimuth shows a distinct "S"-shaped pattern. This pattern is produced when a pipeline is displaced from its initial location. It is reasonable to conclude that the pipeline was initially laid straight through the area and account for the two minor manufactured bends in the recreated heading profile as shown with a dashed line in Figure 4.2.

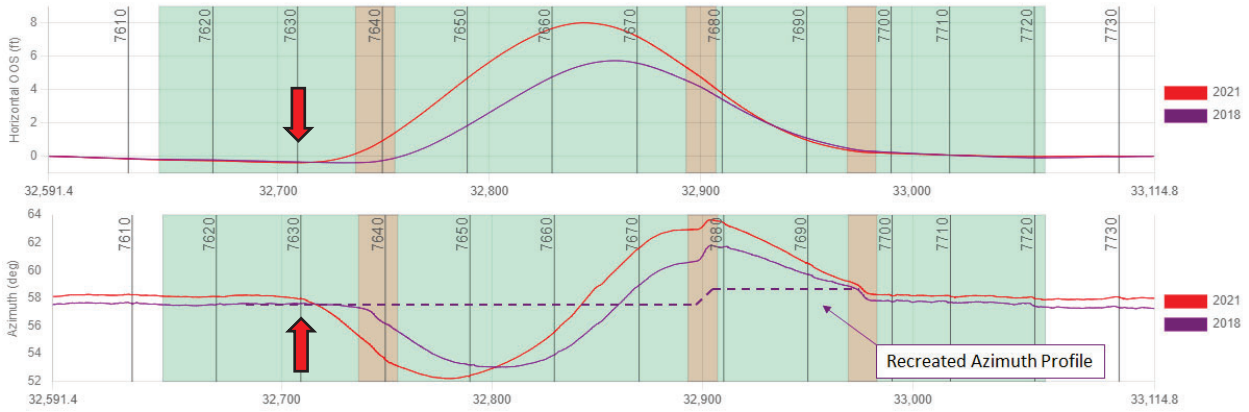

Figure 4.2: Azimuth Recreation

Figure 4.3 provides a comparison of the vertical out-of-straightness profiles and the pitch angles from the 2018 and the 2021 inspections. Both inspections show similar behavior in the pitch angle consistent with external loads acting on the pipeline. Near the beginning of the movement area, both tools enter with a near-flat pitch of approximately 0.5-degrees and exit the movement area with a pitch of approximately 2-degrees. Within the movement area, three small vertical bends can be seen near odometer 32750 feet, 32,900 feet, and 33,990 feet. These vertical bends form an overbend-sagbend-overbend combination that is typical of pipeline construction at shallow crossings. The presence of these vertical manufactured bends confirms the information from the depth of cover assessment that showed a shallow drainage area at this location. It is reasonable to conclude that the pipeline was constructed with shallow bends to cross the drainage. Similar to the azimuth heading angles, the pitch angles in both inspections show the characteristic "S" shape within the movement area as a result of external loads. The recreated pitch profile is shown in Figure 4.3 with the dashed line. The recreated profile preserves the manufactured bends near 32,900 feet and 33,990 feet.

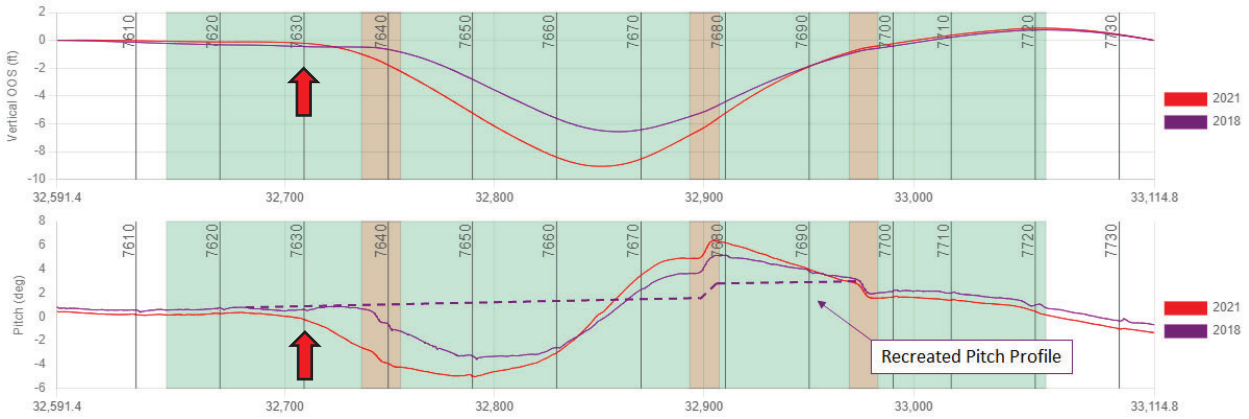

Figure 4.3: Pitch Recreation

The resulting as-laid condition used for the baseline is shown in Figure 4.4 for both the horizontal and vertical profiles. The recreated as-built profile is shown as a green line. The horizontal out-of-straightness shows a near straight trajectory with less than 1-ft of deviation, and the vertical out-of-straightness shows an initial vertical change of approximately 3-ft. This agrees well with the depth of cover information which showed similar deviations in the ground elevation near the drain crossing.

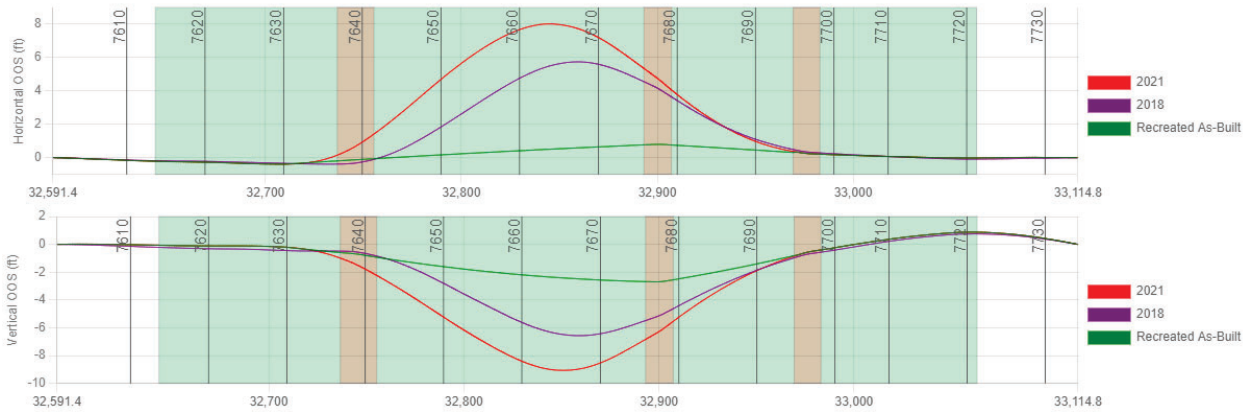

Figure 4.4: Recreated Out-of-Straightness Profiles

4.3 Soil Properties

The Abaqus model used pipe-soil interaction elements (type PSI34) to capture the behavior of the soil at the WoodPat system based on the data captured in the borings. PSI34 elements represent the interaction between the pipeline and the soil as a series of non-linear springs in the horizontal, vertical, and axial direction. The formulations for the soil springs are based on documentation from the American Lifelines Alliance document (American Lifelines Alliance, 2005). The soil was indicated to be primarily made of clay at the pipeline depth with stiffness ranging from soft to firm. Therefore, analysis models were developed using clay (i.e., undrained soil response) formulations that are based on the shear strength of the soil. The upper and lower bound properties used in the assessment are shown in Table 4-1.

Table 4-1: Clay (Undrained) Properties

Property	Lower Bound (weak) Undrained Values	Upper Bound (firm) Undrained Values
Shear Strength	3.62 psi (25 kPa)	7.25 psi (50 kPa)
Alpha	0.94	0.69
Nch (horizontal factor)	6.25	6.25
Ncv (uplift factor)	5.4	5.4
Nc (bearing factor)	5.14	5.14

While the borings did not show sandy material near the depth of the pipeline, the geotechnical review did observe coarse-grained materials (i.e., sand) near the water line. Therefore, the analysis also considered soil properties using sand (i.e., drained soil response) formulations that are based on unit weight and friction angle. Like the clay properties, upper and lower bound values were generated as shown in Table 4-2. The soil friction angle was taken from publicly available sources as this value is not typically characterized for clay soils (Oswell, 2016).

Table 4-2: Sand (Drained) Properties

Property	Lower Bound (weak) Drained Values	Upper Bound (firm) Drained Values
Effective Unit Weight	63.4 pcf	63.4 pcf
Θ, Friction Angle	10°	30°
Nqh (lateral factor)	3.0	7.6
Nqv (uplift factor)	1.0	2.0
Nq (bearing factor)	2.4	18.4
Nγ (bearing factor)	0.5	18.1

4.4 Assessment Methodology

The analysis utilized an iterative approach to determine the strain demand placed on the weld prior to failure. This approach is shown graphically in Figure 4.5. The as-laid configuration as described in the previous section was taken as the starting point for the analysis. The as-laid configuration was assumed to be constructed in a stress-free condition. Displacements were applied to the soil nodes which in turn produce pipeline displacements. The soil displacements are incrementally applied to match the conditions from the 2018 and 2021 inspections as well as the as-found measurements. The strains and resulting pipeline displacements from each increment are compared to the displacements captured from the IMU tool or the as-found survey measurements. If a good match is obtained, the strains at the girth weld of interest are extracted from the model. If a match is not obtained, the displacement profile is iteratively

adjusted until a match is obtained. For the purposes of this report, only the final calibrated models and associated results are presented.

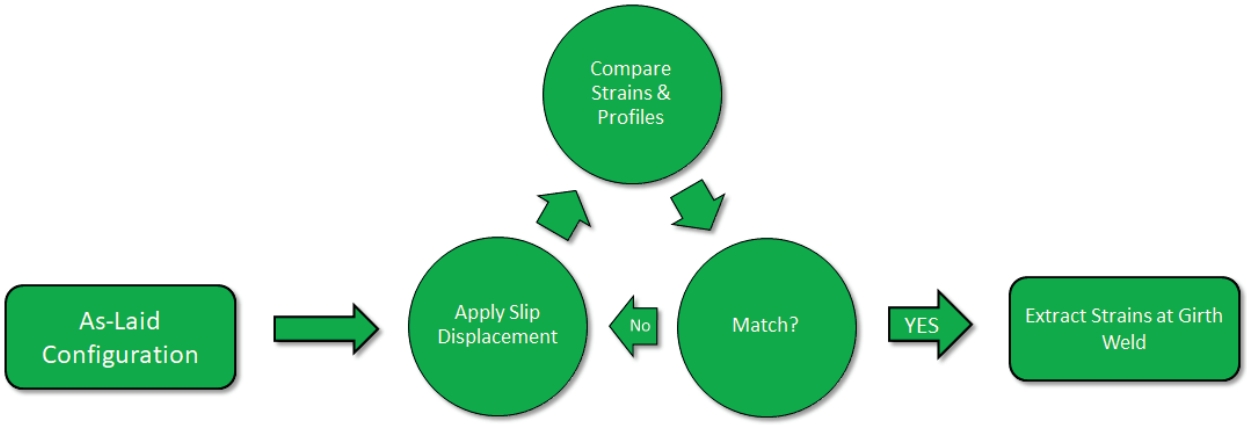

Figure 4.5: Analysis Methodology

4.5 Load Cases

The assessment of the Edwardsville failure addressed four load cases, which are described in Table 4-3. Four load cases were assessed considering variations in the soil type and properties. All load cases included gravity and an internal pressure specified as 476 psi.

Table 4-3: Load Case Description

Load Case	Description
Load Case 1	Upper Bound Undrained (Clay) properties
Load Case 2	Lower Bound Undrained (Clay) properties
Load Case 3	Lower Bound Drained (Sand) properties
Load Case 4	Upper Bound Drained (Sand) Properties

4.6 Post Failure Simulation

The response after the failure was modeled for each load case by “deleting” the elements near the girth weld and allowing the pipeline to respond. The separations observed in the model were then compared to the results recorded during the response shown in Table 3-2.

5.0 RESULTS

The results from the numerical analysis are presented in detail for Load Case 1 and then summarized more briefly for each of the remaining load cases. The process for evaluating the Load Cases is shown graphically in Figure 5.1. The numerical analysis proceeded in steps, and the results are compared for each of the following steps: 2018 alignment, 2021 alignment, and as-found Alignment. Iterative adjustments were made as needed to achieve the results shown for each load case.

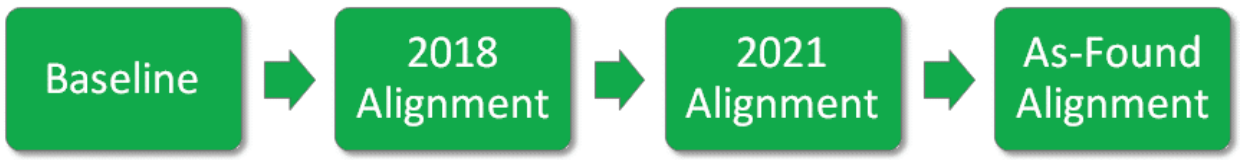

Figure 5.1: Results Comparisons

It is also important to clarify the nomenclature regarding strains. The bending strains determined from the heading angles recorded by the IMU tool and presented in the previous sections are calculated based on curvature in the horizontal and vertical planes. These bending strains do not include membrane strains, which reflect how much the pipe may have "stretched" or "compressed" because of uniform axial loading.

In contrast, the numerical models can provide bending, membrane, and total strains by post-processing the available axial strains at locations around the pipe circumference. The total strain includes both the bending and membrane components. When the results from the numerical models are compared to the IMU bending strain data, the axial strains are processed to render the bending strain components in the horizontal and vertical directions providing an equivalent comparison. When the results present the total strains from the numerical models, these values are inclusive of the membrane and bending strains. The total strains are not compared to the bending strains calculated from IMU.

5.1 Load Case 1 – Upper Bound Undrained Properties

The results for Load Case 1 are shown in Figure 5.2. Except for the total strain panel, each panel compares the results from the IMU tool (or as-found field measurements) to the numerical models with matching colors. Results from the numerical model are shown with dashed lines while the results from the IMU or field measurements are shown with solid lines. It should be noted that strains are not available for the as-found field measurements, but they are presented for the calibrated numerical model representing the same condition. The results of each comparison based on the information in the panels are summarized below:

- Horizontal OOS: The horizontal OOS shows excellent agreement for the 2018, 2021, and as-found data sets. The peak displacements match to within 0.1-ft for each of these conditions.

- Horizontal Bending Strain: The horizontal bending strains show excellent agreement with the available IMU data sets from 2018 and 2021. The horizontal strains for the as-found condition from the numerical model show a sharp increase from the 2021 values near the upstream flank of the landslide with peak horizontal bending strains of 0.38%.

- Vertical OOS: The vertical OOS shows agreement for the 2018, 2021, and as-found data sets.

- Vertical Bending Strain: The vertical bending strains show excellent agreement with the available IMU data sets from 2018 and 2021. There are no significant changes in the vertical strains from 2021 to the as-found condition in the numerical model.

- Combined Bending Strain: The combined bending strains show excellent agreement with the available IMU data sets from 2018 and 2021. The combined strains for the as-found condition from the numerical model show a sharp increase from the 2021 values near the upstream flank of the landslide with peak bending strains of 0.42%. This increase is primarily due to the increase in the horizontal bending strain.

- Total Strain: The total strains show progressive increases from 2018 to 2021 and the as-found condition in the numerical models. The maximum total strain in 2018 was 0.61% located near the peak displacement in the landslide. The maximum total strain in 2021 was 0.76% also located near the peak displacement in the landslide. In addition, the 2021 value shows rapidly changing total strains in the bend near odometer 32,900 feet. This rapid change is due to the “straightening” of the 2-degree field bend at this location. The numerical model also shows significant change near the upstream flank of the landslide adjacent to the failed girth weld 7630 at odometer 32,709 feet. At this location, the total strains show a sharp increase with total strains of 0.83%. This rapid change in total strain near the failure is attributed to the pipe cross section becoming fully yielded (i.e., forming a plastic hinge) near the upstream flank of the landslide thereby creating a location where strains can accumulate.

In summary, the comparison for Load Case 1 shows that the horizontal bending and total strains changed rapidly near the upstream flank of the landslide adjacent to the location of the failed girth weld. While the actual total strains are 0.18% at the location of the failed girth weld, the peak total strain occurs less than 10-feet away from the girth weld. Given the uncertainties with the precise position of the WoodPat pipeline prior to failure with respect to the landslide extents, it is possible that the strains were as high as 0.83% in the weld if the upstream flank of the landslide is shifted slightly upstream from where it is located based on the 2021 IMU data.

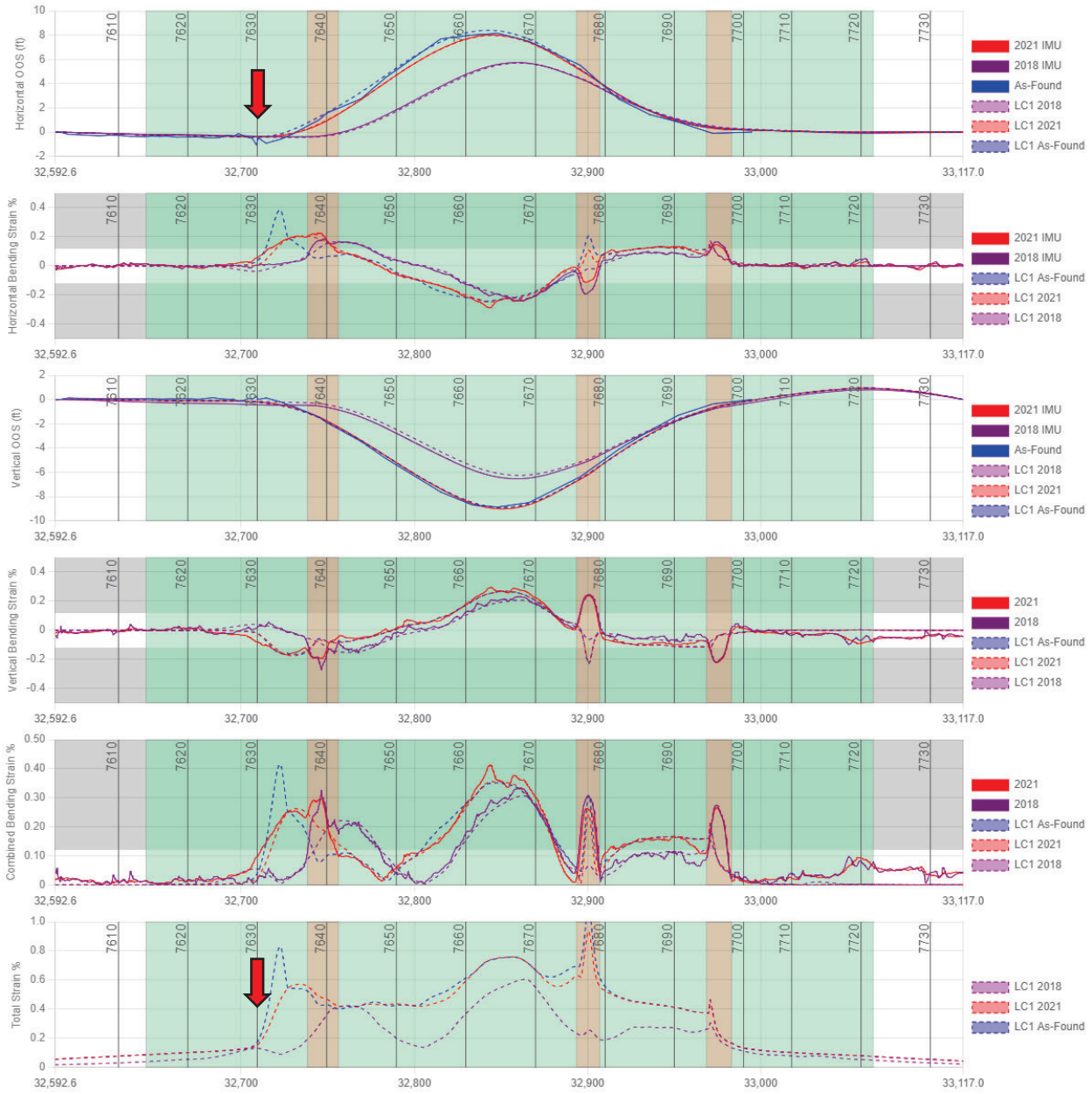

Figure 5.2: Load Case 1, Upper Bound Undrained, Results Comparison

5.2 Load Case 2 – Lower Bound Undrained Properties

The results for Load Case 2 with lower bound undrained properties are shown in Figure 5.3. Except for the total strain panel, each panel compares the results from the IMU tool (or as-found field measurements) to the numerical models with matching colors. Results from the numerical model are shown with dashed lines, while the results from the IMU or field measurements are shown with solid lines. It should be noted that strains are not available for the as-found field measurements, but they are presented for the calibrated numerical model.

With respect to the out-of-straightness plots, the results from Load Case 2 are nearly identical to the results from Load Case 1. Both the horizontal and vertical out-of-straightness plots show excellent agreement with the 2018, 2021, and as-found data sets. However, the results do show differences in the horizontal, combined, and total strains. The sharp peak observed in Load Case 1 is more muted for Load Case 2 with lower overall strains near the upstream flank of the landslide. The horizontal bending strain near the upstream flank is 0.26% while the total strain is 0.61%. The strains are lower for Load Case 2 because the axial and bending resistance of the soil is weaker for the lower-bound load properties. The weaker properties delay the formation of the plastic hinge, but do not prevent its formation.

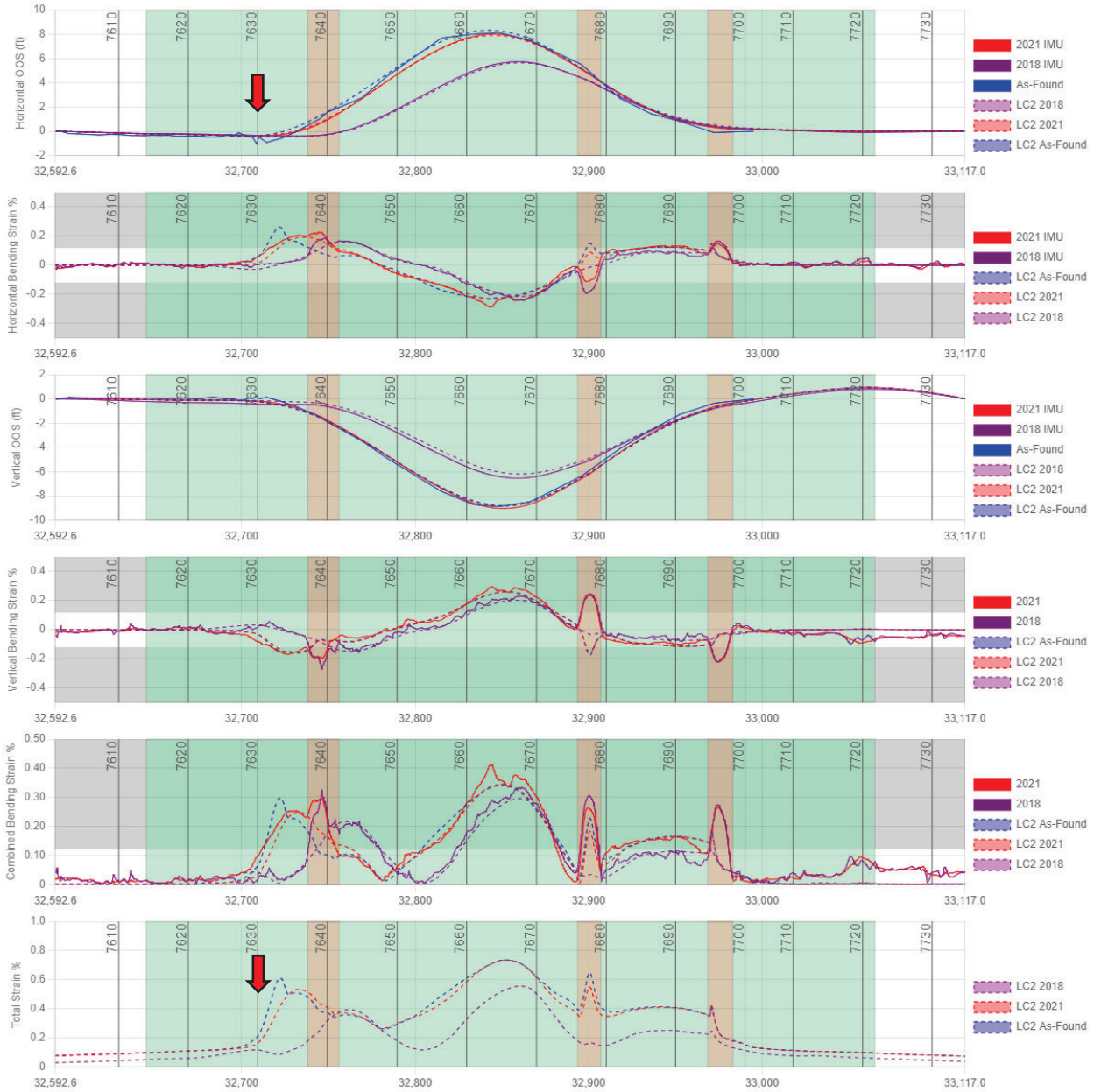

Figure 5.3: Load Case 2, Lower Bound Undrained, Results Comparison

5.3 Load Case 3 – Upper Bound Drained Properties

The comparison of the results for Load Case 3 with upper bound drained properties are shown in Figure 5.4. Except for the total strain panel, each panel compares the results from the IMU tool or as-found field measurements to the numerical models with matching colors. Results from the numerical model are shown with dashed lines while the results from the IMU are shown with solid lines. It should be noted that strains are not available for the as-found field measurements, but they are presented for the calibrated numerical model.

With respect to the out-of-straightness plots, the results for the horizontal displacements from Load Case 3 are nearly identical to the previous results. However, the vertical displacements do not match quite as well. Additionally, the calibration of the vertical displacements required the use of the saturated unit weight (125.4 pcf) rather than the equivalent unit weight (63 pcf). Since the vertical strength of drained materials is a function on the unit weight and the burial depth, this has the effect of increasing the vertical soil resistance. In this assessment, an increase in the unit weight was required to achieve agreement in the displacements.

Regarding the strains, the results from Load Case 3 show similar results to Load Case 1. A localized peak in the strains is evident near the upstream flank of the landslide. The horizontal bending strain near the upstream flank is 0.29% while the total strain is 0.64%. These strains are slightly lower than the results for the upper bound undrained properties in Load Case 1.

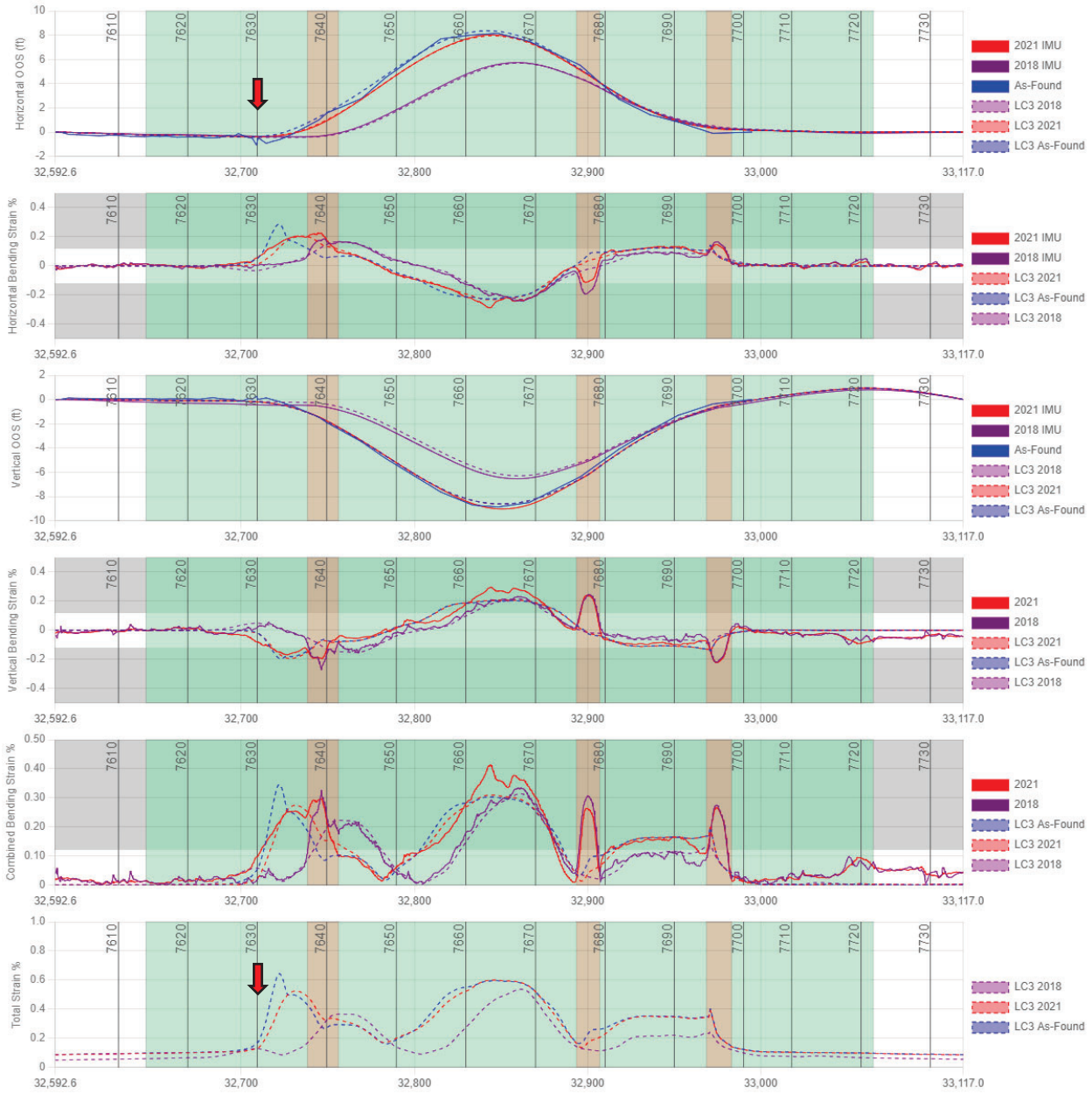

Figure 5.4: Load Case 3, Upper Bound Drained, Results Comparison

5.4 Load Case 4 – Lower Bound Drained Properties

The results for Load Case 4 with lower bound drained properties are shown in Figure 5.5. Except for the total strain panel, each panel compares the results from the IMU tool or as-found field measurements to the numerical models with matching colors. Results from the numerical model are shown with dashed lines while the results from the IMU are shown with solid lines. It should be noted that strains are not available for the as-found field measurements, but they are presented for the calibrated numerical model.

Calibrating the numerical models to the measured strains and displacements based on the recorded IMU data was challenging for Load Case 4. Even with the alteration to the unit weight as described in the previous section, the displacements and strains did not match well. Additionally, the model proved to be numerically unstable at displacements beyond the 2021 values. The comparisons showed that the displacements for the 2018 load case had reasonable agreement, but the comparisons did not match as well as any of the other load cases. In addition, the displacements near the peak and upstream flank of the landslide do not show good agreement for the 2021 load case. The weaker horizontal strength of the soil resulted in a noticeably smoother profile with lower strains near the upstream flank of the landslide.

Regarding the strains, the results for Load Case 4 show significantly lower strains than the other load cases. The vertical and horizontal strains for the 2021 condition show poor agreement with the IMU data. While additional modifications to the soil properties may provide improvements to the comparison, it is unlikely that the vertical displacements will be able to be calibrated. These results indicate that the lower bound drained properties are not an accurate representation of the conditions observed at the failure location based on the 2021 IMU data and information collected at the time of failure. Therefore, the results from Load Case 4 were disregarded for future use.

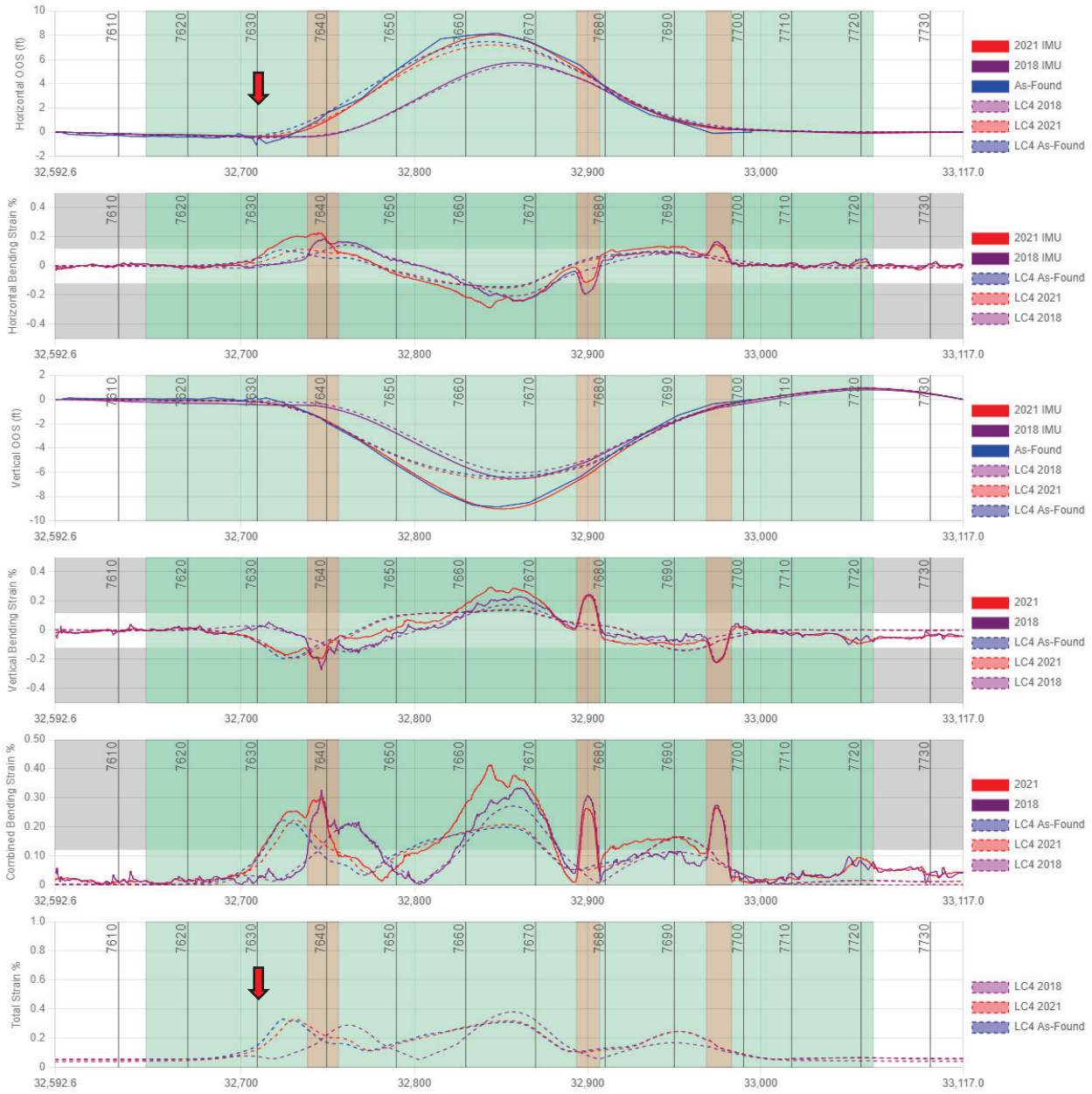

Figure 5.5: Load Case 4, Lower Bound Drained, Results Comparison

5.5 Post Failure Axial Separation

For Load Cases 1 through 3, the analysis models were progressed to simulate the conditions at the time of failure. This was accomplished by deleting the element nearest the girth weld and allowing the pipeline to separate as the soil elements relaxed. It is important to recognize that the results from this step are only considered appropriate when used as a qualitative order-of-magnitude type assessment. The conditions just prior to the failure are not likely to resemble the conditions during the response from 2012 to 2021. The conditions near the girth weld are expected to change as the soil interacts with released

hydrocarbons, and some excavation is required for access to the girth weld. Both conditions will change the local restraint near the girth weld. Nevertheless, the measurements recorded during the investigation provide a useful point of comparison to judge the accuracy of the models.

An average axial separation of 7.3-inches was recorded during the remediation activities. In comparison, Load Case 1 showed a separation of 4.8-inches, and Load Case 2 showed a separation of 6.5-inches. Load Case 3 showed a separation of 6.6-inches. It is interesting that the lower bound undrained properties and the upper bound drained properties showed better agreement than the upper bound undrained properties; however, all the results show reasonable agreement given the challenges in replicating the actual conditions after the failure.

5.6 Other Analysis Considerations

Two additional considerations were addressed in the analysis at the request of MPL. First, the sensitivity of the results to the soil displacements near GW 7630 at the upstream flank of the landslide was investigated. The results from the initial assessments produced a “sharp” change near the upstream flank of the landslide between the 2021 and the as-found simulations. This change was tapered over a 10-ft length to “soften” the change. The results showed no significant difference in the out-of-straightness profiles; however, the total strains did reduce from 0.83% to 0.69% for Load Case 1. These results confirm that the region where the plastic hinge forms adjacent to the girth weld will be sensitive to soil properties and applied displacements.

The second consideration addressed in the analysis was whether repair sleeves installed in 2014 within the displaced section could have influenced the results. Four repair sleeves varying from 1 to 2 feet in length were installed in 2014. The sleeves were located near the following odometers: 32,840 feet, 32,851 feet, 32,900 feet, and 32,911 feet. The failure was located at odometer 32,709 feet, or 131 feet from the nearest sleeve. The sleeves were included in the model by locally increasing the wall thickness for the elements at the sleeve location to account for the additional material. The results showed no difference in the peak strains observed for Load Case 1. Therefore, it was concluded that the presence of the installed sleeves did not contribute to the failure.

5.7 Numerical Analysis Results Summary

The results from the numerical analysis are summarized in Table 5-1. All the load cases showed a sharp increase in strain approximately 10-ft from the girth weld where the incident occurred. The total strains in the girth weld ranged from 0.61 – 0.83%, with the membrane strains accounting for approximately half of these total strains in each load case. While the strains at the girth weld within the model were lower than the maximum values near the girth weld (0.17 – 0.21%), uncertainties in the precise extents of the landslide profile combined with the sharp changes in strain near the girth weld make it likely that the girth weld was experiencing strains higher than the exact values predicted at the girth weld.

Table 5-1: Results Summary

	LC1	LC2	LC3
Total Strain at Girth Weld 7630	0.18%	0.21%	0.17%
Max Bending Strain Near Girth Weld 7630	0.42%	0.30%	0.35%
Max Membrane Strain Near Girth Weld 7630	0.41%	0.31%	0.29%
Max Total Strain Near Girth Weld 7630	0.83%	0.61%	0.64%
Simulated Displacement After Failure (As-found 7.3 inches)	4.8-inches	6.5-inches	6.6-inches

6.0 DISCUSSION

The metallurgical examination (ADV Integrity, 2023) of the girth weld identified two planar features near the failure origin. The largest feature had a length of 7.2-inches with an average depth of 50% nominal wall thickness (NWT) and a peak depth of 88% NWT. The material testing determined that the weld properties and pipe properties were within specifications. The full-size equivalent Charpy energies for the weld centerline and heat affected zone were 58.2 ft-lb and 55.2 ft-lb, respectively. The metallurgical report is included in the appendices.

The tensile strain capacity (TSC) was estimated using PRCI SIA-1-7 with an apparent CTOD value of 0.0177 inches. The exact dimensions of the feature (7.2-inch x 88% NWT) could not be specified as a feature size due to limitations in the SIA-1-7 method. However, a feature was assessed with a size approximating the identified feature with respect to the peak depth. The assessed feature had a length of 3.27 inches with a depth of 80% NWT. This assessed feature is shorter than the actual feature, but with a depth near the measured peak depth. The predicted TSC based on this feature and the measured properties was 0.29%. It is reasonable to conclude that the TSC of the actual feature is not likely to be larger than this value.

This calculated TSC of 0.29% is exceeded by the predicted strains from the numerical model. All the calibrated numerical models indicated that the pipe cross section as fully yielded at a location near the failed girth weld. As a result of the fully plastic cross section, the strains are shown to accumulate rapidly near the failed girth weld with only small increases in additional movement. For example, the peak total strain near the failed girth weld in Load Case 1 was estimated as 0.44% at odometer 32722 feet based on the 2021 IMU inspection. While the pipeline displacements were not substantially different between the 2021 inspection and those recorded after the failure (8 ft vs. 8.2 ft), the peak total strain from the as-found simulation had increased to 0.83% at this same location. These results indicate that the strains near the girth weld increased by 89% with only small changes in movement. The peak total strains at the same location were only 0.1% based on the 2018 inspection.

It is also noteworthy that the maximum overall bending strain did not change as significantly from 2018 to 2021 as the bending strains near the girth weld. The maximum bending strain from the 2018 IMU was 0.33% (total strain 0.60%) while the maximum bending strain in 2021 was 0.41% (total strain 0.76%). This represents an increase of approximately 25% in the reported maximum bending strains. However, the change in bending strain near the girth weld that failed was more significant. The bending strain near the girth weld changed from 0.02% in 2018 to 0.25% in 2021. The bending strain from the as-found condition was estimated at 0.42% representing a 61% increase from 2021 to the time of failure. This information supports the fact that the strains near the critical location were changing more rapidly than the strains near the peak displacement or the location of maximum bending strain within the previously identified area.

Another noteworthy observation in this analysis is that the membrane strains were equal to the calculated bending strains. It is common for pipeline operators to manage geohazard threats based on calculated bending strains alone. For most bending strain locations with smaller displacements and lower strain

values, the membrane strains are not significant and add less than 0.1% strain to the bending strain value. However, at larger displacements, the membrane strains can become significant with magnitudes equal to or greater than the calculated bending strain values as seen in this assessment.

7.0 REFERENCES

ADV Integrity. (2023, June). Woodpat Pipeline Girth Weld Testing, Edwardsville Illinois Pipe Sample .

American Lifelines Alliance. (2005, February). Guidelines for the Design of Buried Steel Pipe.

Oswell, J. M. (2016). *Soil Mechanics for Pipeline Stress Analysis.*

Wang, Y.-Y. (2019). Characterization of Mechanical Properties of Vintage Girth Welds.

APPENDIX A

Metallurgical Report

ADVINTEGRITY

ADVANCING INDUSTRY TOGETHER

Woodpat Pipeline Girth Weld Testing, Edwardsville Illinois Pipe Sample

Final Report

Prepared for

Marathon Pipe Line, LLC

100794-RP01-Rev0-061623

WHEN TECHNOLOGY WORKS, TREMENDOUS THINGS ARE POSSIBLE.

June 2023

Woodpat Pipeline Girth Weld Testing, Edwardsville Illinois Pipe Sample

Final Report

Prepared for

Marathon Pipe Line, LLC

Findlay, OH

June 2023

Prepared by:

David Futch, PE

[redacted]

Reviewed by:

Rhett Dotson, PE

[redacted]

ADVINTEGRITY

ADVANCING INDUSTRY TOGETHER

100794-RP01-Rev0-061623

Rev	Date	Description	Prepared	Checked	Reviewed
B	06.09.2023	Issued for Client Review	DBF	---	RLD
0	06.16.2023	Issued for Use	DBF	---	RLD

Texas Registered Engineering Firm F-19081

www.advintegrity.com

ADV INTEGRITY

ADVANCING INDUSTRY TOGETHER

Friday, June 16, 2023 100794-RP01-Rev0-061623

Nic Roniger, P.E. | *MPL Mainline Integrity Supervisor*
Marathon Pipe Line, LLC
539 S Main St, Findlay, OH 45840

Nic,

Enclosed is our report documenting the mechanical testing and tensile strain capacity estimation of an intact girth weld removed from the Woodpat pipeline segment. This girth weld was removed due to the Edwardsville, Illinois incident occurring on March 11, 2022. Marathon reported that the pipeline in question was installed in 1949 using nominal 22-inch OD x 0.344-inch WT, API 5L, Grade X46 pipe material. Marathon reported that the pipeline transports crude oil at a maximum allowable operating pressure of 881 psig, and the failure occurred at 479 psig.

Thank you for the opportunity to complete this work and please do not hesitate to contact us with any questions.

Regards,

David Futch, PE | Director, Materials Engineering

ADV Integrity, Inc.
4027 Pinehurst Meadow | Magnolia, TX 77355
Office: [redacted] | E-[redacted]
Texas Registered Engineering Firm F-19081

Reviewed by: Rhett Dotson, PE | Chief Engineer – Pipeline Integrity

CONTENTS

LIST OF FIGURES

LIST OF TABLES

1.0 INTRODUCTION AND BACKGROUND

Marathon Pipe Line, LLC (Marathon) contracted ADV Integrity, Inc. (ADV) to perform mechanical testing of an intact girth weld removed from the Woodpat pipeline segment. This girth weld was removed due to the Edwardsville, Illinois incident occurring on March 11, 2022. The National Transportation Safety Board (NTSB) performed a metallurgical examination of the failed girth weld and a partial examination of the intact weld provided. Marathon reported that the pipeline in question was installed in 1949 using nominal 22-inch OD x 0.344-inch WT, API 5L, Grade X46 pipe material. Marathon reported that the pipeline transports crude oil at a maximum allowable operating pressure of 881 psig and the failure occurred at 479 psig.

Marathon requested that ADV perform a series of examinations and mechanical testing to determine the weld's quality and estimate the tensile strain capacity of the weld. To do so, ADV suggested a test matrix to include: pipe body and girth weld tensile tests, Charpy v-Notch testing of the girth weld per API 1104, CTODs of the welds per API 1104, girth weld macros, and full hardness maps. The cross girth weld tensile tests were monitored via digital image correlation (DIC) to provide additional details regarding strain during the tensile test. The results from each examination are summarized in the sections below.

ADV utilized feature dimensions determined via the NTSB examination on the failed girth weld and the feature dimensions present determined via radiographic testing (RT) of the intact girth weld. Based on review of the NTSB data, ADV determined the following:

- Planar feature length within the failed weld:
  - Incomplete Penetration, 7.2-inch long, 1:15 to 1:30 o'clock orientation (0.6 to 1.2 feet); shown in Figure 1 and Figure 2
    - Metallurgical depth of 7.7 mm at deepest point, average 2-4 mm along the length of feature
  - Incomplete Penetration, 1.2-inch long, 3:20 to 3:32 o'clock orientation (1.6 to 1.7 feet)
  - Incomplete Penetration, 0.5 inch long, 6:46 to 6:53 o'clock orientation (3.25 to 3.3 feet)
  - Incomplete Penetration, 0.5 inch long, 10:25 to 10:32 o'clock orientation (5 to 5.05 feet)
- Intact weld: shown in Figure 3
  - Volumetric Features:
    - Elongated slag inclusions and porosity, 0.5 inch long, 12:47 to 12:52 o'clock orientation (4.5 inch to 5 inch)
    - Elongated slag inclusions, 2 inches long, 2:20 to 2:40 o'clock orientation (13.5 inch to 15.5 inch)
    - Elongated slag inclusions, 1.5 inches long, 3:45 to 4:00 o'clock orientation (21.5 inch to 23 inch)
    - Scattered porosity, 5 inches long, 5:12 to 6:05 o'clock orientation (30 inch to 35 inch)
    - Elongated slag inclusions, 3 inches long, 7:38 to 8:10 o'clock orientation (44 inch to 47 inch)
  - Planar features:

- Incomplete Penetration, 0.5-inch long, 4:15 to 4:21 o'clock orientation (24.5 inch to 25 inch)
    - Metallurgical depth 1.3 mm
- Incomplete Fusion, 0.5-inch long, 6:54 to 7:00 o'clock orientation (39.75 inch to 40.25 inch)
- Burn through, 0.25 inch long, 9:20 to 9:23 o'clock orientation (53.75 inch to 54 inch)

Figure 1: Photograph of fracture surface. Numbered scale divisions are inches.

Figure 2: Photograph of fracture surface.

Figure 3: RT image of intact girth weld.

2.0 EXAMINATION OF INTACT WELD

2.1 Tensile Tests

ADV performed tensile testing of the base pipe from both sides of the intact girth weld and three cross weld tensile tests around the circumference of the girth weld. The tensile straps were removed from the top of the pipe (12:00 o'clock orientation) and either the 3:00 o'clock orientation or 9:00 o'clock orientation, and the bottom of the pipe (6:00 o'clock orientation) guided by the RT images in an attempt to avoid flaws present. The cross girth weld tensile tests were monitored via digital image correlation (DIC). DIC utilizes a defined speckle pattern applied to the viewing surface (in this case the through thickness weld profile) created through black and white spray paint to monitor displacement over a given time. Relationship between the starting pattern and how that pattern deforms relative to adjacent patterns is then later interpreted as strain.

The results were compared to the closest API 5L edition from the time of manufacturing: API 5LX, 5th Edition (1954). Tensile test (per ASTM A370) results, summarized in Table 1, respectively, are consistent with the requirements of API 5L, Grade X46 material. The cross girth weld tensile test prepared at the 12:00 and 3:00 o'clock orientation failed in the weld metal with obvious signs of weld flaws (incomplete penetration and porosity). Images of all three tensiles are shown in Figure 4 through Figure 6. Videos of the DIC tests were provided in a separate file. Some of these videos failed outside the virtual extensometer as they failed in the base pipe. These results are considered further in the tensile strain capacity calculations.

Table 1: Tensile Strength Results

Sample	Yield Strength (psi)	Tensile Strength (psi)	Elongation (%)
Pipe Body, Longitudinal, Upstream Pipe	51,200	82,600	30.0
Pipe Body, Longitudinal, Downstream Pipe	55,700	82,000	30.0
API 5LX, Grade X46 5th Edition (1954)	46,000 (min)	63,000 (min)	23.5 (min)
Cross Girth Weld 1 (12:00)	---	69,400 [1]	---
Cross Girth Weld 2 (3:00)	---	69,400 [1]	---
Cross Girth Weld 3 (6:00)	---	81,200 [2]	---

Longitudinal, 3/4" wide reduced sections
[1] Failed in base material, [2] Failed in girth weld or HAZ

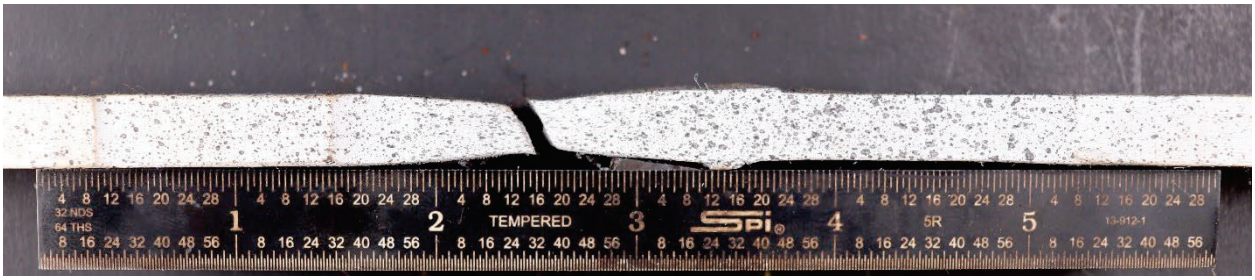

Figure 4: 12:00 o'clock orientation cross girth weld tensile.

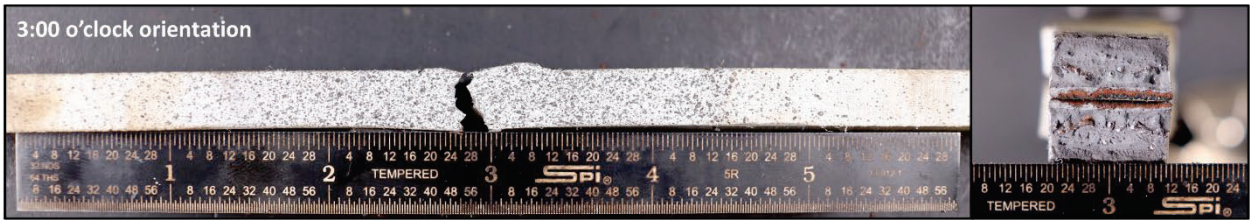

Figure 5: 3:00 o'clock orientation cross girth weld tensile.

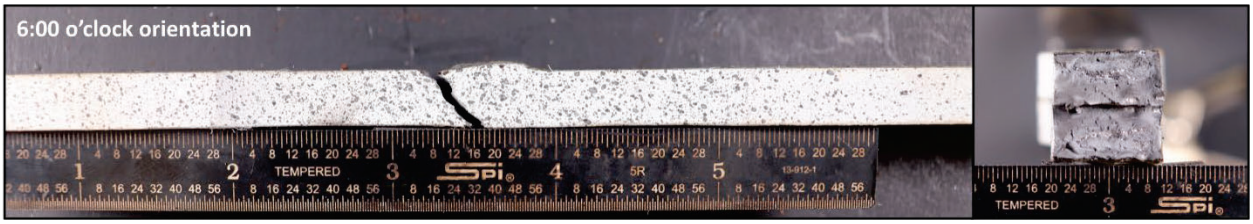

Figure 6: 6:00 o'clock orientation cross girth weld tensile.

2.2 Charpy v-Notch Tests

Girth weld centerline and girth weld heat affected zone (HAZ), two-thirds size Charpy V-notch tests (per ASTM A370) were performed to generate a transition curve; results are summarized in Table 2. Charpy V-notch transition curves were generated using a hyperbolic tangent curve-fit (API 579, Annex 9F) and summarized in Figure 7 and Figure 8.

Table 2: Charpy V-notch Results

Location	Specimen	Temperature	Absorbed Energy (ft-lb)	Approx. Full-Size Equivalent Absorbed Energy (ft-lb)	Percent Shear (%)
Weld Centerline	1	-110	12	17.9	30
	2	-90	4.5	6.7	25
	3	-70	21	31.3	40
	4	-20	22	32.8	60
	5	32	41	61.2	100
	6	74	39	58.2	100
Weld HAZ	1	-70	4	6.0	10
	2	-20	8	11.9	40
	3	32	34	50.7	60
	4	74	37	55.2	70
	5	120	41	61.2	80
	6	170	49	73.1	100

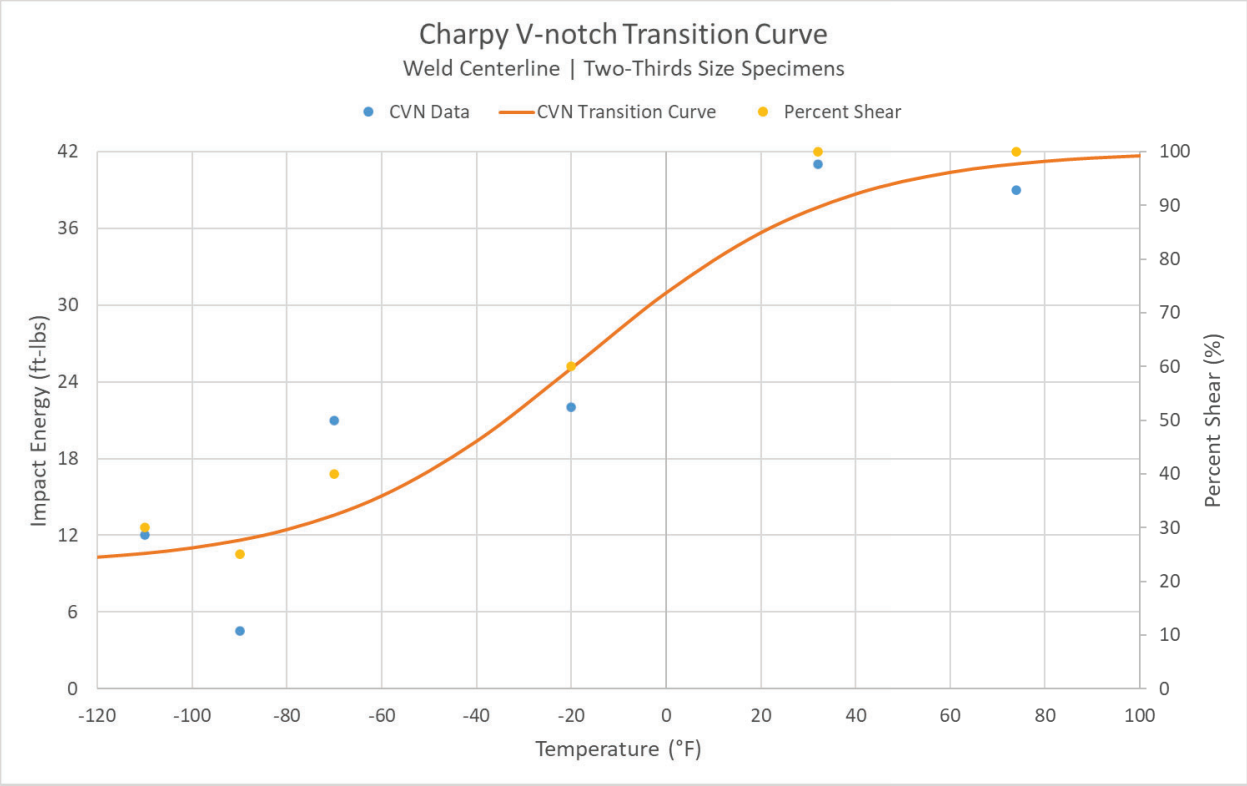

Figure 7: Girth weld centerline CVN transition curve.

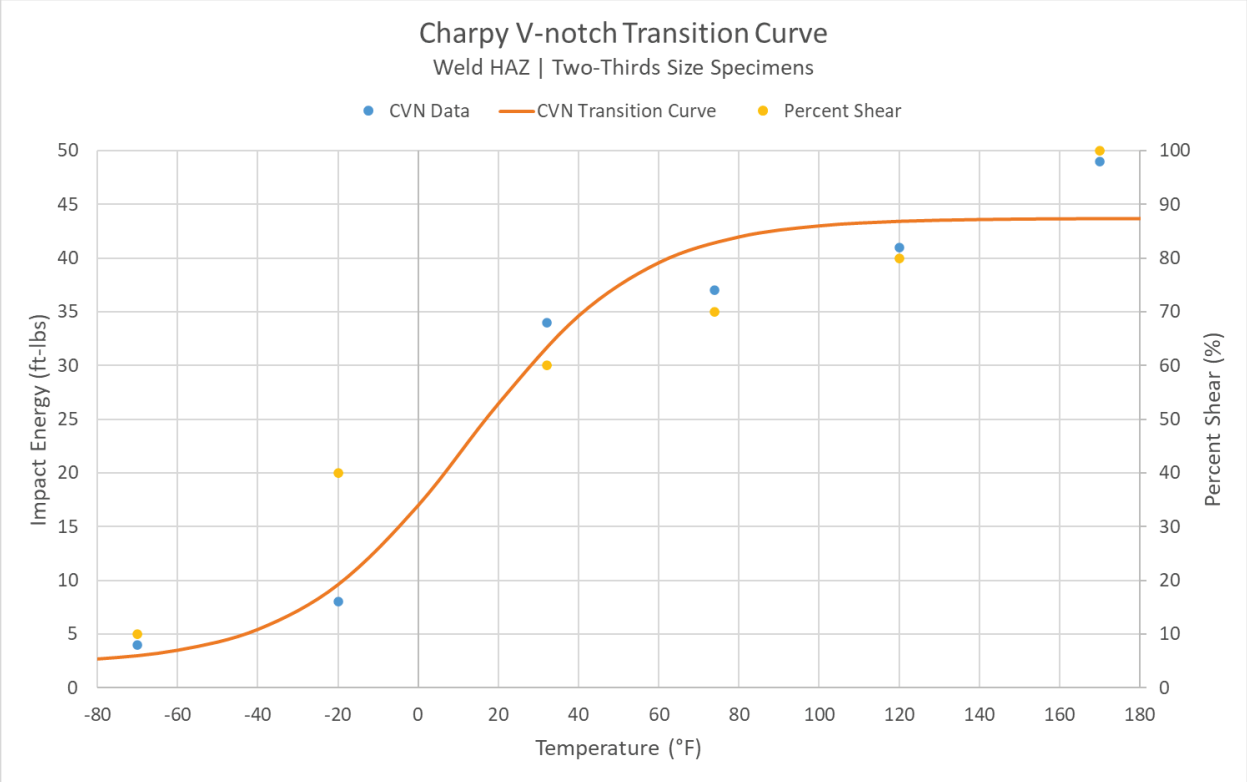

Figure 8: Girth weld HAZ CVN transition curve.

2.3 CTODs

ADV contracted Anderson and Associates to perform Bx2B SE(B) CTODs notched in the weld HAZ and the weld centerline. These tests were performed at ambient temperature at three circumferential locations: 12:00 o'clock, 3:00 o'clock, and 6:00 o'clock orientation. The results are summarized in Table 3.

Table 3: CTOD Results

Location		CTOD (in)	Average CTOD (in)
HAZ	12:00	0.011	0.0097
	3:00	0.0073	
	6:00	0.011	
Weld Centerline	12:00	0.012	0.0109
	3:00	0.011	
	6:00	0.0098 [1]	

[1] Invalid result due to weld flaw present.

2.4 Girth Weld Macros and Hardness Testing

ADV prepared two metallurgical cross sections of the girth weld, one at the 12:00 o'clock and one at the 3:00 o'clock orientation. These cross sections are shown in Figure 9 and Figure 10, respectively. High-lo was identified in the 3:00 o'clock cross section, as annotated in the figure. The high-lo present at the 3:00

o'clock orientation is shown in Figure 11. An area of incomplete penetration was identified connected to the high-lo present. The base pipe microstructure on both sides of the girth weld is consistent with a ferrite-pearlite mixture expected for carbon steel, shown in Figure 12 and Figure 13.

Full hardness maps were performed on the cross sections at a 500-gram load (HV0.5). Images of the hardness traverse are shown in Figure 14 and Figure 15, respectively. No evidence of widespread heat affected zone softening was identified. ADV further calculated a weld strength factor (weld strength / pipe strength) for each macro: both were approximately 0.95. The full hardness reports are attached in Appendix B.

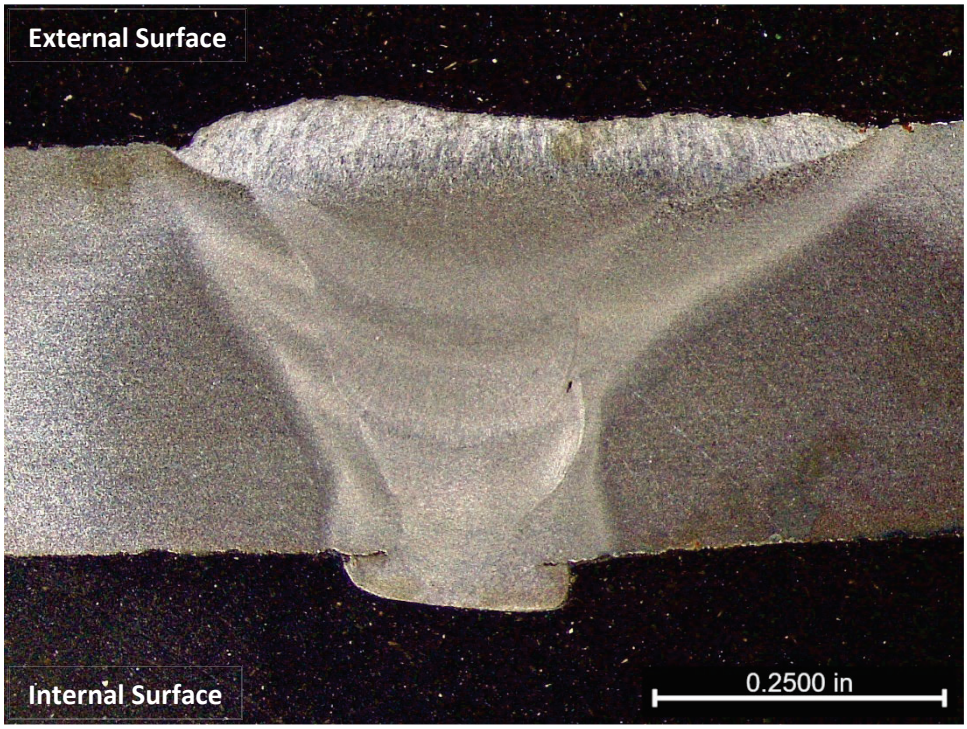

Figure 9: Photomicrograph of across the intact girth weld at the 12:00 o'clock orienation. Etchant is 2% Nital; original mangification is 0.6x.

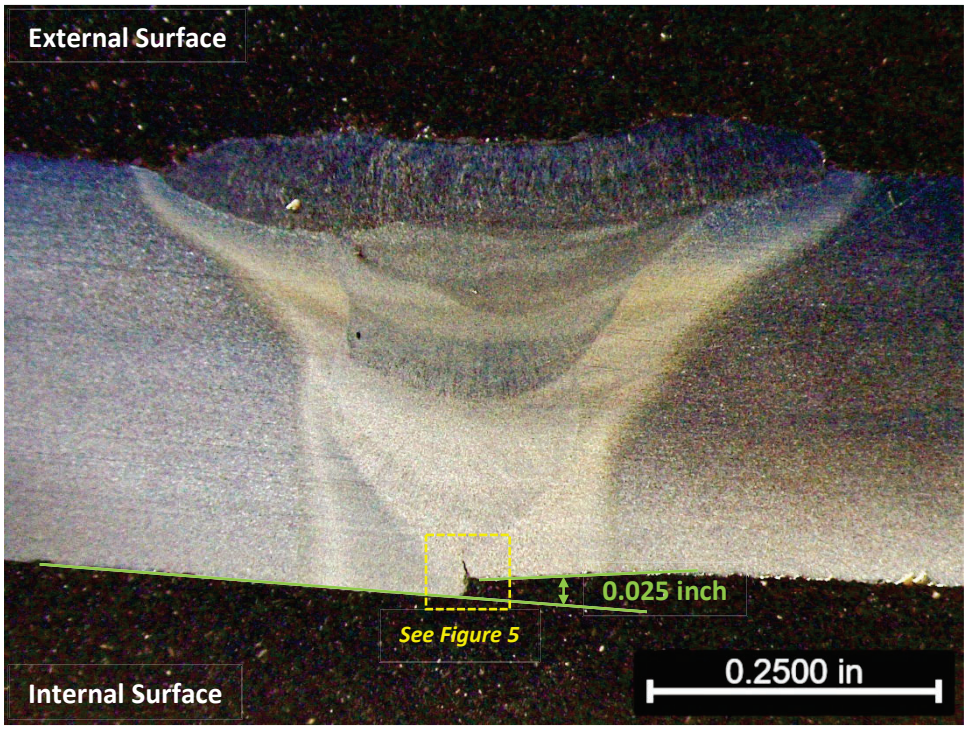

Figure 10: Photomicrograph of across the intact girth weld at the 3:00 o'clock orienation. Etchant is 2% Nital; original mangification is 0.6x.

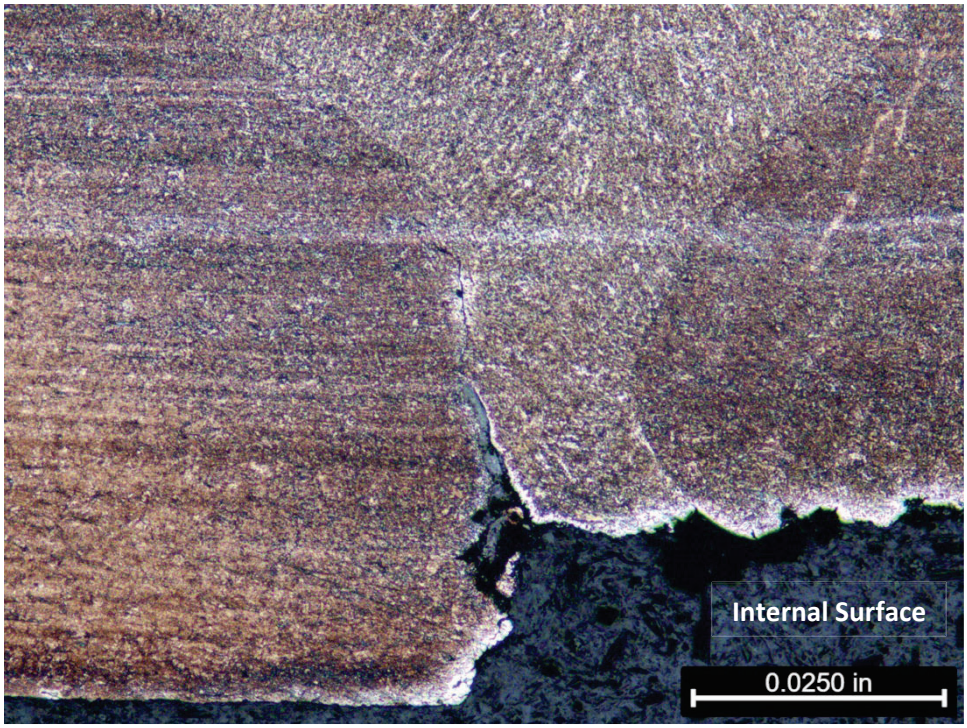

Figure 11: Photomicrograph of girth weld feature present along the internal surface of the 3:00 o'clock cross section. Etchant is 2% Nital; original mangification is 50x.

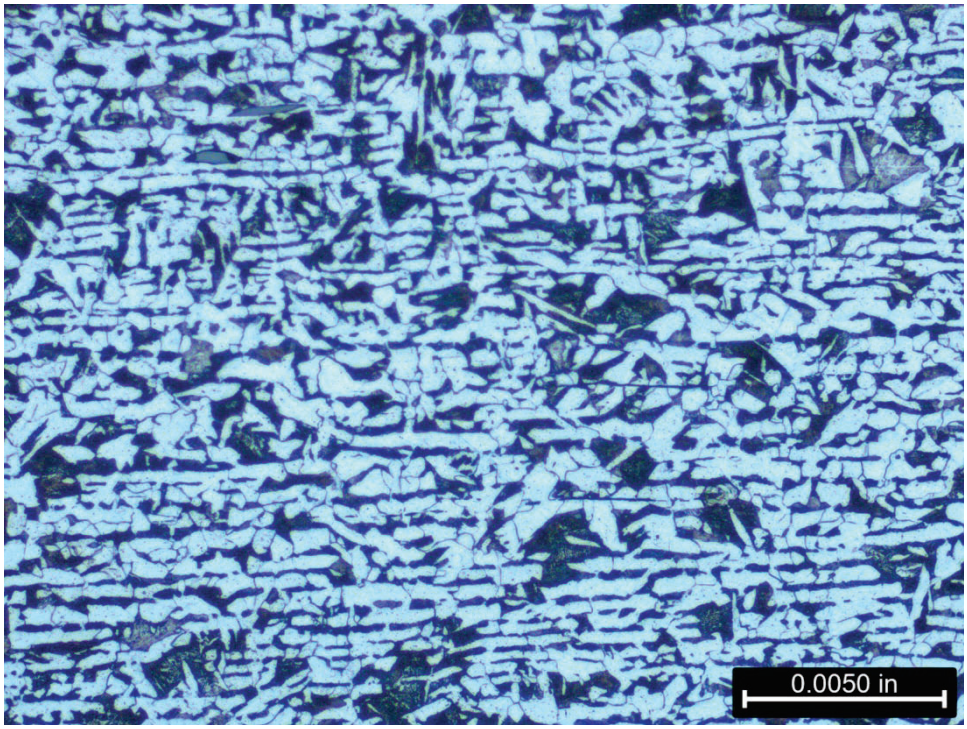

Figure 12: Photomicrograph of the base pipe material upstream of the girth weld. Etchant is 2% Nital; original mangification is 200x.

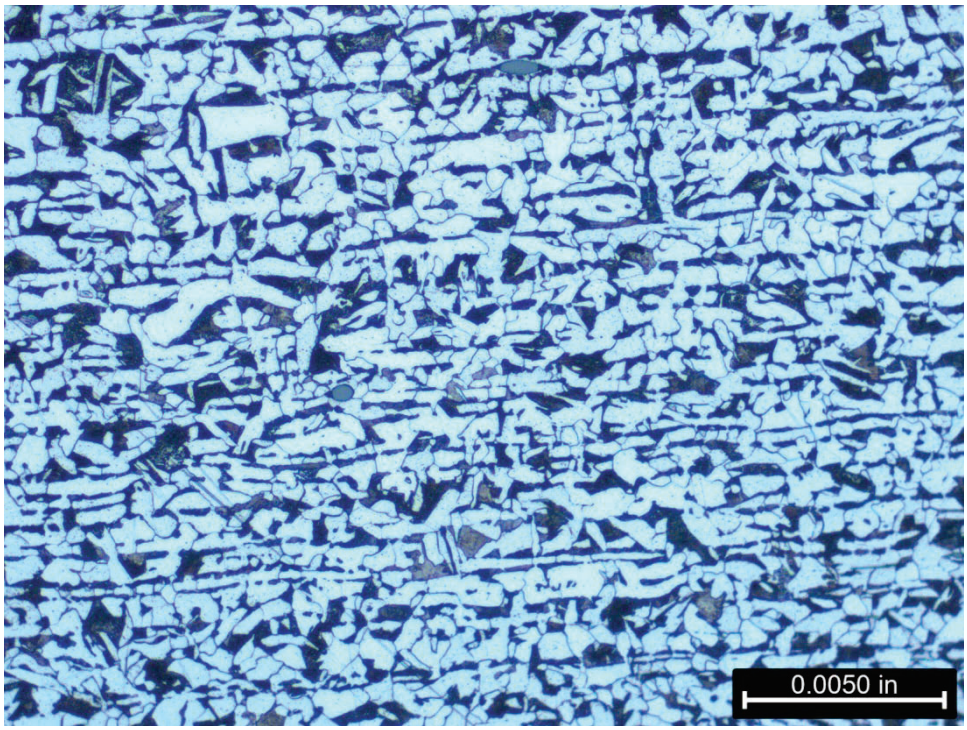

Figure 13: Photomicrograph of the base pipe material downstream of the girth weld. Etchant is 2% Nital; original mangification is 200x.

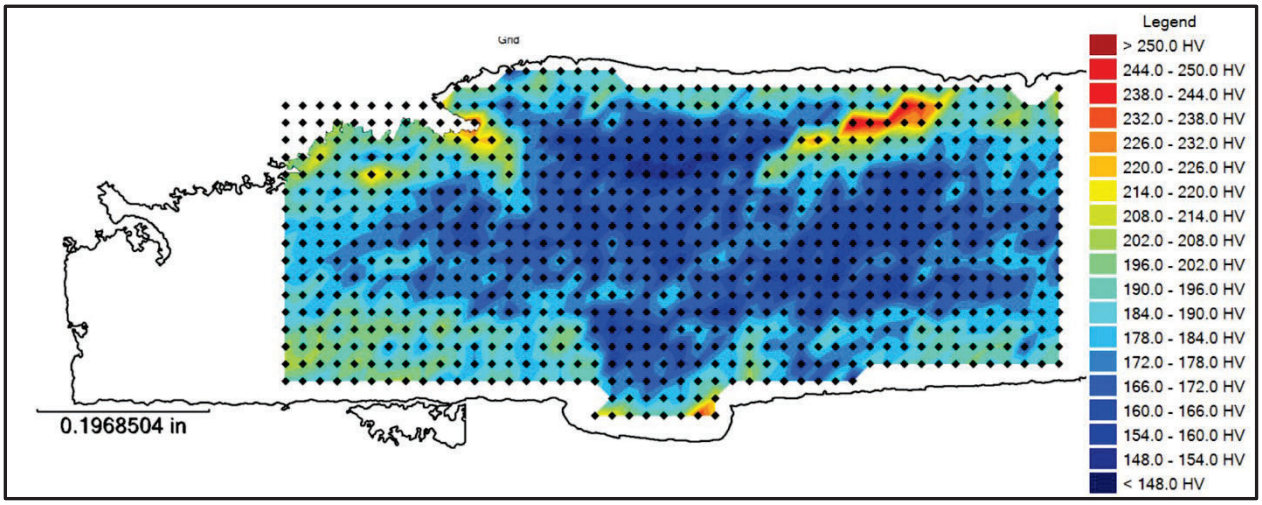

Figure 14: HV0.5 hardness map of weld, 12:00 o'clock orientation.

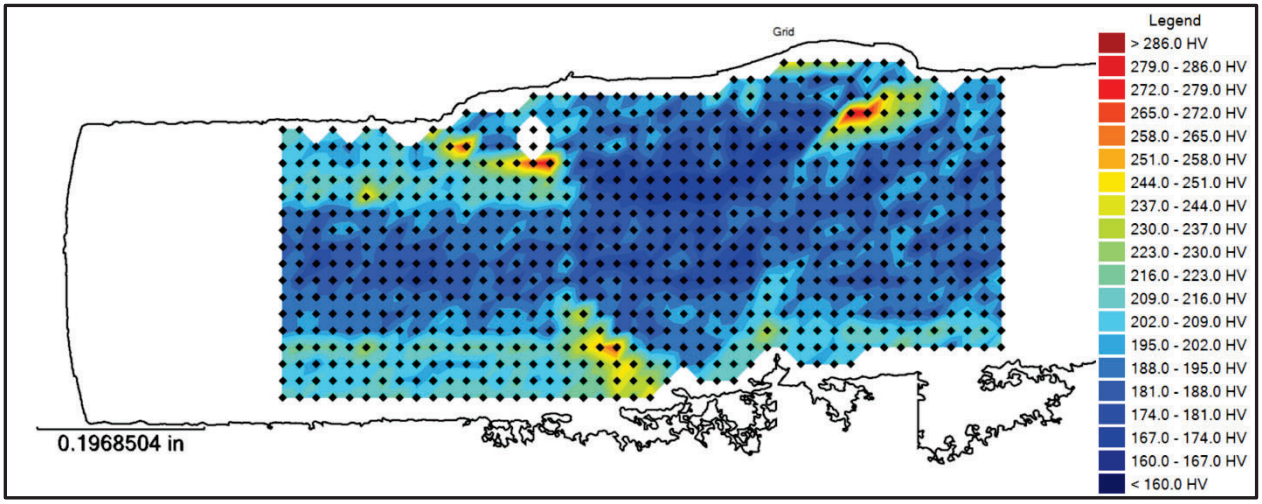

Figure 15: HV0.5 hardness map of weld, 3:00 o'clock orientation.

2.5 Calculated Tensile Strain Capacity (TSC)

ADV followed PRCI SIA-1-7 to estimate the TSC of the weld, which contains a 0.67 safety factor. The assumptions utilized in the calculations are shown in Table 4. These assumptions were based upon the test results described in the subsections above.

Load case 1 was utilized to represent a feature of similar depth to that of the failure origin. The PRCI SIA-1-7 software contains a maximum allowable aspect ratio of 12 and a maximum depth of 80% of the nominal wall thickness. Therefore, the flaw identified is outside the limits of the available industry tool. This limited the analysis to a feature that measured 6.95 mm deep (0.274 inches deep) with a length of 3.27 inches. This resulted in a feature that was slightly shallower (compared to the peak depth) and approximately half the length than found during the metallurgical examination, resulting in a TSC of 0.29. Load case 2 is based on the longest allowable feature within the PRCI SIA-1-7 software with a depth of 3.5

mm (similar to the average depth along the identified feature). Load case 3 is based on the feature length and depth identified via RT and metallography of the intact girth weld provided. These load cases are repeated with the pressure being modified from the MOP (881 psig) to the reported failure pressure (479 psig).

Table 4: Tensile Strain Capacity Inputs and Results

Input	Case					
	1	2	3	4	5	6
Pipe OD (in)	22					
Pipe WT (in)	0.344 (8.7 mm)					
Pipe Grade	Grade X46 (46 ksi yield)					
Pressure Factor	0.61 (881 psi)			0.33 (479 psi)		
Misalignment (mm)	0.80					
Weld Strength Factor	0.95					
Flaw Length (in)	3.27	1.65	0.5	3.27	1.65	0.5
Flaw Depth (mm)	6.95	3.5	1.5	6.95	3.5	1.5
CTOD (in)	0.0097 (Avg), 0.0073 (Low)					
Apparent Toughness, CTODa (in)	0.0177					
Result (TSC %)	**0.29**	**0.89**	**>2.0**	**0.35**	**1.1**	**>2.0**

APPENDIX A: HARDNESS TESTING REPORTS

Hardness Map

ADV PN 100794 12:00 o'clock

Date: 05-25-2023
Tester: Admin
Program: Hardness Map

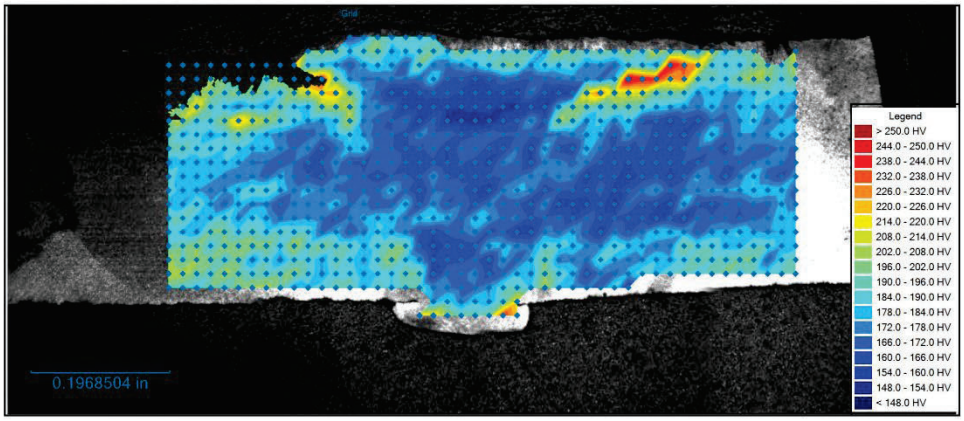

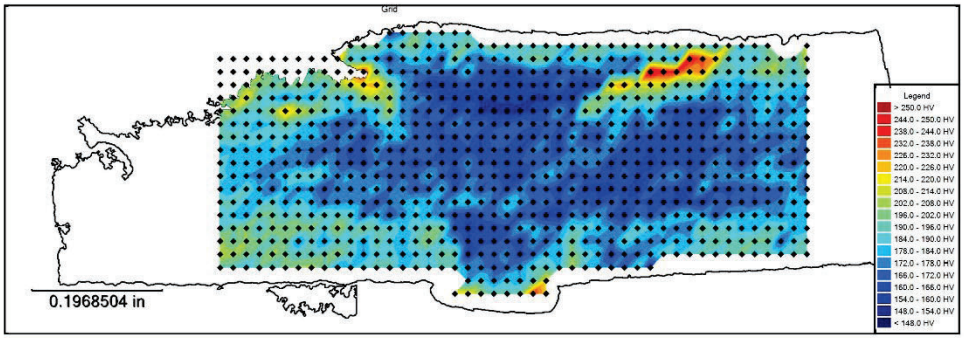

Date: 05-25-2023
Tester: Admin
Program: Hardness Map

Grid

Mean	Minimum	Maximum	Range	Std. deviation
180.3	149.4	252.2	102.9	15.9

Hardness Trace

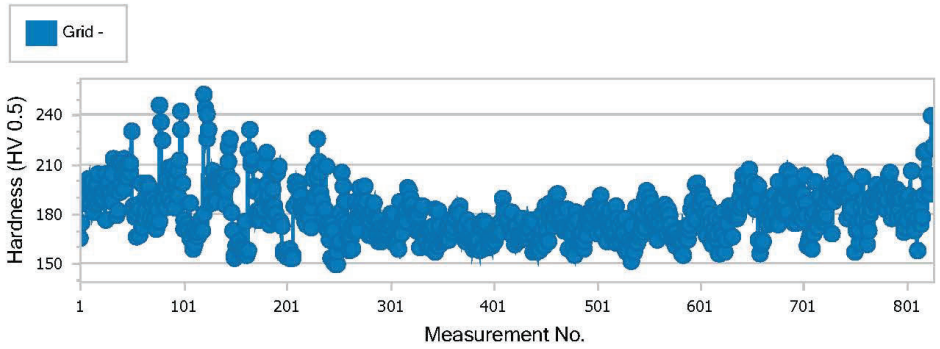

Point	Distance	Hardness	Converted	Diagonal X	Diagonal Y	Comments
1	-	165.0 HV 0.5	85.0 HRB	74.0 µm	75.9 µm	
2	-	174.1 HV 0.5	87.5 HRB	75.9 µm	70.0 µm	
3	-	197.0 HV 0.5	92.4 HRB	68.4 µm	68.8 µm	
4	-	186.1 HV 0.5	90.2 HRB	70.2 µm	70.9 µm	
5	-	192.4 HV 0.5	91.5 HRB	69.6 µm	69.2 µm	
6	-	187.2 HV 0.5	90.4 HRB	70.6 µm	70.2 µm	
7	-	188.9 HV 0.5	90.8 HRB	69.4 µm	70.7 µm	
8	-	195.5 HV 0.5	92.1 HRB	68.7 µm	69.0 µm	
9	-	201.1 HV 0.5	93.2 HRB	68.8 µm	67.0 µm	
10	-	197.8 HV 0.5	92.6 HRB	67.9 µm	69.0 µm	
11	-	186.5 HV 0.5	90.3 HRB	70.6 µm	70.5 µm	
12	-	194.9 HV 0.5	92.0 HRB	68.0 µm	70.0 µm	
13	-	199.4 HV 0.5	92.9 HRB	69.1 µm	67.2 µm	
14	-	180.5 HV 0.5	89.1 HRB	71.7 µm	71.6 µm	
15	-	185.4 HV 0.5	90.1 HRB	72.5 µm	68.9 µm	
16	-	190.6 HV 0.5	91.1 HRB	70.3 µm	69.2 µm	
17	-	197.7 HV 0.5	92.5 HRB	68.7 µm	68.3 µm	
18	-	186.8 HV 0.5	90.4 HRB	70.1 µm	70.8 µm	
19	-	203.9 HV 0.5	93.8 HRB	66.4 µm	68.4 µm	
20	-	191.6 HV 0.5	91.3 HRB	68.3 µm	70.8 µm	
21	-	191.6 HV 0.5	91.3 HRB	68.7 µm	70.5 µm	

Date: 05-25-2023
Tester: Admin
Program: Hardness Map

Point	Distance	Hardness	Converted	Diagonal X	Diagonal Y	Comments
22	-	188.2 HV 0.5	90.6 HRB	70.2 µm	70.2 µm	
23	-	189.0 HV 0.5	90.8 HRB	71.0 µm	69.1 µm	
24	-	194.1 HV 0.5	91.8 HRB	68.3 µm	69.9 µm	
25	-	176.5 HV 0.5	88.1 HRB	72.4 µm	72.6 µm	
26	-	204.2 HV 0.5	93.8 HRB	65.8 µm	68.9 µm	
27	-	196.6 HV 0.5	92.3 HRB	69.6 µm	67.7 µm	
28	-	190.7 HV 0.5	91.1 HRB	70.9 µm	68.6 µm	
29	-	199.1 HV 0.5	92.8 HRB	68.2 µm	68.3 µm	
30	-	193.2 HV 0.5	91.6 HRB	68.0 µm	70.5 µm	
31	-	204.5 HV 0.5	93.9 HRB	67.5 µm	67.2 µm	
32	-	187.4 HV 0.5	90.5 HRB	70.6 µm	70.1 µm	
33	-	213.5 HV 0.5	95.6 HRB	65.8 µm	66.0 µm	
34	-	194.6 HV 0.5	91.9 HRB	70.6 µm	67.5 µm	
35	-	194.9 HV 0.5	92.0 HRB	71.5 µm	66.4 µm	
36	-	179.4 HV 0.5	88.8 HRB	70.3 µm	73.5 µm	
37	-	211.9 HV 0.5	95.3 HRB	65.2 µm	67.1 µm	
38	-	181.6 HV 0.5	89.3 HRB	75.1 µm	67.8 µm	
39	-	192.9 HV 0.5	91.6 HRB	69.5 µm	69.2 µm	
40	-	197.5 HV 0.5	92.5 HRB	68.0 µm	69.0 µm	
41	-	211.0 HV 0.5	95.2 HRB	65.0 µm	67.6 µm	
42	-	203.7 HV 0.5	93.7 HRB	68.7 µm	66.2 µm	
43	-	212.9 HV 0.5	95.5 HRB	67.5 µm	64.5 µm	
44	-	194.5 HV 0.5	91.9 HRB	66.8 µm	71.3 µm	
45	-	205.0 HV 0.5	94.0 HRB	68.6 µm	66.0 µm	
46	-	202.5 HV 0.5	93.5 HRB	67.4 µm	67.9 µm	
47	-	202.3 HV 0.5	93.5 HRB	66.5 µm	68.9 µm	
48	-	211.2 HV 0.5	95.2 HRB	64.8 µm	67.7 µm	
49	-	204.6 HV 0.5	93.9 HRB	65.2 µm	69.4 µm	
50	-	210.9 HV 0.5	95.2 HRB	66.8 µm	65.8 µm	
51	-	230.3 HV 0.5	98.4 HRB	64.2 µm	62.7 µm	
52	-	184.5 HV 0.5	89.9 HRB	71.6 µm	70.2 µm	
53	-	181.5 HV 0.5	89.3 HRB	71.5 µm	71.4 µm	
54	-	178.0 HV 0.5	88.5 HRB	73.1 µm	71.3 µm	
55	-	165.9 HV 0.5	85.2 HRB	75.5 µm	74.0 µm	
56	-	179.5 HV 0.5	88.9 HRB	71.1 µm	72.7 µm	
57	-	185.1 HV 0.5	90.0 HRB	72.6 µm	68.9 µm	
58	-	182.4 HV 0.5	89.5 HRB	71.5 µm	71.1 µm	
59	-	166.9 HV 0.5	85.5 HRB	75.8 µm	73.3 µm	
60	-	198.8 HV 0.5	92.8 HRB	69.3 µm	67.3 µm	

Date: 05-25-2023
Tester: Admin
Program: Hardness Map

Point	Distance	Hardness	Converted	Diagonal X	Diagonal Y	Comments
61	-	173.0 HV 0.5	87.2 HRB	73.4 µm	73.0 µm	
62	-	171.5 HV 0.5	86.8 HRB	74.7 µm	72.4 µm	
63	-	176.7 HV 0.5	88.2 HRB	73.4 µm	71.4 µm	
64	-	181.8 HV 0.5	89.4 HRB	71.5 µm	71.3 µm	
65	-	189.9 HV 0.5	91.0 HRB	69.6 µm	70.2 µm	
66	-	198.4 HV 0.5	92.7 HRB	69.2 µm	67.6 µm	
67	-	196.8 HV 0.5	92.4 HRB	68.7 µm	68.6 µm	
68	-	177.4 HV 0.5	88.4 HRB	73.8 µm	70.8 µm	
69	-	189.0 HV 0.5	90.8 HRB	71.8 µm	68.3 µm	
70	-	185.6 HV 0.5	90.1 HRB	70.9 µm	70.5 µm	
71	-	189.5 HV 0.5	90.9 HRB	70.3 µm	69.6 µm	
72	-	174.3 HV 0.5	87.6 HRB	73.1 µm	72.8 µm	
73	-	177.6 HV 0.5	88.4 HRB	71.8 µm	72.7 µm	
74	-	170.4 HV 0.5	86.5 HRB	73.1 µm	74.5 µm	
75	-	186.4 HV 0.5	90.3 HRB	70.3 µm	70.8 µm	
76	-	183.2 HV 0.5	89.6 HRB	71.8 µm	70.5 µm	
77	-	174.9 HV 0.5	87.7 HRB	72.9 µm	72.7 µm	
78	-	246.0 HV 0.5	-	63.0 µm	59.8 µm	
79	-	235.3 HV 0.5	99.2 HRB	62.1 µm	63.5 µm	
80	-	224.1 HV 0.5	97.4 HRB	64.5 µm	64.1 µm	
81	-	189.2 HV 0.5	90.8 HRB	68.5 µm	71.5 µm	
82	-	188.1 HV 0.5	90.6 HRB	69.2 µm	71.2 µm	
83	-	183.6 HV 0.5	89.7 HRB	72.0 µm	70.1 µm	
84	-	196.3 HV 0.5	92.3 HRB	71.0 µm	66.5 µm	
85	-	201.3 HV 0.5	93.3 HRB	67.8 µm	67.9 µm	
86	-	189.4 HV 0.5	90.9 HRB	69.0 µm	70.9 µm	
87	-	207.6 HV 0.5	94.5 HRB	65.7 µm	67.9 µm	
88	-	198.9 HV 0.5	92.8 HRB	68.4 µm	68.1 µm	
89	-	206.3 HV 0.5	94.3 HRB	69.9 µm	64.2 µm	
90	-	186.6 HV 0.5	90.3 HRB	71.8 µm	69.1 µm	
91	-	208.4 HV 0.5	94.7 HRB	66.2 µm	67.2 µm	
92	-	198.1 HV 0.5	92.6 HRB	68.3 µm	68.6 µm	
93	-	183.8 HV 0.5	89.8 HRB	71.2 µm	70.8 µm	
94	-	200.4 HV 0.5	93.1 HRB	67.2 µm	68.9 µm	
95	-	190.9 HV 0.5	91.2 HRB	68.6 µm	70.8 µm	
96	-	205.7 HV 0.5	94.1 HRB	67.5 µm	66.8 µm	
97	-	212.7 HV 0.5	95.4 HRB	67.0 µm	65.1 µm	
98	-	231.3 HV 0.5	98.6 HRB	64.9 µm	61.7 µm	
99	-	242.1 HV 0.5	-	61.3 µm	62.5 µm	

Date: 05-25-2023
Tester: Admin
Program: Hardness Map

Point	Distance	Hardness	Converted	Diagonal X	Diagonal Y	Comments
100	-	198.7 HV 0.5	92.7 HRB	67.5 µm	69.1 µm	
101	-	176.2 HV 0.5	88.0 HRB	72.7 µm	72.4 µm	
102	-	170.4 HV 0.5	86.5 HRB	73.4 µm	74.1 µm	
103	-	171.5 HV 0.5	86.8 HRB	73.7 µm	73.3 µm	
104	-	173.0 HV 0.5	87.2 HRB	73.4 µm	73.0 µm	
105	-	173.7 HV 0.5	87.4 HRB	72.5 µm	73.7 µm	
106	-	170.0 HV 0.5	86.3 HRB	74.3 µm	73.4 µm	
107	-	186.3 HV 0.5	90.3 HRB	70.3 µm	70.8 µm	
108	-	164.7 HV 0.5	84.9 HRB	76.1 µm	74.0 µm	
109	-	164.5 HV 0.5	84.8 HRB	77.4 µm	72.8 µm	
110	-	158.6 HV 0.5	82.9 HRB	77.3 µm	75.6 µm	
111	-	161.4 HV 0.5	83.8 HRB	75.4 µm	76.2 µm	
112	-	171.5 HV 0.5	86.8 HRB	74.4 µm	72.6 µm	
113	-	167.9 HV 0.5	85.7 HRB	73.1 µm	75.6 µm	
114	-	165.9 HV 0.5	85.2 HRB	75.2 µm	74.3 µm	
115	-	168.5 HV 0.5	85.9 HRB	74.4 µm	74.0 µm	
116	-	172.6 HV 0.5	87.1 HRB	73.2 µm	73.4 µm	
117	-	174.9 HV 0.5	87.7 HRB	74.8 µm	70.8 µm	
118	-	176.0 HV 0.5	88.0 HRB	73.1 µm	72.1 µm	
119	-	169.8 HV 0.5	86.3 HRB	73.2 µm	74.6 µm	
120	-	179.7 HV 0.5	88.9 HRB	70.6 µm	73.1 µm	
121	-	252.2 HV 0.5	-	61.2 µm	60.1 µm	
122	-	243.8 HV 0.5	-	61.8 µm	61.5 µm	
123	-	240.7 HV 0.5	-	61.0 µm	63.1 µm	
124	-	225.1 HV 0.5	97.5 HRB	64.2 µm	64.1 µm	
125	-	231.1 HV 0.5	98.5 HRB	63.7 µm	63.0 µm	
126	-	196.9 HV 0.5	92.4 HRB	69.1 µm	68.2 µm	
127	-	192.1 HV 0.5	91.4 HRB	68.2 µm	70.7 µm	
128	-	186.0 HV 0.5	90.2 HRB	70.9 µm	70.3 µm	
129	-	199.9 HV 0.5	93.0 HRB	67.9 µm	68.4 µm	
130	-	205.6 HV 0.5	94.1 HRB	68.4 µm	65.9 µm	
131	-	200.6 HV 0.5	93.1 HRB	69.2 µm	66.7 µm	
132	-	187.2 HV 0.5	90.4 HRB	70.2 µm	70.5 µm	
133	-	199.3 HV 0.5	92.9 HRB	68.2 µm	68.2 µm	
134	-	199.8 HV 0.5	93.0 HRB	66.3 µm	69.9 µm	
135	-	200.3 HV 0.5	93.1 HRB	68.5 µm	67.6 µm	
136	-	202.6 HV 0.5	93.5 HRB	67.3 µm	68.1 µm	
137	-	200.0 HV 0.5	93.0 HRB	66.7 µm	69.5 µm	
138	-	194.9 HV 0.5	92.0 HRB	68.2 µm	69.7 µm	

Date: 05-25-2023
Tester: Admin
Program: Hardness Map

Point	Distance	Hardness	Converted	Diagonal X	Diagonal Y	Comments
139	-	201.0 HV 0.5	93.2 HRB	68.6 µm	67.3 µm	
140	-	200.6 HV 0.5	93.1 HRB	66.2 µm	69.7 µm	
141	-	194.6 HV 0.5	91.9 HRB	68.0 µm	70.1 µm	
142	-	185.9 HV 0.5	90.2 HRB	68.8 µm	72.5 µm	
143	-	204.0 HV 0.5	93.8 HRB	67.6 µm	67.2 µm	
144	-	211.8 HV 0.5	95.3 HRB	66.3 µm	66.0 µm	
145	-	220.6 HV 0.5	96.8 HRB	64.7 µm	65.0 µm	
146	-	225.8 HV 0.5	97.6 HRB	64.9 µm	63.2 µm	
147	-	200.4 HV 0.5	93.1 HRB	67.4 µm	68.6 µm	
148	-	180.6 HV 0.5	89.1 HRB	71.9 µm	71.4 µm	
149	-	169.5 HV 0.5	86.2 HRB	74.5 µm	73.4 µm	
150	-	152.6 HV 0.5	80.9 HRB	78.4 µm	77.5 µm	
151	-	155.0 HV 0.5	81.7 HRB	76.6 µm	78.1 µm	
152	-	160.2 HV 0.5	83.4 HRB	76.3 µm	75.8 µm	
153	-	162.5 HV 0.5	84.2 HRB	75.0 µm	76.1 µm	
154	-	163.1 HV 0.5	84.4 HRB	75.9 µm	74.9 µm	
155	-	159.6 HV 0.5	83.2 HRB	76.6 µm	75.9 µm	
156	-	156.7 HV 0.5	82.2 HRB	76.6 µm	77.2 µm	
157	-	157.4 HV 0.5	82.5 HRB	76.6 µm	76.9 µm	
158	-	158.5 HV 0.5	82.8 HRB	76.8 µm	76.2 µm	
159	-	156.7 HV 0.5	82.2 HRB	76.4 µm	77.5 µm	
160	-	174.8 HV 0.5	87.7 HRB	73.1 µm	72.6 µm	
161	-	158.1 HV 0.5	82.7 HRB	77.2 µm	76.0 µm	
162	-	154.4 HV 0.5	81.5 HRB	77.5 µm	77.5 µm	
163	-	157.6 HV 0.5	82.5 HRB	75.6 µm	77.8 µm	
164	-	218.7 HV 0.5	96.5 HRB	65.9 µm	64.4 µm	
165	-	231.4 HV 0.5	98.6 HRB	63.5 µm	63.1 µm	
166	-	209.7 HV 0.5	94.9 HRB	66.0 µm	67.0 µm	
167	-	212.4 HV 0.5	95.4 HRB	67.0 µm	65.2 µm	
168	-	213.6 HV 0.5	95.6 HRB	66.2 µm	65.6 µm	
169	-	194.0 HV 0.5	91.8 HRB	69.7 µm	68.6 µm	
170	-	196.9 HV 0.5	92.4 HRB	69.0 µm	68.2 µm	
171	-	195.0 HV 0.5	92.0 HRB	69.1 µm	68.8 µm	
172	-	176.7 HV 0.5	88.2 HRB	72.1 µm	72.8 µm	
173	-	181.9 HV 0.5	89.4 HRB	70.2 µm	72.6 µm	
174	-	177.8 HV 0.5	88.4 HRB	71.4 µm	73.0 µm	
175	-	176.2 HV 0.5	88.1 HRB	69.5 µm	75.5 µm	
176	-	181.8 HV 0.5	89.4 HRB	69.3 µm	73.6 µm	
177	-	190.6 HV 0.5	91.1 HRB	67.5 µm	72.0 µm	

Date: 05-25-2023
Tester: Admin
Program: Hardness Map

Point	Distance	Hardness	Converted	Diagonal X	Diagonal Y	Comments
178	-	184.1 HV 0.5	89.8 HRB	69.7 µm	72.2 µm	
179	-	182.9 HV 0.5	89.6 HRB	72.7 µm	69.7 µm	
180	-	209.3 HV 0.5	94.9 HRB	67.1 µm	66.0 µm	
181	-	197.8 HV 0.5	92.6 HRB	68.1 µm	68.9 µm	
182	-	216.9 HV 0.5	96.1 HRB	62.3 µm	68.4 µm	
183	-	191.4 HV 0.5	91.3 HRB	72.5 µm	66.8 µm	
184	-	183.7 HV 0.5	89.7 HRB	70.5 µm	71.6 µm	
185	-	173.0 HV 0.5	87.3 HRB	70.6 µm	75.8 µm	
186	-	183.4 HV 0.5	89.7 HRB	73.4 µm	68.8 µm	
187	-	176.3 HV 0.5	88.1 HRB	71.2 µm	73.8 µm	
188	-	194.4 HV 0.5	91.9 HRB	68.4 µm	69.7 µm	
189	-	184.7 HV 0.5	89.9 HRB	70.6 µm	71.1 µm	
190	-	180.4 HV 0.5	89.1 HRB	70.2 µm	73.2 µm	
191	-	203.8 HV 0.5	93.8 HRB	67.0 µm	67.9 µm	
192	-	205.0 HV 0.5	94.0 HRB	67.6 µm	66.9 µm	
193	-	209.1 HV 0.5	94.8 HRB	65.6 µm	67.6 µm	
194	-	174.1 HV 0.5	87.5 HRB	74.3 µm	71.7 µm	
195	-	175.0 HV 0.5	87.8 HRB	73.6 µm	71.9 µm	
196	-	172.7 HV 0.5	87.2 HRB	73.4 µm	73.1 µm	
197	-	155.9 HV 0.5	82.0 HRB	77.6 µm	76.6 µm	
198	-	157.3 HV 0.5	82.4 HRB	77.4 µm	76.2 µm	
199	-	155.7 HV 0.5	81.9 HRB	78.1 µm	76.3 µm	
200	-	155.6 HV 0.5	81.9 HRB	76.9 µm	77.5 µm	
201	-	154.1 HV 0.5	81.4 HRB	78.0 µm	77.1 µm	
202	-	155.5 HV 0.5	81.8 HRB	77.7 µm	76.7 µm	
203	-	158.2 HV 0.5	82.7 HRB	76.9 µm	76.2 µm	
204	-	152.6 HV 0.5	80.9 HRB	77.5 µm	78.4 µm	
205	-	153.0 HV 0.5	81.0 HRB	77.5 µm	78.2 µm	
206	-	155.1 HV 0.5	81.7 HRB	78.1 µm	76.5 µm	
207	-	153.0 HV 0.5	81.0 HRB	77.5 µm	78.2 µm	
208	-	184.3 HV 0.5	89.9 HRB	70.7 µm	71.2 µm	
209	-	199.4 HV 0.5	92.9 HRB	66.2 µm	70.2 µm	
210	-	197.1 HV 0.5	92.4 HRB	68.4 µm	68.8 µm	
211	-	187.3 HV 0.5	90.5 HRB	68.7 µm	72.0 µm	
212	-	198.7 HV 0.5	92.7 HRB	67.8 µm	68.8 µm	
213	-	193.8 HV 0.5	91.8 HRB	68.6 µm	69.7 µm	
214	-	190.7 HV 0.5	91.1 HRB	69.0 µm	70.5 µm	
215	-	184.3 HV 0.5	89.9 HRB	69.4 µm	72.5 µm	
216	-	182.0 HV 0.5	89.4 HRB	69.8 µm	73.0 µm	

Date: 05-25-2023
Tester: Admin
Program: Hardness Map

Point	Distance	Hardness	Converted	Diagonal X	Diagonal Y	Comments
217	-	179.1 HV 0.5	88.8 HRB	70.5 µm	73.4 µm	
218	-	175.0 HV 0.5	87.8 HRB	71.7 µm	73.8 µm	
219	-	182.8 HV 0.5	89.6 HRB	71.9 µm	70.5 µm	
220	-	173.2 HV 0.5	87.3 HRB	71.5 µm	74.8 µm	
221	-	180.9 HV 0.5	89.2 HRB	70.4 µm	72.8 µm	
222	-	184.7 HV 0.5	89.9 HRB	72.3 µm	69.4 µm	
223	-	177.3 HV 0.5	88.3 HRB	73.2 µm	71.4 µm	
224	-	183.7 HV 0.5	89.7 HRB	70.0 µm	72.0 µm	
225	-	171.4 HV 0.5	86.8 HRB	72.5 µm	74.6 µm	
226	-	201.3 HV 0.5	93.3 HRB	66.5 µm	69.2 µm	
227	-	206.8 HV 0.5	94.4 HRB	67.4 µm	66.6 µm	
228	-	190.0 HV 0.5	91.0 HRB	68.8 µm	70.9 µm	
229	-	190.0 HV 0.5	91.0 HRB	69.0 µm	70.8 µm	
230	-	201.9 HV 0.5	93.4 HRB	67.4 µm	68.1 µm	
231	-	225.5 HV 0.5	97.6 HRB	66.1 µm	62.1 µm	
232	-	211.7 HV 0.5	95.3 HRB	66.9 µm	65.5 µm	
233	-	205.3 HV 0.5	94.1 HRB	66.3 µm	68.1 µm	
234	-	192.9 HV 0.5	91.6 HRB	67.7 µm	71.0 µm	
235	-	188.5 HV 0.5	90.7 HRB	69.9 µm	70.4 µm	
236	-	180.7 HV 0.5	89.1 HRB	72.5 µm	70.8 µm	
237	-	177.3 HV 0.5	88.3 HRB	72.6 µm	72.0 µm	
238	-	182.7 HV 0.5	89.5 HRB	68.9 µm	73.6 µm	
239	-	208.4 HV 0.5	94.7 HRB	66.9 µm	66.5 µm	
240	-	174.1 HV 0.5	87.5 HRB	72.5 µm	73.5 µm	
241	-	170.1 HV 0.5	86.4 HRB	71.7 µm	75.9 µm	
242	-	164.5 HV 0.5	84.8 HRB	75.8 µm	74.3 µm	
243	-	173.4 HV 0.5	87.3 HRB	74.5 µm	71.7 µm	
244	-	153.0 HV 0.5	81.0 HRB	80.8 µm	74.9 µm	
245	-	169.6 HV 0.5	86.2 HRB	74.1 µm	73.8 µm	
246	-	150.5 HV 0.5	80.2 HRB	76.8 µm	80.2 µm	
247	-	152.0 HV 0.5	80.7 HRB	78.4 µm	77.8 µm	
248	-	149.5 HV 0.5	79.8 HRB	79.7 µm	77.8 µm	
249	-	149.4 HV 0.5	79.8 HRB	80.0 µm	77.5 µm	
250	-	156.4 HV 0.5	82.1 HRB	78.1 µm	75.9 µm	
251	-	162.1 HV 0.5	84.0 HRB	75.3 µm	76.0 µm	
252	-	180.9 HV 0.5	89.2 HRB	71.3 µm	71.8 µm	
253	-	163.0 HV 0.5	84.3 HRB	76.0 µm	74.9 µm	
254	-	204.6 HV 0.5	93.9 HRB	68.3 µm	66.4 µm	
255	-	196.8 HV 0.5	92.4 HRB	68.1 µm	69.2 µm	

Date: 05-25-2023
Tester: Admin
Program: Hardness Map

Point	Distance	Hardness	Converted	Diagonal X	Diagonal Y	Comments
256	-	175.9 HV 0.5	88.0 HRB	70.5 µm	74.7 µm	
257	-	187.2 HV 0.5	90.4 HRB	70.9 µm	69.9 µm	
258	-	174.3 HV 0.5	87.6 HRB	76.0 µm	69.8 µm	
259	-	187.5 HV 0.5	90.5 HRB	70.2 µm	70.5 µm	
260	-	164.8 HV 0.5	84.9 HRB	74.4 µm	75.7 µm	
261	-	165.2 HV 0.5	85.0 HRB	72.2 µm	77.6 µm	
262	-	157.9 HV 0.5	82.6 HRB	77.2 µm	76.1 µm	
263	-	165.1 HV 0.5	85.0 HRB	75.4 µm	74.5 µm	
264	-	158.7 HV 0.5	82.9 HRB	77.5 µm	75.4 µm	
265	-	172.1 HV 0.5	87.0 HRB	72.8 µm	74.0 µm	
266	-	169.9 HV 0.5	86.3 HRB	74.1 µm	73.7 µm	
267	-	177.2 HV 0.5	88.3 HRB	72.6 µm	72.1 µm	
268	-	186.9 HV 0.5	90.4 HRB	70.0 µm	70.8 µm	
269	-	169.6 HV 0.5	86.2 HRB	73.4 µm	74.4 µm	
270	-	178.2 HV 0.5	88.5 HRB	70.7 µm	73.6 µm	
271	-	183.1 HV 0.5	89.6 HRB	70.5 µm	71.8 µm	
272	-	195.8 HV 0.5	92.2 HRB	69.1 µm	68.5 µm	
273	-	180.9 HV 0.5	89.2 HRB	72.0 µm	71.2 µm	
274	-	187.0 HV 0.5	90.4 HRB	68.9 µm	72.0 µm	
275	-	179.8 HV 0.5	88.9 HRB	71.7 µm	71.9 µm	
276	-	183.9 HV 0.5	89.8 HRB	68.1 µm	73.9 µm	
277	-	196.8 HV 0.5	92.4 HRB	68.6 µm	68.7 µm	
278	-	187.3 HV 0.5	90.5 HRB	69.8 µm	70.9 µm	
279	-	178.6 HV 0.5	88.7 HRB	71.8 µm	72.3 µm	
280	-	176.1 HV 0.5	88.0 HRB	72.1 µm	73.0 µm	
281	-	166.9 HV 0.5	85.5 HRB	73.4 µm	75.7 µm	
282	-	167.7 HV 0.5	85.7 HRB	72.5 µm	76.2 µm	
283	-	175.2 HV 0.5	87.8 HRB	72.5 µm	73.0 µm	
284	-	181.9 HV 0.5	89.4 HRB	71.1 µm	71.8 µm	
285	-	186.8 HV 0.5	90.4 HRB	71.5 µm	69.4 µm	
286	-	177.4 HV 0.5	88.4 HRB	71.5 µm	73.1 µm	
287	-	167.4 HV 0.5	85.6 HRB	73.1 µm	75.7 µm	
288	-	166.7 HV 0.5	85.4 HRB	73.6 µm	75.6 µm	
289	-	163.4 HV 0.5	84.5 HRB	75.0 µm	75.6 µm	
290	-	176.0 HV 0.5	88.0 HRB	72.9 µm	72.2 µm	
291	-	169.2 HV 0.5	86.1 HRB	73.5 µm	74.5 µm	
292	-	171.7 HV 0.5	86.9 HRB	73.9 µm	73.1 µm	
293	-	163.4 HV 0.5	84.5 HRB	74.7 µm	76.0 µm	
294	-	165.5 HV 0.5	85.1 HRB	75.1 µm	74.6 µm	

Date: 05-25-2023
Tester: Admin
Program: Hardness Map

Point	Distance	Hardness	Converted	Diagonal X	Diagonal Y	Comments
295	-	170.9 HV 0.5	86.6 HRB	73.6 µm	73.7 µm	
296	-	166.7 HV 0.5	85.4 HRB	74.2 µm	75.0 µm	
297	-	167.0 HV 0.5	85.5 HRB	73.0 µm	76.1 µm	
298	-	167.2 HV 0.5	85.6 HRB	73.3 µm	75.6 µm	
299	-	169.5 HV 0.5	86.2 HRB	74.4 µm	73.5 µm	
300	-	172.1 HV 0.5	87.0 HRB	74.7 µm	72.1 µm	
301	-	174.5 HV 0.5	87.6 HRB	75.3 µm	70.5 µm	
302	-	179.7 HV 0.5	88.9 HRB	72.1 µm	71.6 µm	
303	-	178.4 HV 0.5	88.6 HRB	72.7 µm	71.5 µm	
304	-	162.8 HV 0.5	84.3 HRB	76.7 µm	74.3 µm	
305	-	180.2 HV 0.5	89.0 HRB	71.9 µm	71.5 µm	
306	-	168.6 HV 0.5	85.9 HRB	74.1 µm	74.2 µm	
307	-	164.4 HV 0.5	84.8 HRB	73.3 µm	76.9 µm	
308	-	162.2 HV 0.5	84.1 HRB	74.5 µm	76.7 µm	
309	-	158.4 HV 0.5	82.8 HRB	75.5 µm	77.5 µm	
310	-	169.8 HV 0.5	86.3 HRB	74.8 µm	73.0 µm	
311	-	187.2 HV 0.5	90.4 HRB	68.7 µm	72.1 µm	
312	-	168.3 HV 0.5	85.8 HRB	73.7 µm	74.7 µm	
313	-	177.5 HV 0.5	88.4 HRB	70.4 µm	74.2 µm	
314	-	177.0 HV 0.5	88.2 HRB	70.6 µm	74.2 µm	
315	-	178.1 HV 0.5	88.5 HRB	73.3 µm	71.0 µm	
316	-	182.5 HV 0.5	89.5 HRB	73.7 µm	68.8 µm	
317	-	174.8 HV 0.5	87.7 HRB	71.8 µm	73.8 µm	
318	-	196.2 HV 0.5	92.2 HRB	70.4 µm	67.1 µm	
319	-	194.0 HV 0.5	91.8 HRB	66.9 µm	71.4 µm	
320	-	185.5 HV 0.5	90.1 HRB	68.4 µm	73.0 µm	
321	-	189.1 HV 0.5	90.8 HRB	68.6 µm	71.4 µm	
322	-	183.9 HV 0.5	89.8 HRB	72.3 µm	69.7 µm	
323	-	185.5 HV 0.5	90.1 HRB	69.3 µm	72.1 µm	
324	-	180.2 HV 0.5	89.0 HRB	69.8 µm	73.6 µm	
325	-	180.4 HV 0.5	89.1 HRB	71.4 µm	72.0 µm	
326	-	176.8 HV 0.5	88.2 HRB	70.0 µm	74.9 µm	
327	-	169.9 HV 0.5	86.3 HRB	74.7 µm	73.0 µm	
328	-	179.3 HV 0.5	88.8 HRB	70.8 µm	73.1 µm	
329	-	159.5 HV 0.5	83.2 HRB	74.9 µm	77.6 µm	
330	-	169.2 HV 0.5	86.1 HRB	73.4 µm	74.6 µm	
331	-	182.7 HV 0.5	89.5 HRB	70.5 µm	72.0 µm	
332	-	184.2 HV 0.5	89.8 HRB	69.6 µm	72.3 µm	
333	-	167.1 HV 0.5	85.5 HRB	74.5 µm	74.4 µm	

Date: 05-25-2023
Tester: Admin
Program: Hardness Map

Point	Distance	Hardness	Converted	Diagonal X	Diagonal Y	Comments
334	-	166.4 HV 0.5	85.4 HRB	73.1 µm	76.2 µm	
335	-	163.1 HV 0.5	84.4 HRB	75.1 µm	75.7 µm	
336	-	164.4 HV 0.5	84.8 HRB	76.1 µm	74.1 µm	
337	-	170.8 HV 0.5	86.6 HRB	73.4 µm	74.0 µm	
338	-	159.4 HV 0.5	83.1 HRB	76.1 µm	76.4 µm	
339	-	169.0 HV 0.5	86.0 HRB	73.5 µm	74.6 µm	
340	-	171.0 HV 0.5	86.7 HRB	73.9 µm	73.4 µm	
341	-	163.4 HV 0.5	84.5 HRB	75.6 µm	75.1 µm	
342	-	160.6 HV 0.5	83.5 HRB	77.3 µm	74.6 µm	
343	-	172.7 HV 0.5	87.2 HRB	73.1 µm	73.5 µm	
344	-	156.6 HV 0.5	82.2 HRB	77.4 µm	76.5 µm	
345	-	182.4 HV 0.5	89.5 HRB	73.4 µm	69.2 µm	
346	-	163.5 HV 0.5	84.5 HRB	74.4 µm	76.2 µm	
347	-	160.2 HV 0.5	83.4 HRB	76.0 µm	76.1 µm	
348	-	182.1 HV 0.5	89.4 HRB	70.8 µm	72.0 µm	
349	-	172.0 HV 0.5	87.0 HRB	75.0 µm	71.8 µm	
350	-	164.2 HV 0.5	84.7 HRB	76.1 µm	74.2 µm	
351	-	163.1 HV 0.5	84.4 HRB	74.1 µm	76.7 µm	
352	-	166.7 HV 0.5	85.4 HRB	73.1 µm	76.0 µm	
353	-	163.3 HV 0.5	84.4 HRB	75.4 µm	75.2 µm	
354	-	164.5 HV 0.5	84.8 HRB	74.3 µm	75.9 µm	
355	-	165.1 HV 0.5	85.0 HRB	74.9 µm	75.0 µm	
356	-	171.5 HV 0.5	86.8 HRB	74.5 µm	72.6 µm	
357	-	167.2 HV 0.5	85.5 HRB	74.7 µm	74.3 µm	
358	-	164.0 HV 0.5	84.7 HRB	72.1 µm	78.3 µm	
359	-	176.7 HV 0.5	88.2 HRB	71.4 µm	73.5 µm	
360	-	169.6 HV 0.5	86.2 HRB	71.2 µm	76.7 µm	
361	-	169.0 HV 0.5	86.0 HRB	71.1 µm	77.0 µm	
362	-	172.8 HV 0.5	87.2 HRB	71.5 µm	75.0 µm	
363	-	171.3 HV 0.5	86.8 HRB	73.2 µm	74.0 µm	
364	-	176.9 HV 0.5	88.2 HRB	71.6 µm	73.2 µm	
365	-	182.1 HV 0.5	89.4 HRB	71.2 µm	71.5 µm	
366	-	182.2 HV 0.5	89.4 HRB	70.8 µm	71.9 µm	
367	-	180.1 HV 0.5	89.0 HRB	70.5 µm	73.0 µm	
368	-	184.5 HV 0.5	89.9 HRB	69.5 µm	72.3 µm	
369	-	180.2 HV 0.5	89.0 HRB	72.4 µm	71.1 µm	
370	-	171.5 HV 0.5	86.8 HRB	72.5 µm	74.5 µm	
371	-	171.9 HV 0.5	87.0 HRB	73.7 µm	73.2 µm	
372	-	165.8 HV 0.5	85.2 HRB	74.3 µm	75.3 µm	

Date: 05-25-2023
Tester: Admin
Program: Hardness Map

Point	Distance	Hardness	Converted	Diagonal X	Diagonal Y	Comments
373	-	171.8 HV 0.5	86.9 HRB	75.0 µm	71.9 µm	
374	-	163.4 HV 0.5	84.5 HRB	73.4 µm	77.3 µm	
375	-	165.9 HV 0.5	85.2 HRB	74.8 µm	74.8 µm	
376	-	176.5 HV 0.5	88.1 HRB	73.0 µm	72.0 µm	
377	-	164.9 HV 0.5	85.0 HRB	73.7 µm	76.2 µm	
378	-	164.3 HV 0.5	84.8 HRB	75.5 µm	74.8 µm	
379	-	169.5 HV 0.5	86.2 HRB	73.9 µm	74.0 µm	
380	-	172.8 HV 0.5	87.2 HRB	73.2 µm	73.3 µm	
381	-	163.7 HV 0.5	84.6 HRB	74.3 µm	76.2 µm	
382	-	158.7 HV 0.5	82.9 HRB	75.9 µm	77.0 µm	
383	-	164.7 HV 0.5	84.9 HRB	76.3 µm	73.8 µm	
384	-	159.2 HV 0.5	83.1 HRB	76.6 µm	76.0 µm	
385	-	166.4 HV 0.5	85.4 HRB	75.2 µm	74.1 µm	
386	-	164.0 HV 0.5	84.7 HRB	74.7 µm	75.7 µm	
387	-	157.9 HV 0.5	82.6 HRB	75.5 µm	77.8 µm	
388	-	173.8 HV 0.5	87.5 HRB	72.7 µm	73.3 µm	
389	-	171.3 HV 0.5	86.8 HRB	74.0 µm	73.2 µm	
390	-	158.3 HV 0.5	82.8 HRB	76.3 µm	76.8 µm	
391	-	175.0 HV 0.5	87.7 HRB	72.3 µm	73.3 µm	
392	-	175.0 HV 0.5	87.8 HRB	73.5 µm	72.0 µm	
393	-	170.2 HV 0.5	86.4 HRB	73.7 µm	73.9 µm	
394	-	174.4 HV 0.5	87.6 HRB	71.9 µm	73.9 µm	
395	-	163.8 HV 0.5	84.6 HRB	74.8 µm	75.6 µm	
396	-	161.4 HV 0.5	83.8 HRB	76.3 µm	75.2 µm	
397	-	159.3 HV 0.5	83.1 HRB	76.1 µm	76.5 µm	
398	-	165.5 HV 0.5	85.1 HRB	73.7 µm	76.0 µm	
399	-	160.3 HV 0.5	83.4 HRB	73.6 µm	78.5 µm	
400	-	161.8 HV 0.5	83.9 HRB	76.1 µm	75.2 µm	
401	-	166.1 HV 0.5	85.3 HRB	73.8 µm	75.7 µm	
402	-	163.4 HV 0.5	84.5 HRB	74.9 µm	75.8 µm	
403	-	170.0 HV 0.5	86.3 HRB	74.7 µm	73.0 µm	
404	-	167.4 HV 0.5	85.6 HRB	75.9 µm	72.9 µm	
405	-	168.5 HV 0.5	85.9 HRB	73.4 µm	75.0 µm	
406	-	172.2 HV 0.5	87.0 HRB	71.9 µm	74.8 µm	
407	-	174.2 HV 0.5	87.5 HRB	72.9 µm	73.1 µm	
408	-	172.8 HV 0.5	87.2 HRB	73.0 µm	73.5 µm	
409	-	168.9 HV 0.5	86.0 HRB	75.9 µm	72.3 µm	
410	-	189.2 HV 0.5	90.8 HRB	69.6 µm	70.5 µm	
411	-	179.0 HV 0.5	88.7 HRB	71.3 µm	72.6 µm	

Date: 05-25-2023
Tester: Admin
Program: Hardness Map

Point	Distance	Hardness	Converted	Diagonal X	Diagonal Y	Comments
412	-	182.6 HV 0.5	89.5 HRB	71.7 µm	70.9 µm	
413	-	182.2 HV 0.5	89.4 HRB	70.7 µm	72.0 µm	
414	-	175.7 HV 0.5	87.9 HRB	70.6 µm	74.7 µm	
415	-	174.1 HV 0.5	87.5 HRB	72.6 µm	73.3 µm	
416	-	175.2 HV 0.5	87.8 HRB	70.4 µm	75.1 µm	
417	-	169.1 HV 0.5	86.0 HRB	72.6 µm	75.5 µm	
418	-	180.9 HV 0.5	89.2 HRB	71.0 µm	72.2 µm	
419	-	170.8 HV 0.5	86.6 HRB	73.1 µm	74.3 µm	
420	-	166.3 HV 0.5	85.3 HRB	73.7 µm	75.6 µm	
421	-	161.8 HV 0.5	83.9 HRB	74.9 µm	76.5 µm	
422	-	172.6 HV 0.5	87.2 HRB	72.6 µm	73.9 µm	
423	-	172.8 HV 0.5	87.2 HRB	71.3 µm	75.2 µm	
424	-	166.7 HV 0.5	85.4 HRB	73.8 µm	75.3 µm	
425	-	162.8 HV 0.5	84.3 HRB	77.0 µm	74.0 µm	
426	-	166.3 HV 0.5	85.3 HRB	74.3 µm	75.0 µm	
427	-	166.7 HV 0.5	85.4 HRB	75.7 µm	73.4 µm	
428	-	164.6 HV 0.5	84.9 HRB	75.0 µm	75.2 µm	
429	-	177.3 HV 0.5	88.3 HRB	73.4 µm	71.3 µm	
430	-	164.7 HV 0.5	84.9 HRB	73.8 µm	76.2 µm	
431	-	165.1 HV 0.5	85.0 HRB	75.3 µm	74.6 µm	
432	-	165.4 HV 0.5	85.1 HRB	74.4 µm	75.3 µm	
433	-	165.1 HV 0.5	85.0 HRB	75.0 µm	74.9 µm	
434	-	167.8 HV 0.5	85.7 HRB	73.8 µm	74.9 µm	
435	-	170.7 HV 0.5	86.6 HRB	73.3 µm	74.1 µm	
436	-	176.3 HV 0.5	88.1 HRB	72.2 µm	72.9 µm	
437	-	171.0 HV 0.5	86.7 HRB	73.3 µm	74.0 µm	
438	-	176.3 HV 0.5	88.1 HRB	72.8 µm	72.3 µm	
439	-	175.1 HV 0.5	87.8 HRB	72.8 µm	72.7 µm	
440	-	156.7 HV 0.5	82.2 HRB	78.0 µm	75.8 µm	
441	-	165.0 HV 0.5	85.0 HRB	73.1 µm	76.8 µm	
442	-	161.6 HV 0.5	83.9 HRB	74.2 µm	77.3 µm	
443	-	156.3 HV 0.5	82.1 HRB	75.9 µm	78.2 µm	
444	-	161.9 HV 0.5	84.0 HRB	75.2 µm	76.2 µm	
445	-	165.3 HV 0.5	85.1 HRB	73.9 µm	75.9 µm	
446	-	157.5 HV 0.5	82.5 HRB	75.8 µm	77.7 µm	
447	-	163.1 HV 0.5	84.4 HRB	74.6 µm	76.2 µm	
448	-	179.8 HV 0.5	89.0 HRB	71.5 µm	72.1 µm	
449	-	171.0 HV 0.5	86.7 HRB	72.4 µm	74.9 µm	
450	-	160.4 HV 0.5	83.5 HRB	75.0 µm	77.0 µm	

Date: 05-25-2023
Tester: Admin
Program: Hardness Map

Point	Distance	Hardness	Converted	Diagonal X	Diagonal Y	Comments
451	-	174.5 HV 0.5	87.6 HRB	72.3 µm	73.5 µm	
452	-	184.1 HV 0.5	89.8 HRB	71.5 µm	70.4 µm	
453	-	169.4 HV 0.5	86.1 HRB	72.5 µm	75.4 µm	
454	-	163.2 HV 0.5	84.4 HRB	73.4 µm	77.3 µm	
455	-	178.6 HV 0.5	88.6 HRB	71.8 µm	72.3 µm	
456	-	186.8 HV 0.5	90.4 HRB	71.9 µm	69.0 µm	
457	-	181.8 HV 0.5	89.4 HRB	72.0 µm	70.8 µm	
458	-	178.5 HV 0.5	88.6 HRB	71.1 µm	73.1 µm	
459	-	173.0 HV 0.5	87.2 HRB	71.2 µm	75.2 µm	
460	-	178.5 HV 0.5	88.6 HRB	72.1 µm	72.1 µm	
461	-	182.4 HV 0.5	89.5 HRB	70.8 µm	71.8 µm	
462	-	191.3 HV 0.5	91.3 HRB	71.5 µm	67.8 µm	
463	-	191.7 HV 0.5	91.3 HRB	68.7 µm	70.4 µm	
464	-	182.9 HV 0.5	89.6 HRB	71.3 µm	71.1 µm	
465	-	174.4 HV 0.5	87.6 HRB	72.9 µm	72.9 µm	
466	-	180.9 HV 0.5	89.2 HRB	71.7 µm	71.5 µm	
467	-	175.2 HV 0.5	87.8 HRB	72.0 µm	73.5 µm	
468	-	171.5 HV 0.5	86.8 HRB	73.1 µm	74.0 µm	
469	-	169.5 HV 0.5	86.2 HRB	72.4 µm	75.5 µm	
470	-	171.6 HV 0.5	86.9 HRB	73.5 µm	73.5 µm	
471	-	169.6 HV 0.5	86.2 HRB	73.9 µm	74.0 µm	
472	-	182.5 HV 0.5	89.5 HRB	71.2 µm	71.3 µm	
473	-	168.7 HV 0.5	85.9 HRB	74.0 µm	74.3 µm	
474	-	158.5 HV 0.5	82.8 HRB	76.1 µm	76.9 µm	
475	-	171.9 HV 0.5	87.0 HRB	74.6 µm	72.3 µm	
476	-	170.9 HV 0.5	86.6 HRB	74.3 µm	73.0 µm	
477	-	166.8 HV 0.5	85.4 HRB	75.2 µm	73.9 µm	
478	-	160.0 HV 0.5	83.3 HRB	76.4 µm	75.9 µm	
479	-	155.3 HV 0.5	81.8 HRB	73.1 µm	81.4 µm	
480	-	173.7 HV 0.5	87.4 HRB	74.0 µm	72.1 µm	
481	-	180.5 HV 0.5	89.1 HRB	72.6 µm	70.8 µm	
482	-	176.5 HV 0.5	88.1 HRB	73.7 µm	71.3 µm	
483	-	162.2 HV 0.5	84.1 HRB	76.3 µm	74.9 µm	
484	-	167.2 HV 0.5	85.5 HRB	72.3 µm	76.6 µm	
485	-	165.2 HV 0.5	85.1 HRB	72.8 µm	77.0 µm	
486	-	162.3 HV 0.5	84.1 HRB	75.3 µm	75.9 µm	
487	-	168.7 HV 0.5	85.9 HRB	72.9 µm	75.4 µm	
488	-	158.6 HV 0.5	82.9 HRB	77.5 µm	75.4 µm	
489	-	163.5 HV 0.5	84.5 HRB	74.7 µm	75.9 µm	

Date: 05-25-2023
Tester: Admin
Program: Hardness Map

Point	Distance	Hardness	Converted	Diagonal X	Diagonal Y	Comments
490	-	173.5 HV 0.5	87.4 HRB	74.6 µm	71.6 µm	
491	-	180.0 HV 0.5	89.0 HRB	71.4 µm	72.1 µm	
492	-	166.7 HV 0.5	85.4 HRB	72.3 µm	76.8 µm	
493	-	173.4 HV 0.5	87.4 HRB	69.6 µm	76.6 µm	
494	-	175.3 HV 0.5	87.8 HRB	72.0 µm	73.5 µm	
495	-	179.8 HV 0.5	89.0 HRB	71.3 µm	72.3 µm	
496	-	178.1 HV 0.5	88.5 HRB	73.7 µm	70.6 µm	
497	-	179.0 HV 0.5	88.8 HRB	72.5 µm	71.5 µm	
498	-	184.7 HV 0.5	89.9 HRB	70.2 µm	71.5 µm	
499	-	183.9 HV 0.5	89.8 HRB	69.2 µm	72.8 µm	
500	-	184.5 HV 0.5	89.9 HRB	70.6 µm	71.2 µm	
501	-	167.6 HV 0.5	85.6 HRB	75.7 µm	73.0 µm	
502	-	181.9 HV 0.5	89.4 HRB	70.5 µm	72.3 µm	
503	-	177.2 HV 0.5	88.3 HRB	71.0 µm	73.6 µm	
504	-	191.1 HV 0.5	91.2 HRB	69.1 µm	70.2 µm	
505	-	179.3 HV 0.5	88.8 HRB	70.1 µm	73.7 µm	
506	-	168.8 HV 0.5	86.0 HRB	75.3 µm	73.0 µm	
507	-	182.4 HV 0.5	89.5 HRB	69.7 µm	72.9 µm	
508	-	175.4 HV 0.5	87.9 HRB	72.7 µm	72.7 µm	
509	-	176.7 HV 0.5	88.2 HRB	72.2 µm	72.7 µm	
510	-	163.3 HV 0.5	84.4 HRB	75.4 µm	75.2 µm	
511	-	175.7 HV 0.5	87.9 HRB	71.0 µm	74.2 µm	
512	-	171.5 HV 0.5	86.8 HRB	71.2 µm	75.8 µm	
513	-	176.0 HV 0.5	88.0 HRB	71.8 µm	73.4 µm	
514	-	181.6 HV 0.5	89.3 HRB	72.2 µm	70.7 µm	
515	-	171.0 HV 0.5	86.7 HRB	72.2 µm	75.1 µm	
516	-	174.3 HV 0.5	87.6 HRB	74.0 µm	71.9 µm	
517	-	165.8 HV 0.5	85.2 HRB	76.4 µm	73.1 µm	
518	-	167.7 HV 0.5	85.7 HRB	73.5 µm	75.2 µm	
519	-	184.3 HV 0.5	89.9 HRB	71.6 µm	70.3 µm	
520	-	162.7 HV 0.5	84.2 HRB	75.3 µm	75.7 µm	
521	-	177.2 HV 0.5	88.3 HRB	71.6 µm	73.1 µm	
522	-	164.6 HV 0.5	84.9 HRB	74.9 µm	75.2 µm	
523	-	172.6 HV 0.5	87.2 HRB	73.0 µm	73.6 µm	
524	-	162.7 HV 0.5	84.2 HRB	75.2 µm	75.8 µm	
525	-	175.1 HV 0.5	87.8 HRB	73.4 µm	72.1 µm	
526	-	166.7 HV 0.5	85.4 HRB	74.4 µm	74.8 µm	
527	-	168.1 HV 0.5	85.8 HRB	73.1 µm	75.4 µm	
528	-	158.8 HV 0.5	82.9 HRB	75.5 µm	77.3 µm	

Date: 05-25-2023
Tester: Admin
Program: Hardness Map

Point	Distance	Hardness	Converted	Diagonal X	Diagonal Y	Comments
529	-	176.9 HV 0.5	88.2 HRB	73.0 µm	71.7 µm	
530	-	156.6 HV 0.5	82.2 HRB	76.6 µm	77.3 µm	
531	-	157.9 HV 0.5	82.6 HRB	75.8 µm	77.5 µm	
532	-	157.3 HV 0.5	82.4 HRB	76.2 µm	77.3 µm	
533	-	163.8 HV 0.5	84.6 HRB	74.9 µm	75.6 µm	
534	-	151.6 HV 0.5	80.5 HRB	75.5 µm	80.9 µm	
535	-	172.5 HV 0.5	87.1 HRB	73.8 µm	72.8 µm	
536	-	162.8 HV 0.5	84.3 HRB	73.6 µm	77.4 µm	
537	-	161.2 HV 0.5	83.7 HRB	74.4 µm	77.3 µm	
538	-	156.5 HV 0.5	82.2 HRB	77.1 µm	76.9 µm	
539	-	183.9 HV 0.5	89.8 HRB	70.6 µm	71.4 µm	
540	-	164.6 HV 0.5	84.9 HRB	73.6 µm	76.5 µm	
541	-	162.7 HV 0.5	84.2 HRB	74.4 µm	76.6 µm	
542	-	167.7 HV 0.5	85.7 HRB	73.6 µm	75.1 µm	
543	-	166.4 HV 0.5	85.4 HRB	72.5 µm	76.7 µm	
544	-	172.7 HV 0.5	87.2 HRB	73.0 µm	73.5 µm	
545	-	168.7 HV 0.5	85.9 HRB	73.9 µm	74.3 µm	
546	-	180.4 HV 0.5	89.1 HRB	69.9 µm	73.5 µm	
547	-	172.0 HV 0.5	87.0 HRB	70.6 µm	76.2 µm	
548	-	190.2 HV 0.5	91.0 HRB	67.5 µm	72.2 µm	
549	-	193.4 HV 0.5	91.7 HRB	67.8 µm	70.7 µm	
550	-	182.3 HV 0.5	89.5 HRB	68.3 µm	74.3 µm	
551	-	183.4 HV 0.5	89.7 HRB	71.1 µm	71.1 µm	
552	-	190.2 HV 0.5	91.0 HRB	68.4 µm	71.2 µm	
553	-	175.1 HV 0.5	87.8 HRB	70.2 µm	75.3 µm	
554	-	186.9 HV 0.5	90.4 HRB	69.2 µm	71.7 µm	
555	-	181.1 HV 0.5	89.2 HRB	70.7 µm	72.4 µm	
556	-	171.4 HV 0.5	86.8 HRB	72.2 µm	74.9 µm	
557	-	175.3 HV 0.5	87.8 HRB	71.8 µm	73.7 µm	
558	-	177.5 HV 0.5	88.4 HRB	71.2 µm	73.3 µm	
559	-	173.8 HV 0.5	87.5 HRB	71.4 µm	74.7 µm	
560	-	163.9 HV 0.5	84.6 HRB	72.9 µm	77.5 µm	
561	-	174.0 HV 0.5	87.5 HRB	72.0 µm	74.0 µm	
562	-	179.8 HV 0.5	88.9 HRB	71.7 µm	71.9 µm	
563	-	183.7 HV 0.5	89.7 HRB	71.5 µm	70.5 µm	
564	-	182.7 HV 0.5	89.5 HRB	71.1 µm	71.4 µm	
565	-	171.6 HV 0.5	86.9 HRB	73.9 µm	73.1 µm	
566	-	183.4 HV 0.5	89.7 HRB	70.6 µm	71.6 µm	
567	-	185.6 HV 0.5	90.1 HRB	70.9 µm	70.5 µm	

Date: 05-25-2023
Tester: Admin
Program: Hardness Map

Point	Distance	Hardness	Converted	Diagonal X	Diagonal Y	Comments
568	-	181.4 HV 0.5	89.3 HRB	71.1 µm	71.9 µm	
569	-	168.2 HV 0.5	85.8 HRB	74.2 µm	74.3 µm	
570	-	182.8 HV 0.5	89.6 HRB	70.8 µm	71.6 µm	
571	-	179.4 HV 0.5	88.8 HRB	72.0 µm	71.8 µm	
572	-	170.6 HV 0.5	86.5 HRB	73.7 µm	73.7 µm	
573	-	173.5 HV 0.5	87.4 HRB	73.2 µm	73.0 µm	
574	-	164.3 HV 0.5	84.8 HRB	75.4 µm	74.9 µm	
575	-	167.1 HV 0.5	85.5 HRB	75.3 µm	73.7 µm	
576	-	169.1 HV 0.5	86.0 HRB	73.5 µm	74.6 µm	
577	-	160.9 HV 0.5	83.6 HRB	76.6 µm	75.2 µm	
578	-	169.1 HV 0.5	86.0 HRB	73.8 µm	74.3 µm	
579	-	164.2 HV 0.5	84.7 HRB	75.4 µm	74.9 µm	
580	-	165.3 HV 0.5	85.1 HRB	75.2 µm	74.6 µm	
581	-	162.7 HV 0.5	84.2 HRB	74.8 µm	76.2 µm	
582	-	163.7 HV 0.5	84.6 HRB	75.6 µm	74.9 µm	
583	-	155.9 HV 0.5	82.0 HRB	75.5 µm	78.7 µm	
584	-	163.0 HV 0.5	84.3 HRB	74.9 µm	75.9 µm	
585	-	155.1 HV 0.5	81.7 HRB	79.0 µm	75.6 µm	
586	-	172.0 HV 0.5	87.0 HRB	72.0 µm	74.8 µm	
587	-	166.8 HV 0.5	85.4 HRB	72.0 µm	77.1 µm	
588	-	169.0 HV 0.5	86.0 HRB	74.7 µm	73.4 µm	
589	-	164.6 HV 0.5	84.9 HRB	75.0 µm	75.1 µm	
590	-	170.0 HV 0.5	86.3 HRB	71.5 µm	76.2 µm	
591	-	173.8 HV 0.5	87.4 HRB	72.5 µm	73.6 µm	
592	-	183.2 HV 0.5	89.6 HRB	72.1 µm	70.2 µm	
593	-	184.3 HV 0.5	89.9 HRB	71.5 µm	70.4 µm	
594	-	187.3 HV 0.5	90.5 HRB	68.9 µm	71.8 µm	
595	-	182.2 HV 0.5	89.4 HRB	70.0 µm	72.7 µm	
596	-	176.6 HV 0.5	88.2 HRB	71.0 µm	73.9 µm	
597	-	197.5 HV 0.5	92.5 HRB	69.7 µm	67.3 µm	
598	-	198.1 HV 0.5	92.6 HRB	67.7 µm	69.1 µm	
599	-	185.6 HV 0.5	90.1 HRB	70.9 µm	70.5 µm	
600	-	193.3 HV 0.5	91.7 HRB	69.1 µm	69.4 µm	
601	-	185.2 HV 0.5	90.0 HRB	71.1 µm	70.4 µm	
602	-	192.0 HV 0.5	91.4 HRB	70.1 µm	68.9 µm	
603	-	189.3 HV 0.5	90.9 HRB	70.0 µm	69.9 µm	
604	-	189.1 HV 0.5	90.8 HRB	69.8 µm	70.2 µm	
605	-	169.9 HV 0.5	86.3 HRB	73.4 µm	74.4 µm	
606	-	181.0 HV 0.5	89.2 HRB	71.4 µm	71.7 µm	

Date: 05-25-2023
Tester: Admin
Program: Hardness Map

Point	Distance	Hardness	Converted	Diagonal X	Diagonal Y	Comments
607	-	166.6 HV 0.5	85.4 HRB	71.4 µm	77.8 µm	
608	-	175.1 HV 0.5	87.8 HRB	71.4 µm	74.1 µm	
609	-	184.9 HV 0.5	90.0 HRB	70.1 µm	71.5 µm	
610	-	179.5 HV 0.5	88.9 HRB	73.4 µm	70.3 µm	
611	-	174.1 HV 0.5	87.5 HRB	70.0 µm	76.0 µm	
612	-	163.1 HV 0.5	84.4 HRB	76.3 µm	74.5 µm	
613	-	161.0 HV 0.5	83.7 HRB	75.1 µm	76.7 µm	
614	-	167.0 HV 0.5	85.5 HRB	75.2 µm	73.8 µm	
615	-	170.3 HV 0.5	86.4 HRB	71.6 µm	75.9 µm	
616	-	176.9 HV 0.5	88.2 HRB	73.7 µm	71.1 µm	
617	-	163.7 HV 0.5	84.6 HRB	73.7 µm	76.8 µm	
618	-	167.7 HV 0.5	85.7 HRB	76.3 µm	72.4 µm	
619	-	155.8 HV 0.5	81.9 HRB	76.5 µm	77.8 µm	
620	-	156.0 HV 0.5	82.0 HRB	75.0 µm	79.2 µm	
621	-	175.0 HV 0.5	87.7 HRB	73.0 µm	72.6 µm	
622	-	170.4 HV 0.5	86.5 HRB	74.2 µm	73.3 µm	
623	-	180.6 HV 0.5	89.1 HRB	71.6 µm	71.7 µm	
624	-	166.6 HV 0.5	85.4 HRB	74.8 µm	74.4 µm	
625	-	156.6 HV 0.5	82.2 HRB	78.3 µm	75.6 µm	
626	-	174.6 HV 0.5	87.7 HRB	71.5 µm	74.2 µm	
627	-	163.7 HV 0.5	84.6 HRB	76.2 µm	74.3 µm	
628	-	174.5 HV 0.5	87.6 HRB	71.5 µm	74.3 µm	
629	-	184.4 HV 0.5	89.9 HRB	69.5 µm	72.3 µm	
630	-	182.9 HV 0.5	89.6 HRB	71.4 µm	71.0 µm	
631	-	179.7 HV 0.5	88.9 HRB	69.6 µm	74.1 µm	
632	-	165.7 HV 0.5	85.2 HRB	74.4 µm	75.2 µm	
633	-	179.0 HV 0.5	88.8 HRB	72.0 µm	71.9 µm	
634	-	180.0 HV 0.5	89.0 HRB	69.6 µm	74.0 µm	
635	-	185.7 HV 0.5	90.1 HRB	69.9 µm	71.4 µm	
636	-	178.7 HV 0.5	88.7 HRB	72.5 µm	71.6 µm	
637	-	176.7 HV 0.5	88.2 HRB	71.9 µm	73.0 µm	
638	-	178.6 HV 0.5	88.7 HRB	69.3 µm	74.8 µm	
639	-	183.4 HV 0.5	89.7 HRB	70.7 µm	71.5 µm	
640	-	190.5 HV 0.5	91.1 HRB	69.3 µm	70.3 µm	
641	-	195.3 HV 0.5	92.1 HRB	66.7 µm	71.1 µm	
642	-	203.0 HV 0.5	93.6 HRB	68.1 µm	67.1 µm	
643	-	185.1 HV 0.5	90.0 HRB	72.0 µm	69.6 µm	
644	-	199.9 HV 0.5	93.0 HRB	67.8 µm	68.4 µm	
645	-	201.5 HV 0.5	93.3 HRB	68.5 µm	67.1 µm	

Date: 05-25-2023
Tester: Admin
Program: Hardness Map

Point	Distance	Hardness	Converted	Diagonal X	Diagonal Y	Comments
646	-	201.3 HV 0.5	93.3 HRB	65.9 µm	69.8 µm	
647	-	200.8 HV 0.5	93.2 HRB	67.8 µm	68.1 µm	
648	-	185.6 HV 0.5	90.1 HRB	70.2 µm	71.2 µm	
649	-	207.1 HV 0.5	94.4 HRB	66.1 µm	67.7 µm	
650	-	189.7 HV 0.5	90.9 HRB	70.1 µm	69.8 µm	
651	-	199.7 HV 0.5	92.9 HRB	67.7 µm	68.6 µm	
652	-	191.8 HV 0.5	91.4 HRB	71.8 µm	67.2 µm	
653	-	190.9 HV 0.5	91.2 HRB	71.5 µm	67.9 µm	
654	-	182.4 HV 0.5	89.5 HRB	68.3 µm	74.3 µm	
655	-	187.5 HV 0.5	90.5 HRB	71.2 µm	69.4 µm	
656	-	197.3 HV 0.5	92.5 HRB	68.6 µm	68.5 µm	
657	-	197.1 HV 0.5	92.4 HRB	69.7 µm	67.5 µm	
658	-	164.5 HV 0.5	84.8 HRB	74.1 µm	76.1 µm	
659	-	155.9 HV 0.5	82.0 HRB	76.9 µm	77.3 µm	
660	-	161.5 HV 0.5	83.8 HRB	74.1 µm	77.4 µm	
661	-	161.0 HV 0.5	83.7 HRB	75.1 µm	76.7 µm	
662	-	163.5 HV 0.5	84.5 HRB	73.8 µm	76.8 µm	
663	-	182.1 HV 0.5	89.4 HRB	71.1 µm	71.7 µm	
664	-	181.0 HV 0.5	89.2 HRB	71.0 µm	72.2 µm	
665	-	176.6 HV 0.5	88.2 HRB	70.7 µm	74.2 µm	
666	-	173.6 HV 0.5	87.4 HRB	71.0 µm	75.2 µm	
667	-	188.6 HV 0.5	90.7 HRB	69.7 µm	70.5 µm	
668	-	187.8 HV 0.5	90.6 HRB	68.7 µm	71.8 µm	
669	-	183.0 HV 0.5	89.6 HRB	69.9 µm	72.5 µm	
670	-	177.5 HV 0.5	88.4 HRB	70.9 µm	73.6 µm	
671	-	174.1 HV 0.5	87.5 HRB	73.9 µm	72.0 µm	
672	-	190.8 HV 0.5	91.2 HRB	69.0 µm	70.4 µm	
673	-	184.4 HV 0.5	89.9 HRB	72.0 µm	69.8 µm	
674	-	179.6 HV 0.5	88.9 HRB	71.9 µm	71.8 µm	
675	-	174.3 HV 0.5	87.6 HRB	72.4 µm	73.4 µm	
676	-	173.0 HV 0.5	87.2 HRB	73.7 µm	72.7 µm	
677	-	199.3 HV 0.5	92.9 HRB	66.3 µm	70.1 µm	
678	-	188.4 HV 0.5	90.7 HRB	69.3 µm	71.0 µm	
679	-	190.4 HV 0.5	91.1 HRB	69.8 µm	69.8 µm	
680	-	180.7 HV 0.5	89.1 HRB	70.9 µm	72.3 µm	
681	-	180.6 HV 0.5	89.1 HRB	72.8 µm	70.5 µm	
682	-	191.3 HV 0.5	91.3 HRB	70.4 µm	68.9 µm	
683	-	189.7 HV 0.5	90.9 HRB	69.9 µm	70.0 µm	
684	-	179.5 HV 0.5	88.9 HRB	72.5 µm	71.3 µm	

Date: 05-25-2023
Tester: Admin
Program: Hardness Map

Point	Distance	Hardness	Converted	Diagonal X	Diagonal Y	Comments
685	-	180.6 HV 0.5	89.1 HRB	69.4 µm	73.9 µm	
686	-	206.1 HV 0.5	94.2 HRB	67.1 µm	67.0 µm	
687	-	193.4 HV 0.5	91.7 HRB	69.6 µm	68.9 µm	
688	-	203.9 HV 0.5	93.8 HRB	66.9 µm	68.0 µm	
689	-	198.3 HV 0.5	92.7 HRB	68.0 µm	68.7 µm	
690	-	191.9 HV 0.5	91.4 HRB	66.4 µm	72.6 µm	
691	-	198.4 HV 0.5	92.7 HRB	67.5 µm	69.2 µm	
692	-	174.8 HV 0.5	87.7 HRB	73.1 µm	72.6 µm	
693	-	190.8 HV 0.5	91.2 HRB	70.0 µm	69.4 µm	
694	-	174.5 HV 0.5	87.6 HRB	73.6 µm	72.2 µm	
695	-	189.6 HV 0.5	90.9 HRB	70.4 µm	69.5 µm	
696	-	189.3 HV 0.5	90.9 HRB	69.4 µm	70.6 µm	
697	-	178.0 HV 0.5	88.5 HRB	72.5 µm	71.9 µm	
698	-	193.3 HV 0.5	91.7 HRB	66.7 µm	71.8 µm	
699	-	186.5 HV 0.5	90.3 HRB	71.5 µm	69.5 µm	
700	-	176.5 HV 0.5	88.1 HRB	72.3 µm	72.7 µm	
701	-	191.7 HV 0.5	91.3 HRB	70.1 µm	69.0 µm	
702	-	203.5 HV 0.5	93.7 HRB	68.2 µm	66.8 µm	
703	-	186.4 HV 0.5	90.3 HRB	72.2 µm	68.9 µm	
704	-	178.6 HV 0.5	88.7 HRB	72.2 µm	71.9 µm	
705	-	160.2 HV 0.5	83.4 HRB	74.9 µm	77.2 µm	
706	-	162.6 HV 0.5	84.2 HRB	76.9 µm	74.1 µm	
707	-	164.6 HV 0.5	84.9 HRB	76.6 µm	73.5 µm	
708	-	167.5 HV 0.5	85.6 HRB	74.5 µm	74.3 µm	
709	-	158.1 HV 0.5	82.7 HRB	76.5 µm	76.7 µm	
710	-	179.0 HV 0.5	88.7 HRB	72.4 µm	71.6 µm	
711	-	167.8 HV 0.5	85.7 HRB	74.5 µm	74.2 µm	
712	-	180.7 HV 0.5	89.1 HRB	71.7 µm	71.5 µm	
713	-	199.1 HV 0.5	92.8 HRB	67.7 µm	68.8 µm	
714	-	173.5 HV 0.5	87.4 HRB	73.8 µm	72.4 µm	
715	-	175.6 HV 0.5	87.9 HRB	71.7 µm	73.6 µm	
716	-	171.2 HV 0.5	86.7 HRB	74.0 µm	73.2 µm	
717	-	190.7 HV 0.5	91.1 HRB	69.1 µm	70.4 µm	
718	-	179.7 HV 0.5	88.9 HRB	70.4 µm	73.2 µm	
719	-	175.4 HV 0.5	87.9 HRB	71.7 µm	73.7 µm	
720	-	177.8 HV 0.5	88.4 HRB	72.3 µm	72.1 µm	
721	-	183.9 HV 0.5	89.8 HRB	70.4 µm	71.6 µm	
722	-	179.3 HV 0.5	88.8 HRB	69.9 µm	73.9 µm	
723	-	187.5 HV 0.5	90.5 HRB	70.6 µm	70.1 µm	

Date: 05-25-2023
Tester: Admin
Program: Hardness Map

Point	Distance	Hardness	Converted	Diagonal X	Diagonal Y	Comments
724	-	194.9 HV 0.5	92.0 HRB	69.2 µm	68.7 µm	
725	-	189.9 HV 0.5	91.0 HRB	69.5 µm	70.2 µm	
726	-	193.6 HV 0.5	91.7 HRB	68.1 µm	70.3 µm	
727	-	196.4 HV 0.5	92.3 HRB	67.8 µm	69.6 µm	
728	-	197.7 HV 0.5	92.5 HRB	67.3 µm	69.6 µm	
729	-	167.9 HV 0.5	85.7 HRB	69.4 µm	79.2 µm	
730	-	187.1 HV 0.5	90.4 HRB	70.3 µm	70.5 µm	
731	-	193.9 HV 0.5	91.8 HRB	67.7 µm	70.6 µm	
732	-	210.1 HV 0.5	95.0 HRB	65.4 µm	67.5 µm	
733	-	205.8 HV 0.5	94.2 HRB	67.5 µm	66.7 µm	
734	-	198.7 HV 0.5	92.7 HRB	68.9 µm	67.7 µm	
735	-	192.6 HV 0.5	91.5 HRB	67.7 µm	71.1 µm	
736	-	204.7 HV 0.5	93.9 HRB	67.4 µm	67.2 µm	
737	-	197.4 HV 0.5	92.5 HRB	68.4 µm	68.7 µm	
738	-	189.8 HV 0.5	91.0 HRB	70.5 µm	69.3 µm	
739	-	191.9 HV 0.5	91.4 HRB	69.0 µm	70.0 µm	
740	-	194.7 HV 0.5	91.9 HRB	66.8 µm	71.2 µm	
741	-	201.1 HV 0.5	93.2 HRB	68.0 µm	67.8 µm	
742	-	189.9 HV 0.5	91.0 HRB	69.6 µm	70.1 µm	
743	-	176.7 HV 0.5	88.2 HRB	74.1 µm	70.7 µm	
744	-	189.4 HV 0.5	90.9 HRB	69.8 µm	70.2 µm	
745	-	188.7 HV 0.5	90.7 HRB	69.6 µm	70.6 µm	
746	-	179.9 HV 0.5	89.0 HRB	71.8 µm	71.8 µm	
747	-	184.5 HV 0.5	89.9 HRB	70.3 µm	71.4 µm	
748	-	183.9 HV 0.5	89.8 HRB	70.4 µm	71.7 µm	
749	-	197.1 HV 0.5	92.4 HRB	68.2 µm	69.0 µm	
750	-	196.1 HV 0.5	92.2 HRB	68.2 µm	69.3 µm	
751	-	156.9 HV 0.5	82.3 HRB	75.0 µm	78.7 µm	
752	-	171.6 HV 0.5	86.9 HRB	73.9 µm	73.1 µm	
753	-	169.5 HV 0.5	86.2 HRB	73.3 µm	74.6 µm	
754	-	175.4 HV 0.5	87.8 HRB	72.3 µm	73.1 µm	
755	-	162.5 HV 0.5	84.2 HRB	75.0 µm	76.1 µm	
756	-	169.5 HV 0.5	86.2 HRB	74.3 µm	73.6 µm	
757	-	183.5 HV 0.5	89.7 HRB	71.1 µm	71.1 µm	
758	-	176.6 HV 0.5	88.2 HRB	70.1 µm	74.8 µm	
759	-	201.8 HV 0.5	93.4 HRB	67.2 µm	68.4 µm	
760	-	188.3 HV 0.5	90.7 HRB	69.1 µm	71.2 µm	
761	-	182.2 HV 0.5	89.4 HRB	70.6 µm	72.0 µm	
762	-	161.1 HV 0.5	83.7 HRB	74.0 µm	77.8 µm	

Date: 05-25-2023
Tester: Admin
Program: Hardness Map

Point	Distance	Hardness	Converted	Diagonal X	Diagonal Y	Comments
763	-	173.3 HV 0.5	87.3 HRB	74.0 µm	72.3 µm	
764	-	170.1 HV 0.5	86.4 HRB	73.8 µm	73.9 µm	
765	-	179.8 HV 0.5	88.9 HRB	72.2 µm	71.4 µm	
766	-	188.5 HV 0.5	90.7 HRB	69.3 µm	71.0 µm	
767	-	182.4 HV 0.5	89.5 HRB	70.9 µm	71.7 µm	
768	-	190.1 HV 0.5	91.0 HRB	70.2 µm	69.4 µm	
769	-	191.3 HV 0.5	91.3 HRB	69.9 µm	69.3 µm	
770	-	186.7 HV 0.5	90.3 HRB	70.0 µm	71.0 µm	
771	-	193.3 HV 0.5	91.7 HRB	69.0 µm	69.5 µm	
772	-	197.9 HV 0.5	92.6 HRB	68.7 µm	68.2 µm	
773	-	186.7 HV 0.5	90.3 HRB	70.2 µm	70.7 µm	
774	-	192.5 HV 0.5	91.5 HRB	68.5 µm	70.3 µm	
775	-	185.7 HV 0.5	90.1 HRB	70.2 µm	71.1 µm	
776	-	191.0 HV 0.5	91.2 HRB	68.6 µm	70.7 µm	
777	-	194.9 HV 0.5	92.0 HRB	68.3 µm	69.6 µm	
778	-	194.0 HV 0.5	91.8 HRB	65.4 µm	72.9 µm	
779	-	191.1 HV 0.5	91.2 HRB	68.5 µm	70.8 µm	
780	-	183.1 HV 0.5	89.6 HRB	69.5 µm	72.8 µm	
781	-	196.3 HV 0.5	92.3 HRB	70.5 µm	67.0 µm	
782	-	188.6 HV 0.5	90.7 HRB	68.8 µm	71.4 µm	
783	-	200.9 HV 0.5	93.2 HRB	68.4 µm	67.4 µm	
784	-	203.3 HV 0.5	93.7 HRB	66.5 µm	68.6 µm	
785	-	205.2 HV 0.5	94.0 HRB	67.2 µm	67.2 µm	
786	-	195.5 HV 0.5	92.1 HRB	69.2 µm	68.5 µm	
787	-	176.9 HV 0.5	88.2 HRB	72.2 µm	72.6 µm	
788	-	182.6 HV 0.5	89.5 HRB	71.0 µm	71.5 µm	
789	-	188.5 HV 0.5	90.7 HRB	69.3 µm	71.0 µm	
790	-	191.3 HV 0.5	91.3 HRB	69.6 µm	69.6 µm	
791	-	194.4 HV 0.5	91.9 HRB	67.8 µm	70.3 µm	
792	-	177.6 HV 0.5	88.4 HRB	69.6 µm	74.9 µm	
793	-	193.1 HV 0.5	91.6 HRB	70.0 µm	68.6 µm	
794	-	182.9 HV 0.5	89.6 HRB	70.5 µm	71.9 µm	
795	-	192.1 HV 0.5	91.4 HRB	68.7 µm	70.2 µm	
796	-	189.4 HV 0.5	90.9 HRB	70.1 µm	69.9 µm	
797	-	177.4 HV 0.5	88.4 HRB	72.6 µm	72.0 µm	
798	-	172.9 HV 0.5	87.2 HRB	72.3 µm	74.1 µm	
799	-	169.2 HV 0.5	86.1 HRB	74.2 µm	73.9 µm	
800	-	171.4 HV 0.5	86.8 HRB	72.1 µm	75.0 µm	
801	-	176.5 HV 0.5	88.1 HRB	73.8 µm	71.2 µm	

Date: 05-25-2023
Tester: Admin
Program: Hardness Map

Point	Distance	Hardness	Converted	Diagonal X	Diagonal Y	Comments
802	-	189.5 HV 0.5	90.9 HRB	70.3 µm	69.6 µm	
803	-	191.3 HV 0.5	91.3 HRB	69.5 µm	69.7 µm	
804	-	182.9 HV 0.5	89.6 HRB	70.5 µm	71.9 µm	
805	-	206.2 HV 0.5	94.2 HRB	66.4 µm	67.7 µm	
806	-	183.6 HV 0.5	89.7 HRB	71.0 µm	71.2 µm	
807	-	179.3 HV 0.5	88.8 HRB	71.5 µm	72.3 µm	
808	-	173.4 HV 0.5	87.3 HRB	74.6 µm	71.7 µm	
809	-	169.4 HV 0.5	86.1 HRB	73.8 µm	74.2 µm	
810	-	189.4 HV 0.5	90.9 HRB	68.6 µm	71.4 µm	
811	-	157.9 HV 0.5	82.6 HRB	82.0 µm	71.3 µm	
812	-	177.2 HV 0.5	88.3 HRB	71.1 µm	73.6 µm	
813	-	187.9 HV 0.5	90.6 HRB	70.5 µm	70.0 µm	
814	-	173.0 HV 0.5	87.3 HRB	71.9 µm	74.5 µm	
815	-	184.9 HV 0.5	90.0 HRB	69.6 µm	72.1 µm	
816	-	178.5 HV 0.5	88.6 HRB	72.9 µm	71.3 µm	
817	-	191.4 HV 0.5	91.3 HRB	67.6 µm	71.6 µm	
818	-	217.0 HV 0.5	96.2 HRB	65.3 µm	65.4 µm	
819	-	217.7 HV 0.5	96.3 HRB	64.7 µm	65.8 µm	
820	-	218.2 HV 0.5	96.4 HRB	65.4 µm	64.9 µm	
821	-	203.8 HV 0.5	93.8 HRB	67.7 µm	67.2 µm	
822	-	192.3 HV 0.5	91.5 HRB	68.3 µm	70.5 µm	
823	-	192.4 HV 0.5	91.5 HRB	69.4 µm	69.4 µm	
824	-	197.8 HV 0.5	92.6 HRB	65.8 µm	71.2 µm	
825	-	239.2 HV 0.5	99.9 HRB	61.8 µm	62.7 µm	
826	-	221.1 HV 0.5	96.8 HRB	64.1 µm	65.4 µm	

Hardness Map

ADV PN 100794 3:00 o'clock

Date: 05-24-2023
Tester: Admin
Program: Hardness Map

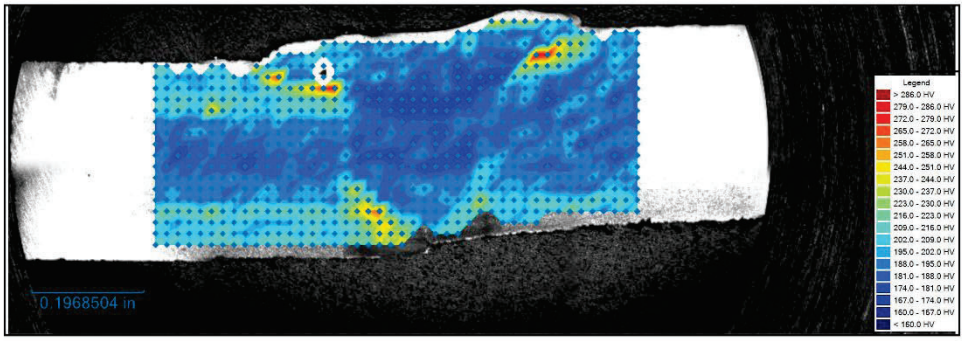

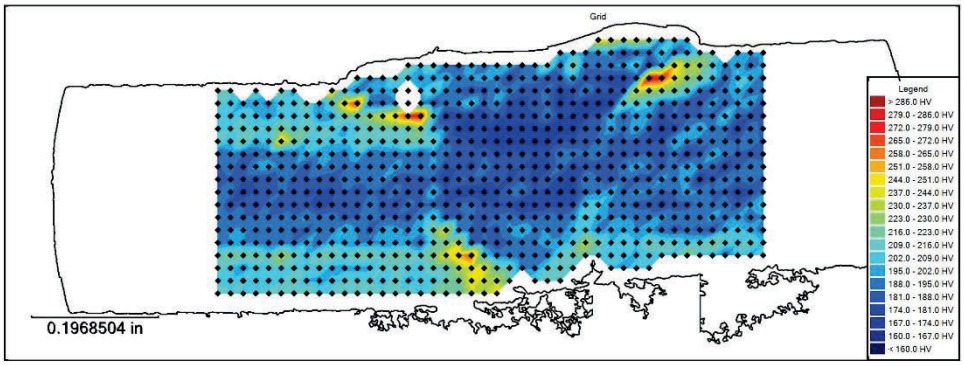

Date: 05-24-2023
Tester: Admin
Program: Hardness Map

Grid

Mean	Minimum	Maximum	Range	Std. deviation
197.2	166.4	283.7	117.3	16.9

Hardness Trace

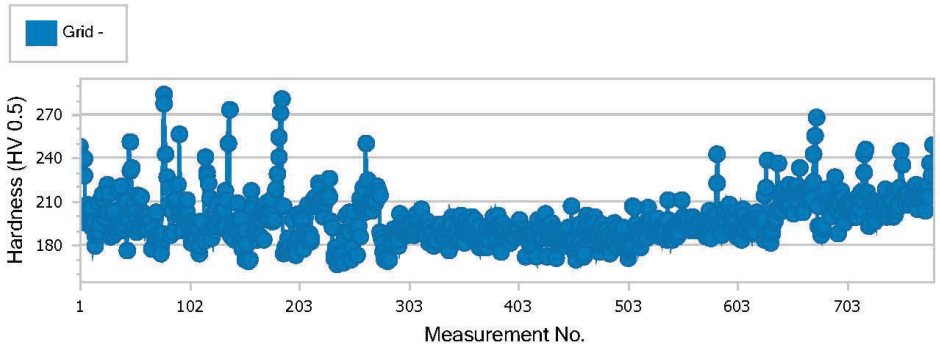

Point	Distance	Hardness	Converted	Diagonal X	Diagonal Y	Comments
1	-	247.8 HV 0.5	-	61.4 µm	61.0 µm	
2	-	241.5 HV 0.5	-	61.2 µm	62.8 µm	
3	-	227.3 HV 0.5	97.9 HRB	63.9 µm	63.8 µm	
4	-	239.9 HV 0.5	100.0 HRB	61.2 µm	63.2 µm	
5	-	227.3 HV 0.5	97.9 HRB	63.6 µm	64.1 µm	
6	-	195.1 HV 0.5	92.0 HRB	68.3 µm	69.5 µm	
7	-	207.3 HV 0.5	94.5 HRB	67.1 µm	66.7 µm	
8	-	198.9 HV 0.5	92.8 HRB	69.3 µm	67.3 µm	
9	-	200.6 HV 0.5	93.1 HRB	67.4 µm	68.6 µm	
10	-	205.4 HV 0.5	94.1 HRB	67.4 µm	67.0 µm	
11	-	191.6 HV 0.5	91.3 HRB	68.7 µm	70.5 µm	
12	-	196.0 HV 0.5	92.2 HRB	68.0 µm	69.5 µm	
13	-	196.0 HV 0.5	92.2 HRB	67.7 µm	69.8 µm	
14	-	179.1 HV 0.5	88.8 HRB	72.8 µm	71.1 µm	
15	-	186.5 HV 0.5	90.3 HRB	71.5 µm	69.5 µm	
16	-	188.1 HV 0.5	90.6 HRB	70.6 µm	69.8 µm	
17	-	208.3 HV 0.5	94.7 HRB	66.8 µm	66.7 µm	
18	-	188.1 HV 0.5	90.6 HRB	69.6 µm	70.8 µm	
19	-	195.3 HV 0.5	92.1 HRB	68.9 µm	68.9 µm	
20	-	211.4 HV 0.5	95.2 HRB	66.1 µm	66.3 µm	
21	-	215.4 HV 0.5	95.9 HRB	64.9 µm	66.4 µm	

Date: 05-24-2023
Tester: Admin
Program: Hardness Map

Point	Distance	Hardness	Converted	Diagonal X	Diagonal Y	Comments
22	-	200.5 HV 0.5	93.1 HRB	66.8 µm	69.2 µm	
23	-	197.6 HV 0.5	92.5 HRB	66.5 µm	70.5 µm	
24	-	198.3 HV 0.5	92.7 HRB	67.4 µm	69.4 µm	
25	-	221.8 HV 0.5	97.0 HRB	64.5 µm	64.8 µm	
26	-	202.5 HV 0.5	93.5 HRB	66.4 µm	68.9 µm	
27	-	215.4 HV 0.5	95.9 HRB	65.2 µm	66.0 µm	
28	-	188.2 HV 0.5	90.6 HRB	70.9 µm	69.5 µm	
29	-	185.0 HV 0.5	90.0 HRB	71.2 µm	70.4 µm	
30	-	202.5 HV 0.5	93.5 HRB	66.8 µm	68.6 µm	
31	-	186.4 HV 0.5	90.3 HRB	69.6 µm	71.4 µm	
32	-	201.6 HV 0.5	93.3 HRB	67.1 µm	68.6 µm	
33	-	203.4 HV 0.5	93.7 HRB	66.8 µm	68.3 µm	
34	-	188.2 HV 0.5	90.6 HRB	67.7 µm	72.7 µm	
35	-	193.0 HV 0.5	91.6 HRB	69.7 µm	68.9 µm	
36	-	218.7 HV 0.5	96.4 HRB	65.8 µm	64.4 µm	
37	-	190.7 HV 0.5	91.1 HRB	68.7 µm	70.8 µm	
38	-	220.7 HV 0.5	96.8 HRB	65.8 µm	63.9 µm	
39	-	189.8 HV 0.5	91.0 HRB	68.7 µm	71.1 µm	
40	-	190.8 HV 0.5	91.2 HRB	67.7 µm	71.7 µm	
41	-	194.2 HV 0.5	91.8 HRB	69.6 µm	68.6 µm	
42	-	197.9 HV 0.5	92.6 HRB	69.0 µm	67.9 µm	
43	-	209.3 HV 0.5	94.9 HRB	67.7 µm	65.4 µm	
44	-	176.0 HV 0.5	88.0 HRB	73.1 µm	72.1 µm	
45	-	195.8 HV 0.5	92.2 HRB	68.7 µm	68.9 µm	
46	-	250.7 HV 0.5	-	62.0 µm	59.6 µm	
47	-	231.3 HV 0.5	98.5 HRB	64.1 µm	62.5 µm	
48	-	232.7 HV 0.5	98.8 HRB	62.4 µm	63.8 µm	
49	-	207.0 HV 0.5	94.4 HRB	68.2 µm	65.6 µm	
50	-	191.6 HV 0.5	91.3 HRB	69.5 µm	69.7 µm	
51	-	202.4 HV 0.5	93.5 HRB	68.1 µm	67.3 µm	
52	-	188.4 HV 0.5	90.7 HRB	67.1 µm	73.2 µm	
53	-	197.8 HV 0.5	92.6 HRB	66.8 µm	70.2 µm	
54	-	214.0 HV 0.5	95.7 HRB	65.3 µm	66.4 µm	
55	-	191.6 HV 0.5	91.3 HRB	69.6 µm	69.5 µm	
56	-	195.1 HV 0.5	92.0 HRB	68.3 µm	69.5 µm	
57	-	213.4 HV 0.5	95.6 HRB	65.8 µm	66.0 µm	
58	-	202.5 HV 0.5	93.5 HRB	68.0 µm	67.3 µm	
59	-	195.6 HV 0.5	92.1 HRB	67.7 µm	70.0 µm	
60	-	196.9 HV 0.5	92.4 HRB	69.9 µm	67.3 µm	

Date: 05-24-2023
Tester: Admin
Program: Hardness Map

Point	Distance	Hardness	Converted	Diagonal X	Diagonal Y	Comments
61	-	200.6 HV 0.5	93.1 HRB	66.8 µm	69.2 µm	
62	-	190.9 HV 0.5	91.2 HRB	70.2 µm	69.1 µm	
63	-	196.9 HV 0.5	92.4 HRB	68.3 µm	68.9 µm	
64	-	200.6 HV 0.5	93.1 HRB	67.1 µm	68.9 µm	
65	-	195.6 HV 0.5	92.1 HRB	69.2 µm	68.5 µm	
66	-	177.1 HV 0.5	88.3 HRB	70.1 µm	74.6 µm	
67	-	191.6 HV 0.5	91.3 HRB	69.3 µm	69.8 µm	
68	-	191.2 HV 0.5	91.2 HRB	69.9 µm	69.4 µm	
69	-	184.0 HV 0.5	89.8 HRB	70.9 µm	71.1 µm	
70	-	186.6 HV 0.5	90.3 HRB	70.5 µm	70.5 µm	
71	-	202.5 HV 0.5	93.5 HRB	68.0 µm	67.3 µm	
72	-	182.2 HV 0.5	89.4 HRB	72.4 µm	70.2 µm	
73	-	180.7 HV 0.5	89.1 HRB	72.1 µm	71.1 µm	
74	-	178.4 HV 0.5	88.6 HRB	74.0 µm	70.2 µm	
75	-	173.9 HV 0.5	87.5 HRB	72.4 µm	73.7 µm	
76	-	187.3 HV 0.5	90.5 HRB	70.2 µm	70.5 µm	
77	-	283.7 HV 0.5	-	57.3 µm	57.0 µm	
78	-	277.4 HV 0.5	-	59.5 µm	56.1 µm	
79	-	242.3 HV 0.5	-	61.2 µm	62.5 µm	
80	-	226.3 HV 0.5	97.7 HRB	63.6 µm	64.4 µm	
81	-	218.7 HV 0.5	96.5 HRB	65.1 µm	65.1 µm	
82	-	207.8 HV 0.5	94.6 HRB	67.6 µm	66.0 µm	
83	-	186.1 HV 0.5	90.2 HRB	70.4 µm	70.7 µm	
84	-	203.9 HV 0.5	93.8 HRB	67.5 µm	67.3 µm	
85	-	203.5 HV 0.5	93.7 HRB	68.7 µm	66.4 µm	
86	-	188.9 HV 0.5	90.8 HRB	70.0 µm	70.2 µm	
87	-	209.8 HV 0.5	95.0 HRB	66.7 µm	66.2 µm	
88	-	210.6 HV 0.5	95.1 HRB	66.9 µm	65.9 µm	
89	-	211.5 HV 0.5	95.3 HRB	65.1 µm	67.3 µm	
90	-	221.0 HV 0.5	96.8 HRB	65.6 µm	63.9 µm	
91	-	200.6 HV 0.5	93.1 HRB	65.9 µm	70.1 µm	
92	-	256.3 HV 0.5	-	59.5 µm	60.8 µm	
93	-	202.5 HV 0.5	93.5 HRB	67.4 µm	67.9 µm	
94	-	189.8 HV 0.5	91.0 HRB	68.7 µm	71.1 µm	
95	-	200.0 HV 0.5	93.0 HRB	67.6 µm	68.6 µm	
96	-	197.8 HV 0.5	92.6 HRB	67.4 µm	69.5 µm	
97	-	201.6 HV 0.5	93.3 HRB	68.0 µm	67.6 µm	
98	-	Deleted	-	-	-	
99	-	202.5 HV 0.5	93.5 HRB	67.4 µm	67.9 µm	

Date: 05-24-2023
Tester: Admin
Program: Hardness Map

Point	Distance	Hardness	Converted	Diagonal X	Diagonal Y	Comments
100	-	210.3 HV 0.5	95.1 HRB	67.1 µm	65.7 µm	
101	-	195.1 HV 0.5	92.0 HRB	69.9 µm	67.9 µm	
102	-	187.3 HV 0.5	90.5 HRB	70.6 µm	70.2 µm	
103	-	181.5 HV 0.5	89.3 HRB	70.9 µm	72.1 µm	
104	-	184.0 HV 0.5	89.8 HRB	70.9 µm	71.1 µm	
105	-	196.0 HV 0.5	92.2 HRB	69.0 µm	68.6 µm	
106	-	193.3 HV 0.5	91.7 HRB	68.7 µm	69.8 µm	
107	-	184.3 HV 0.5	89.9 HRB	72.0 µm	69.8 µm	
108	-	184.8 HV 0.5	90.0 HRB	69.9 µm	71.8 µm	
109	-	190.6 HV 0.5	91.1 HRB	69.3 µm	70.2 µm	
110	-	173.7 HV 0.5	87.4 HRB	73.1 µm	73.0 µm	
111	-	179.1 HV 0.5	88.8 HRB	72.4 µm	71.4 µm	
112	-	196.0 HV 0.5	92.2 HRB	68.0 µm	69.5 µm	
113	-	184.8 HV 0.5	90.0 HRB	69.9 µm	71.8 µm	
114	-	183.0 HV 0.5	89.6 HRB	71.8 µm	70.6 µm	
115	-	182.4 HV 0.5	89.5 HRB	71.2 µm	71.4 µm	
116	-	240.6 HV 0.5	-	62.1 µm	62.0 µm	
117	-	229.7 HV 0.5	98.3 HRB	62.2 µm	64.8 µm	
118	-	228.2 HV 0.5	98.0 HRB	64.0 µm	63.4 µm	
119	-	222.3 HV 0.5	97.1 HRB	63.7 µm	65.4 µm	
120	-	211.4 HV 0.5	95.2 HRB	66.1 µm	66.4 µm	
121	-	190.5 HV 0.5	91.1 HRB	69.1 µm	70.5 µm	
122	-	184.1 HV 0.5	89.8 HRB	72.4 µm	69.5 µm	
123	-	191.8 HV 0.5	91.4 HRB	68.7 µm	70.4 µm	
124	-	203.2 HV 0.5	93.6 HRB	65.2 µm	69.9 µm	
125	-	190.1 HV 0.5	91.0 HRB	68.5 µm	71.2 µm	
126	-	192.4 HV 0.5	91.5 HRB	70.6 µm	68.3 µm	
127	-	210.1 HV 0.5	95.0 HRB	64.9 µm	67.9 µm	
128	-	207.3 HV 0.5	94.5 HRB	66.6 µm	67.2 µm	
129	-	198.0 HV 0.5	92.6 HRB	67.4 µm	69.5 µm	
130	-	197.8 HV 0.5	92.6 HRB	68.6 µm	68.3 µm	
131	-	192.5 HV 0.5	91.5 HRB	72.1 µm	66.7 µm	
132	-	204.7 HV 0.5	93.9 HRB	67.9 µm	66.7 µm	
133	-	203.6 HV 0.5	93.7 HRB	67.7 µm	67.2 µm	
134	-	217.1 HV 0.5	96.2 HRB	66.7 µm	64.0 µm	
135	-	193.3 HV 0.5	91.7 HRB	68.2 µm	70.4 µm	
136	-	210.7 HV 0.5	95.1 HRB	65.0 µm	67.7 µm	
137	-	249.8 HV 0.5	-	60.6 µm	61.2 µm	
138	-	273.1 HV 0.5	-	59.0 µm	57.5 µm	

Date: 05-24-2023
Tester: Admin
Program: Hardness Map

Point	Distance	Hardness	Converted	Diagonal X	Diagonal Y	Comments
139	-	187.3 HV 0.5	90.5 HRB	71.8 µm	68.9 µm	
140	-	185.6 HV 0.5	90.1 HRB	69.0 µm	72.4 µm	
141	-	193.3 HV 0.5	91.7 HRB	67.4 µm	71.1 µm	
142	-	Deleted	-	-	-	
143	-	195.1 HV 0.5	92.0 HRB	69.0 µm	68.9 µm	
144	-	183.5 HV 0.5	89.7 HRB	70.2 µm	71.9 µm	
145	-	192.5 HV 0.5	91.5 HRB	68.7 µm	70.2 µm	
146	-	196.9 HV 0.5	92.4 HRB	67.7 µm	69.5 µm	
147	-	208.3 HV 0.5	94.7 HRB	68.0 µm	65.4 µm	
148	-	186.5 HV 0.5	90.3 HRB	70.2 µm	70.8 µm	
149	-	198.6 HV 0.5	92.7 HRB	67.4 µm	69.2 µm	
150	-	180.7 HV 0.5	89.1 HRB	71.8 µm	71.4 µm	
151	-	177.2 HV 0.5	88.3 HRB	72.8 µm	71.9 µm	
152	-	185.7 HV 0.5	90.1 HRB	70.5 µm	70.8 µm	
153	-	189.8 HV 0.5	91.0 HRB	69.3 µm	70.5 µm	
154	-	169.6 HV 0.5	86.2 HRB	74.0 µm	73.9 µm	
155	-	179.9 HV 0.5	89.0 HRB	71.8 µm	71.8 µm	
156	-	168.6 HV 0.5	85.9 HRB	74.3 µm	74.0 µm	
157	-	168.4 HV 0.5	85.8 HRB	74.1 µm	74.3 µm	
158	-	170.0 HV 0.5	86.3 HRB	73.7 µm	74.0 µm	
159	-	216.6 HV 0.5	96.1 HRB	65.4 µm	65.4 µm	
160	-	208.0 HV 0.5	94.6 HRB	67.7 µm	65.9 µm	
161	-	204.5 HV 0.5	93.9 HRB	67.4 µm	67.3 µm	
162	-	189.3 HV 0.5	90.9 HRB	68.5 µm	71.4 µm	
163	-	189.7 HV 0.5	90.9 HRB	68.1 µm	71.8 µm	
164	-	186.1 HV 0.5	90.2 HRB	72.1 µm	69.1 µm	
165	-	183.7 HV 0.5	89.7 HRB	67.9 µm	74.1 µm	
166	-	199.2 HV 0.5	92.8 HRB	69.0 µm	67.4 µm	
167	-	185.0 HV 0.5	90.0 HRB	70.2 µm	71.4 µm	
168	-	196.5 HV 0.5	92.3 HRB	66.2 µm	71.2 µm	
169	-	201.0 HV 0.5	93.2 HRB	66.9 µm	68.9 µm	
170	-	182.9 HV 0.5	89.6 HRB	70.6 µm	71.9 µm	
171	-	205.7 HV 0.5	94.1 HRB	66.3 µm	68.0 µm	
172	-	201.8 HV 0.5	93.4 HRB	67.0 µm	68.6 µm	
173	-	208.5 HV 0.5	94.7 HRB	65.8 µm	67.5 µm	
174	-	202.7 HV 0.5	93.5 HRB	66.5 µm	68.8 µm	
175	-	197.4 HV 0.5	92.5 HRB	67.9 µm	69.1 µm	
176	-	204.3 HV 0.5	93.9 HRB	66.1 µm	68.6 µm	
177	-	202.6 HV 0.5	93.5 HRB	66.8 µm	68.5 µm	

Date: 05-24-2023
Tester: Admin
Program: Hardness Map

Point	Distance	Hardness	Converted	Diagonal X	Diagonal Y	Comments
178	-	211.0 HV 0.5	95.2 HRB	65.9 µm	66.7 µm	
179	-	195.4 HV 0.5	92.1 HRB	68.3 µm	69.5 µm	
180	-	197.5 HV 0.5	92.5 HRB	67.6 µm	69.5 µm	
181	-	217.9 HV 0.5	96.3 HRB	66.1 µm	64.3 µm	
182	-	217.8 HV 0.5	96.3 HRB	66.1 µm	64.4 µm	
183	-	228.9 HV 0.5	98.2 HRB	62.2 µm	65.1 µm	
184	-	240.2 HV 0.5	-	61.9 µm	62.3 µm	
185	-	254.0 HV 0.5	-	59.8 µm	61.0 µm	
186	-	271.4 HV 0.5	-	59.4 µm	57.5 µm	
187	-	280.7 HV 0.5	-	57.8 µm	57.1 µm	
188	-	206.5 HV 0.5	94.3 HRB	66.1 µm	67.9 µm	
189	-	173.5 HV 0.5	87.4 HRB	72.9 µm	73.3 µm	
190	-	177.6 HV 0.5	88.4 HRB	71.8 µm	72.7 µm	
191	-	174.7 HV 0.5	87.7 HRB	73.1 µm	72.6 µm	
192	-	177.4 HV 0.5	88.3 HRB	71.6 µm	73.0 µm	
193	-	184.7 HV 0.5	89.9 HRB	71.1 µm	70.6 µm	
194	-	178.3 HV 0.5	88.6 HRB	71.8 µm	72.4 µm	
195	-	176.0 HV 0.5	88.0 HRB	71.8 µm	73.3 µm	
196	-	179.1 HV 0.5	88.8 HRB	70.6 µm	73.3 µm	
197	-	196.9 HV 0.5	92.4 HRB	68.7 µm	68.6 µm	
198	-	176.8 HV 0.5	88.2 HRB	72.8 µm	72.1 µm	
199	-	172.9 HV 0.5	87.2 HRB	73.2 µm	73.2 µm	
200	-	175.2 HV 0.5	87.8 HRB	71.8 µm	73.7 µm	
201	-	182.7 HV 0.5	89.5 HRB	69.0 µm	73.4 µm	
202	-	201.0 HV 0.5	93.2 HRB	68.0 µm	67.9 µm	
203	-	185.4 HV 0.5	90.1 HRB	69.3 µm	72.2 µm	
204	-	198.6 HV 0.5	92.7 HRB	69.3 µm	67.4 µm	
205	-	196.5 HV 0.5	92.3 HRB	67.7 µm	69.7 µm	
206	-	177.4 HV 0.5	88.3 HRB	72.4 µm	72.3 µm	
207	-	188.4 HV 0.5	90.7 HRB	69.9 µm	70.4 µm	
208	-	185.6 HV 0.5	90.1 HRB	69.6 µm	71.7 µm	
209	-	187.6 HV 0.5	90.5 HRB	69.6 µm	71.0 µm	
210	-	185.6 HV 0.5	90.1 HRB	69.3 µm	72.1 µm	
211	-	207.4 HV 0.5	94.5 HRB	66.3 µm	67.4 µm	
212	-	187.4 HV 0.5	90.5 HRB	71.2 µm	69.4 µm	
213	-	182.6 HV 0.5	89.5 HRB	71.3 µm	71.3 µm	
214	-	184.2 HV 0.5	89.8 HRB	71.7 µm	70.2 µm	
215	-	206.8 HV 0.5	94.4 HRB	65.9 µm	68.1 µm	
216	-	209.3 HV 0.5	94.9 HRB	66.4 µm	66.7 µm	

Date: 05-24-2023
Tester: Admin
Program: Hardness Map

Point	Distance	Hardness	Converted	Diagonal X	Diagonal Y	Comments
217	-	211.5 HV 0.5	95.2 HRB	66.4 µm	66.0 µm	
218	-	212.4 HV 0.5	95.4 HRB	65.3 µm	66.9 µm	
219	-	209.1 HV 0.5	94.8 HRB	65.3 µm	67.8 µm	
220	-	222.0 HV 0.5	97.0 HRB	64.7 µm	64.6 µm	
221	-	206.7 HV 0.5	94.3 HRB	66.1 µm	67.9 µm	
222	-	218.9 HV 0.5	96.5 HRB	65.9 µm	64.3 µm	
223	-	208.1 HV 0.5	94.6 HRB	67.9 µm	65.6 µm	
224	-	211.6 HV 0.5	95.3 HRB	66.1 µm	66.3 µm	
225	-	198.9 HV 0.5	92.8 HRB	68.7 µm	67.9 µm	
226	-	208.4 HV 0.5	94.7 HRB	68.5 µm	64.9 µm	
227	-	212.4 HV 0.5	95.4 HRB	65.5 µm	66.6 µm	
228	-	214.4 HV 0.5	95.7 HRB	65.6 µm	65.9 µm	
229	-	215.2 HV 0.5	95.9 HRB	65.3 µm	65.9 µm	
230	-	213.0 HV 0.5	95.5 HRB	65.7 µm	66.2 µm	
231	-	226.0 HV 0.5	97.7 HRB	64.5 µm	63.6 µm	
232	-	196.0 HV 0.5	92.2 HRB	68.7 µm	68.9 µm	
233	-	192.1 HV 0.5	91.4 HRB	70.2 µm	68.7 µm	
234	-	173.0 HV 0.5	87.2 HRB	72.8 µm	73.7 µm	
235	-	170.5 HV 0.5	86.5 HRB	73.7 µm	73.8 µm	
236	-	178.2 HV 0.5	88.6 HRB	72.1 µm	72.1 µm	
237	-	166.4 HV 0.5	85.4 HRB	72.4 µm	76.8 µm	
238	-	173.0 HV 0.5	87.2 HRB	72.8 µm	73.7 µm	
239	-	171.3 HV 0.5	86.8 HRB	73.2 µm	74.0 µm	
240	-	170.6 HV 0.5	86.5 HRB	74.1 µm	73.3 µm	
241	-	172.2 HV 0.5	87.1 HRB	73.1 µm	73.7 µm	
242	-	167.0 HV 0.5	85.5 HRB	74.0 µm	75.0 µm	
243	-	167.6 HV 0.5	85.7 HRB	75.4 µm	73.3 µm	
244	-	188.9 HV 0.5	90.8 HRB	69.6 µm	70.5 µm	
245	-	185.0 HV 0.5	90.0 HRB	70.9 µm	70.7 µm	
246	-	200.2 HV 0.5	93.0 HRB	68.7 µm	67.4 µm	
247	-	188.8 HV 0.5	90.8 HRB	70.4 µm	69.8 µm	
248	-	202.3 HV 0.5	93.5 HRB	67.9 µm	67.5 µm	
249	-	188.9 HV 0.5	90.8 HRB	70.7 µm	69.4 µm	
250	-	169.7 HV 0.5	86.2 HRB	73.3 µm	74.5 µm	
251	-	177.8 HV 0.5	88.4 HRB	67.8 µm	76.6 µm	
252	-	195.9 HV 0.5	92.2 HRB	69.1 µm	68.5 µm	
253	-	202.5 HV 0.5	93.5 HRB	66.7 µm	68.7 µm	
254	-	190.7 HV 0.5	91.1 HRB	67.7 µm	71.7 µm	
255	-	192.1 HV 0.5	91.4 HRB	70.9 µm	68.1 µm	

Date: 05-24-2023
Tester: Admin
Program: Hardness Map

Point	Distance	Hardness	Converted	Diagonal X	Diagonal Y	Comments
256	-	172.5 HV 0.5	87.1 HRB	71.8 µm	74.9 µm	
257	-	193.2 HV 0.5	91.6 HRB	69.3 µm	69.3 µm	
258	-	185.2 HV 0.5	90.0 HRB	70.6 µm	70.9 µm	
259	-	211.4 HV 0.5	95.2 HRB	66.1 µm	66.4 µm	
260	-	205.3 HV 0.5	94.1 HRB	67.8 µm	66.6 µm	
261	-	219.1 HV 0.5	96.5 HRB	65.2 µm	64.9 µm	
262	-	202.4 HV 0.5	93.5 HRB	67.2 µm	68.2 µm	
263	-	204.7 HV 0.5	93.9 HRB	67.8 µm	66.8 µm	
264	-	249.6 HV 0.5	-	59.6 µm	62.3 µm	
265	-	224.3 HV 0.5	97.4 HRB	64.5 µm	64.1 µm	
266	-	205.0 HV 0.5	94.0 HRB	65.0 µm	69.5 µm	
267	-	210.9 HV 0.5	95.1 HRB	67.0 µm	65.6 µm	
268	-	204.5 HV 0.5	93.9 HRB	65.2 µm	69.5 µm	
269	-	203.0 HV 0.5	93.6 HRB	65.2 µm	69.9 µm	
270	-	211.9 HV 0.5	95.3 HRB	66.3 µm	66.0 µm	
271	-	217.0 HV 0.5	96.2 HRB	65.9 µm	64.8 µm	
272	-	208.9 HV 0.5	94.8 HRB	66.2 µm	67.1 µm	
273	-	210.3 HV 0.5	95.0 HRB	63.9 µm	69.0 µm	
274	-	219.9 HV 0.5	96.7 HRB	64.4 µm	65.4 µm	
275	-	216.7 HV 0.5	96.1 HRB	67.1 µm	63.7 µm	
276	-	214.3 HV 0.5	95.7 HRB	64.9 µm	66.7 µm	
277	-	188.1 HV 0.5	90.6 HRB	69.1 µm	71.3 µm	
278	-	184.7 HV 0.5	89.9 HRB	71.3 µm	70.4 µm	
279	-	181.3 HV 0.5	89.3 HRB	71.3 µm	71.8 µm	
280	-	174.6 HV 0.5	87.6 HRB	74.7 µm	71.0 µm	
281	-	169.7 HV 0.5	86.2 HRB	71.4 µm	76.4 µm	
282	-	169.4 HV 0.5	86.1 HRB	74.6 µm	73.3 µm	
283	-	171.5 HV 0.5	86.8 HRB	74.5 µm	72.6 µm	
284	-	168.2 HV 0.5	85.8 HRB	74.6 µm	73.9 µm	
285	-	169.3 HV 0.5	86.1 HRB	73.4 µm	74.6 µm	
286	-	182.3 HV 0.5	89.5 HRB	70.9 µm	71.7 µm	
287	-	179.6 HV 0.5	88.9 HRB	71.9 µm	71.8 µm	
288	-	181.5 HV 0.5	89.3 HRB	71.5 µm	71.4 µm	
289	-	190.6 HV 0.5	91.1 HRB	69.2 µm	70.3 µm	
290	-	186.4 HV 0.5	90.3 HRB	70.3 µm	70.8 µm	
291	-	185.9 HV 0.5	90.2 HRB	69.7 µm	71.5 µm	
292	-	185.7 HV 0.5	90.1 HRB	69.3 µm	72.0 µm	
293	-	179.4 HV 0.5	88.8 HRB	71.9 µm	71.9 µm	
294	-	183.1 HV 0.5	89.6 HRB	69.6 µm	72.7 µm	

Date: 05-24-2023
Tester: Admin
Program: Hardness Map

Point	Distance	Hardness	Converted	Diagonal X	Diagonal Y	Comments
295	-	201.0 HV 0.5	93.2 HRB	68.6 µm	67.2 µm	
296	-	194.4 HV 0.5	91.9 HRB	68.3 µm	69.8 µm	
297	-	191.5 HV 0.5	91.3 HRB	68.7 µm	70.5 µm	
298	-	188.9 HV 0.5	90.8 HRB	68.7 µm	71.4 µm	
299	-	190.7 HV 0.5	91.1 HRB	69.3 µm	70.2 µm	
300	-	187.4 HV 0.5	90.5 HRB	68.1 µm	72.6 µm	
301	-	193.1 HV 0.5	91.6 HRB	68.4 µm	70.2 µm	
302	-	186.4 HV 0.5	90.3 HRB	71.6 µm	69.5 µm	
303	-	187.4 HV 0.5	90.5 HRB	69.6 µm	71.1 µm	
304	-	193.2 HV 0.5	91.6 HRB	68.0 µm	70.5 µm	
305	-	188.0 HV 0.5	90.6 HRB	68.7 µm	71.8 µm	
306	-	187.0 HV 0.5	90.4 HRB	70.1 µm	70.7 µm	
307	-	190.1 HV 0.5	91.0 HRB	70.5 µm	69.2 µm	
308	-	186.5 HV 0.5	90.3 HRB	69.5 µm	71.6 µm	
309	-	189.7 HV 0.5	90.9 HRB	68.2 µm	71.7 µm	
310	-	201.1 HV 0.5	93.2 HRB	67.0 µm	68.8 µm	
311	-	195.6 HV 0.5	92.1 HRB	68.6 µm	69.1 µm	
312	-	195.8 HV 0.5	92.2 HRB	67.8 µm	69.8 µm	
313	-	190.0 HV 0.5	91.0 HRB	68.6 µm	71.1 µm	
314	-	204.8 HV 0.5	94.0 HRB	66.5 µm	68.1 µm	
315	-	187.1 HV 0.5	90.4 HRB	69.7 µm	71.1 µm	
316	-	192.1 HV 0.5	91.4 HRB	67.9 µm	71.0 µm	
317	-	190.0 HV 0.5	91.0 HRB	70.9 µm	68.8 µm	
318	-	192.5 HV 0.5	91.5 HRB	70.2 µm	68.6 µm	
319	-	186.6 HV 0.5	90.3 HRB	69.2 µm	71.8 µm	
320	-	195.6 HV 0.5	92.1 HRB	68.3 µm	69.4 µm	
321	-	191.4 HV 0.5	91.3 HRB	70.1 µm	69.1 µm	
322	-	181.7 HV 0.5	89.3 HRB	71.0 µm	71.9 µm	
323	-	183.5 HV 0.5	89.7 HRB	71.5 µm	70.6 µm	
324	-	188.1 HV 0.5	90.6 HRB	70.2 µm	70.2 µm	
325	-	179.0 HV 0.5	88.8 HRB	72.1 µm	71.8 µm	
326	-	182.6 HV 0.5	89.5 HRB	71.1 µm	71.4 µm	
327	-	182.4 HV 0.5	89.5 HRB	71.5 µm	71.1 µm	
328	-	180.9 HV 0.5	89.2 HRB	71.4 µm	71.8 µm	
329	-	181.8 HV 0.5	89.4 HRB	71.4 µm	71.4 µm	
330	-	193.8 HV 0.5	91.8 HRB	68.4 µm	69.9 µm	
331	-	193.0 HV 0.5	91.6 HRB	70.0 µm	68.6 µm	
332	-	189.3 HV 0.5	90.9 HRB	69.8 µm	70.2 µm	
333	-	193.8 HV 0.5	91.8 HRB	68.1 µm	70.2 µm	

Date: 05-24-2023
Tester: Admin
Program: Hardness Map

Point	Distance	Hardness	Converted	Diagonal X	Diagonal Y	Comments
334	-	185.6 HV 0.5	90.1 HRB	70.3 µm	71.1 µm	
335	-	183.8 HV 0.5	89.8 HRB	70.8 µm	71.3 µm	
336	-	186.4 HV 0.5	90.3 HRB	70.7 µm	70.3 µm	
337	-	189.2 HV 0.5	90.8 HRB	70.1 µm	69.9 µm	
338	-	178.9 HV 0.5	88.7 HRB	69.8 µm	74.2 µm	
339	-	193.2 HV 0.5	91.6 HRB	67.8 µm	70.7 µm	
340	-	175.9 HV 0.5	88.0 HRB	72.0 µm	73.2 µm	
341	-	184.5 HV 0.5	89.9 HRB	70.2 µm	71.6 µm	
342	-	199.4 HV 0.5	92.9 HRB	67.1 µm	69.2 µm	
343	-	193.6 HV 0.5	91.7 HRB	69.3 µm	69.1 µm	
344	-	186.9 HV 0.5	90.4 HRB	70.7 µm	70.2 µm	
345	-	184.5 HV 0.5	89.9 HRB	71.2 µm	70.6 µm	
346	-	182.4 HV 0.5	89.5 HRB	70.5 µm	72.1 µm	
347	-	187.5 HV 0.5	90.5 HRB	70.0 µm	70.7 µm	
348	-	191.3 HV 0.5	91.3 HRB	68.9 µm	70.3 µm	
349	-	181.7 HV 0.5	89.3 HRB	71.1 µm	71.8 µm	
350	-	199.1 HV 0.5	92.8 HRB	67.1 µm	69.4 µm	
351	-	200.1 HV 0.5	93.0 HRB	67.9 µm	68.2 µm	
352	-	192.3 HV 0.5	91.5 HRB	68.5 µm	70.4 µm	
353	-	194.3 HV 0.5	91.9 HRB	68.2 µm	70.0 µm	
354	-	181.2 HV 0.5	89.2 HRB	70.2 µm	72.9 µm	
355	-	197.3 HV 0.5	92.5 HRB	69.0 µm	68.2 µm	
356	-	192.1 HV 0.5	91.4 HRB	69.0 µm	70.0 µm	
357	-	187.8 HV 0.5	90.6 HRB	70.0 µm	70.6 µm	
358	-	189.9 HV 0.5	91.0 HRB	68.2 µm	71.6 µm	
359	-	195.4 HV 0.5	92.1 HRB	68.0 µm	69.7 µm	
360	-	188.1 HV 0.5	90.6 HRB	70.2 µm	70.2 µm	
361	-	199.0 HV 0.5	92.8 HRB	67.1 µm	69.4 µm	
362	-	190.7 HV 0.5	91.1 HRB	69.7 µm	69.7 µm	
363	-	192.4 HV 0.5	91.5 HRB	68.8 µm	70.0 µm	
364	-	196.6 HV 0.5	92.3 HRB	68.3 µm	69.0 µm	
365	-	181.2 HV 0.5	89.2 HRB	72.8 µm	70.3 µm	
366	-	183.8 HV 0.5	89.8 HRB	70.9 µm	71.1 µm	
367	-	177.9 HV 0.5	88.5 HRB	73.6 µm	70.8 µm	
368	-	193.2 HV 0.5	91.6 HRB	69.4 µm	69.1 µm	
369	-	183.6 HV 0.5	89.7 HRB	71.5 µm	70.6 µm	
370	-	181.6 HV 0.5	89.3 HRB	71.8 µm	71.1 µm	
371	-	181.5 HV 0.5	89.3 HRB	70.9 µm	72.1 µm	
372	-	178.6 HV 0.5	88.7 HRB	72.2 µm	71.9 µm	

Date: 05-24-2023
Tester: Admin
Program: Hardness Map

Point	Distance	Hardness	Converted	Diagonal X	Diagonal Y	Comments
373	-	177.6 HV 0.5	88.4 HRB	72.8 µm	71.8 µm	
374	-	192.6 HV 0.5	91.5 HRB	67.9 µm	70.9 µm	
375	-	177.9 HV 0.5	88.5 HRB	73.1 µm	71.3 µm	
376	-	183.7 HV 0.5	89.7 HRB	70.6 µm	71.5 µm	
377	-	182.3 HV 0.5	89.5 HRB	71.8 µm	70.8 µm	
378	-	182.8 HV 0.5	89.6 HRB	71.8 µm	70.6 µm	
379	-	192.4 HV 0.5	91.5 HRB	67.9 µm	70.9 µm	
380	-	198.9 HV 0.5	92.8 HRB	70.0 µm	66.6 µm	
381	-	193.3 HV 0.5	91.7 HRB	69.2 µm	69.3 µm	
382	-	185.1 HV 0.5	90.0 HRB	70.1 µm	71.4 µm	
383	-	191.8 HV 0.5	91.4 HRB	67.7 µm	71.4 µm	
384	-	199.7 HV 0.5	92.9 HRB	68.2 µm	68.1 µm	
385	-	193.7 HV 0.5	91.7 HRB	68.9 µm	69.4 µm	
386	-	190.6 HV 0.5	91.1 HRB	68.1 µm	71.4 µm	
387	-	174.9 HV 0.5	87.7 HRB	71.5 µm	74.1 µm	
388	-	186.5 HV 0.5	90.3 HRB	70.0 µm	71.1 µm	
389	-	195.2 HV 0.5	92.0 HRB	68.5 µm	69.3 µm	
390	-	191.0 HV 0.5	91.2 HRB	68.7 µm	70.7 µm	
391	-	184.6 HV 0.5	89.9 HRB	70.4 µm	71.3 µm	
392	-	188.3 HV 0.5	90.7 HRB	70.1 µm	70.2 µm	
393	-	183.7 HV 0.5	89.7 HRB	70.6 µm	71.5 µm	
394	-	182.6 HV 0.5	89.5 HRB	70.4 µm	72.1 µm	
395	-	180.6 HV 0.5	89.1 HRB	71.3 µm	72.0 µm	
396	-	190.2 HV 0.5	91.0 HRB	67.6 µm	72.1 µm	
397	-	186.8 HV 0.5	90.4 HRB	69.3 µm	71.6 µm	
398	-	187.8 HV 0.5	90.6 HRB	68.2 µm	72.4 µm	
399	-	185.4 HV 0.5	90.1 HRB	70.6 µm	70.8 µm	
400	-	184.4 HV 0.5	89.9 HRB	69.3 µm	72.5 µm	
401	-	191.2 HV 0.5	91.2 HRB	68.3 µm	70.9 µm	
402	-	190.7 HV 0.5	91.1 HRB	67.6 µm	71.8 µm	
403	-	192.2 HV 0.5	91.4 HRB	68.7 µm	70.2 µm	
404	-	196.8 HV 0.5	92.4 HRB	67.4 µm	69.8 µm	
405	-	185.8 HV 0.5	90.2 HRB	69.6 µm	71.7 µm	
406	-	185.4 HV 0.5	90.1 HRB	70.6 µm	70.9 µm	
407	-	186.2 HV 0.5	90.2 HRB	70.8 µm	70.3 µm	
408	-	188.0 HV 0.5	90.6 HRB	70.2 µm	70.3 µm	
409	-	172.0 HV 0.5	87.0 HRB	72.6 µm	74.2 µm	
410	-	190.6 HV 0.5	91.1 HRB	69.3 µm	70.2 µm	
411	-	187.3 HV 0.5	90.5 HRB	69.9 µm	70.8 µm	

Date: 05-24-2023
Tester: Admin
Program: Hardness Map

Point	Distance	Hardness	Converted	Diagonal X	Diagonal Y	Comments
412	-	186.1 HV 0.5	90.2 HRB	70.2 µm	70.9 µm	
413	-	185.6 HV 0.5	90.1 HRB	70.2 µm	71.1 µm	
414	-	178.8 HV 0.5	88.7 HRB	71.3 µm	72.8 µm	
415	-	187.1 HV 0.5	90.4 HRB	70.6 µm	70.2 µm	
416	-	176.9 HV 0.5	88.2 HRB	71.5 µm	73.3 µm	
417	-	188.1 HV 0.5	90.6 HRB	69.9 µm	70.5 µm	
418	-	177.8 HV 0.5	88.5 HRB	72.3 µm	72.1 µm	
419	-	172.0 HV 0.5	87.0 HRB	73.4 µm	73.4 µm	
420	-	196.9 HV 0.5	92.4 HRB	68.9 µm	68.3 µm	
421	-	188.1 HV 0.5	90.6 HRB	70.6 µm	69.8 µm	
422	-	182.8 HV 0.5	89.6 HRB	71.9 µm	70.6 µm	
423	-	190.5 HV 0.5	91.1 HRB	69.6 µm	70.0 µm	
424	-	184.2 HV 0.5	89.8 HRB	70.6 µm	71.3 µm	
425	-	185.4 HV 0.5	90.1 HRB	69.7 µm	71.8 µm	
426	-	197.2 HV 0.5	92.4 HRB	68.2 µm	68.9 µm	
427	-	191.6 HV 0.5	91.3 HRB	69.7 µm	69.4 µm	
428	-	200.8 HV 0.5	93.2 HRB	67.1 µm	68.8 µm	
429	-	171.8 HV 0.5	86.9 HRB	77.1 µm	69.8 µm	
430	-	185.7 HV 0.5	90.1 HRB	68.5 µm	72.8 µm	
431	-	193.5 HV 0.5	91.7 HRB	69.4 µm	69.0 µm	
432	-	188.7 HV 0.5	90.7 HRB	68.5 µm	71.7 µm	
433	-	195.1 HV 0.5	92.0 HRB	69.6 µm	68.3 µm	
434	-	185.6 HV 0.5	90.1 HRB	69.6 µm	71.8 µm	
435	-	188.4 HV 0.5	90.7 HRB	70.8 µm	69.5 µm	
436	-	190.4 HV 0.5	91.1 HRB	70.6 µm	68.9 µm	
437	-	170.8 HV 0.5	86.6 HRB	77.5 µm	69.8 µm	
438	-	182.1 HV 0.5	89.4 HRB	72.6 µm	70.1 µm	
439	-	183.1 HV 0.5	89.6 HRB	71.5 µm	70.9 µm	
440	-	189.2 HV 0.5	90.8 HRB	69.5 µm	70.6 µm	
441	-	186.7 HV 0.5	90.3 HRB	70.4 µm	70.6 µm	
442	-	179.9 HV 0.5	89.0 HRB	69.3 µm	74.3 µm	
443	-	181.0 HV 0.5	89.2 HRB	70.1 µm	73.0 µm	
444	-	178.7 HV 0.5	88.7 HRB	70.3 µm	73.8 µm	
445	-	188.6 HV 0.5	90.7 HRB	69.1 µm	71.1 µm	
446	-	182.4 HV 0.5	89.5 HRB	68.8 µm	73.8 µm	
447	-	188.7 HV 0.5	90.7 HRB	68.6 µm	71.6 µm	
448	-	183.4 HV 0.5	89.7 HRB	71.1 µm	71.1 µm	
449	-	191.7 HV 0.5	91.3 HRB	68.9 µm	70.2 µm	
450	-	183.0 HV 0.5	89.6 HRB	69.7 µm	72.6 µm	

Date: 05-24-2023
Tester: Admin
Program: Hardness Map

Point	Distance	Hardness	Converted	Diagonal X	Diagonal Y	Comments
451	-	183.3 HV 0.5	89.7 HRB	71.6 µm	70.6 µm	
452	-	206.1 HV 0.5	94.2 HRB	67.5 µm	66.6 µm	
453	-	181.6 HV 0.5	89.3 HRB	70.5 µm	72.4 µm	
454	-	174.7 HV 0.5	87.7 HRB	72.4 µm	73.3 µm	
455	-	174.9 HV 0.5	87.7 HRB	72.1 µm	73.5 µm	
456	-	169.1 HV 0.5	86.0 HRB	73.9 µm	74.2 µm	
457	-	178.7 HV 0.5	88.7 HRB	71.4 µm	72.7 µm	
458	-	191.1 HV 0.5	91.2 HRB	69.0 µm	70.3 µm	
459	-	194.1 HV 0.5	91.8 HRB	68.6 µm	69.6 µm	
460	-	181.4 HV 0.5	89.3 HRB	71.0 µm	72.0 µm	
461	-	176.9 HV 0.5	88.2 HRB	73.5 µm	71.2 µm	
462	-	172.1 HV 0.5	87.0 HRB	72.6 µm	74.2 µm	
463	-	173.6 HV 0.5	87.4 HRB	72.7 µm	73.4 µm	
464	-	189.7 HV 0.5	90.9 HRB	70.1 µm	69.7 µm	
465	-	194.4 HV 0.5	91.9 HRB	69.0 µm	69.2 µm	
466	-	200.7 HV 0.5	93.1 HRB	67.4 µm	68.6 µm	
467	-	186.4 HV 0.5	90.3 HRB	70.6 µm	70.5 µm	
468	-	197.4 HV 0.5	92.5 HRB	70.1 µm	67.0 µm	
469	-	194.2 HV 0.5	91.8 HRB	68.4 µm	69.8 µm	
470	-	187.2 HV 0.5	90.4 HRB	70.4 µm	70.3 µm	
471	-	188.8 HV 0.5	90.8 HRB	69.1 µm	71.0 µm	
472	-	199.1 HV 0.5	92.8 HRB	68.0 µm	68.4 µm	
473	-	194.8 HV 0.5	92.0 HRB	67.4 µm	70.6 µm	
474	-	187.9 HV 0.5	90.6 HRB	70.5 µm	70.0 µm	
475	-	186.6 HV 0.5	90.3 HRB	69.7 µm	71.2 µm	
476	-	174.4 HV 0.5	87.6 HRB	73.2 µm	72.6 µm	
477	-	180.1 HV 0.5	89.0 HRB	70.1 µm	73.4 µm	
478	-	191.9 HV 0.5	91.4 HRB	68.6 µm	70.4 µm	
479	-	193.9 HV 0.5	91.8 HRB	66.3 µm	72.0 µm	
480	-	181.6 HV 0.5	89.3 HRB	71.2 µm	71.7 µm	
481	-	189.0 HV 0.5	90.8 HRB	69.5 µm	70.6 µm	
482	-	180.6 HV 0.5	89.1 HRB	70.3 µm	73.0 µm	
483	-	191.0 HV 0.5	91.2 HRB	67.7 µm	71.6 µm	
484	-	179.9 HV 0.5	89.0 HRB	70.9 µm	72.7 µm	
485	-	185.1 HV 0.5	90.0 HRB	69.1 µm	72.5 µm	
486	-	182.7 HV 0.5	89.5 HRB	71.1 µm	71.4 µm	
487	-	173.5 HV 0.5	87.4 HRB	69.0 µm	77.2 µm	
488	-	182.8 HV 0.5	89.6 HRB	69.0 µm	73.4 µm	
489	-	181.5 HV 0.5	89.3 HRB	71.4 µm	71.6 µm	

Date: 05-24-2023
Tester: Admin
Program: Hardness Map

Point	Distance	Hardness	Converted	Diagonal X	Diagonal Y	Comments
490	-	182.7 HV 0.5	89.5 HRB	70.7 µm	71.8 µm	
491	-	194.5 HV 0.5	91.9 HRB	67.3 µm	70.8 µm	
492	-	186.1 HV 0.5	90.2 HRB	68.4 µm	72.7 µm	
493	-	178.2 HV 0.5	88.6 HRB	70.1 µm	74.2 µm	
494	-	191.9 HV 0.5	91.4 HRB	68.9 µm	70.1 µm	
495	-	185.2 HV 0.5	90.0 HRB	70.2 µm	71.3 µm	
496	-	187.3 HV 0.5	90.5 HRB	70.8 µm	69.9 µm	
497	-	180.1 HV 0.5	89.0 HRB	71.6 µm	71.9 µm	
498	-	188.9 HV 0.5	90.8 HRB	70.0 µm	70.2 µm	
499	-	191.6 HV 0.5	91.3 HRB	69.1 µm	70.0 µm	
500	-	182.3 HV 0.5	89.5 HRB	71.8 µm	70.8 µm	
501	-	179.8 HV 0.5	89.0 HRB	72.3 µm	71.3 µm	
502	-	180.0 HV 0.5	89.0 HRB	72.0 µm	71.5 µm	
503	-	170.5 HV 0.5	86.5 HRB	73.9 µm	73.6 µm	
504	-	176.0 HV 0.5	88.0 HRB	71.6 µm	73.5 µm	
505	-	176.5 HV 0.5	88.1 HRB	72.1 µm	72.9 µm	
506	-	177.8 HV 0.5	88.4 HRB	71.8 µm	72.6 µm	
507	-	180.5 HV 0.5	89.1 HRB	71.4 µm	72.0 µm	
508	-	206.4 HV 0.5	94.3 HRB	66.4 µm	67.6 µm	
509	-	205.5 HV 0.5	94.1 HRB	67.0 µm	67.3 µm	
510	-	194.1 HV 0.5	91.8 HRB	70.6 µm	67.7 µm	
511	-	189.9 HV 0.5	91.0 HRB	70.0 µm	69.8 µm	
512	-	185.4 HV 0.5	90.1 HRB	70.2 µm	71.2 µm	
513	-	184.9 HV 0.5	90.0 HRB	69.8 µm	71.8 µm	
514	-	177.7 HV 0.5	88.4 HRB	71.5 µm	73.0 µm	
515	-	183.7 HV 0.5	89.7 HRB	68.1 µm	74.0 µm	
516	-	185.3 HV 0.5	90.1 HRB	70.7 µm	70.8 µm	
517	-	190.3 HV 0.5	91.1 HRB	69.4 µm	70.2 µm	
518	-	188.2 HV 0.5	90.6 HRB	67.5 µm	72.9 µm	
519	-	193.1 HV 0.5	91.6 HRB	68.6 µm	70.0 µm	
520	-	183.8 HV 0.5	89.8 HRB	67.9 µm	74.2 µm	
521	-	196.5 HV 0.5	92.3 HRB	68.8 µm	68.6 µm	
522	-	206.0 HV 0.5	94.2 HRB	68.0 µm	66.2 µm	
523	-	196.2 HV 0.5	92.2 HRB	68.3 µm	69.2 µm	
524	-	191.0 HV 0.5	91.2 HRB	69.0 µm	70.4 µm	
525	-	188.6 HV 0.5	90.7 HRB	68.5 µm	71.8 µm	
526	-	188.8 HV 0.5	90.8 HRB	70.6 µm	69.6 µm	
527	-	188.1 HV 0.5	90.6 HRB	68.7 µm	71.7 µm	
528	-	191.5 HV 0.5	91.3 HRB	68.0 µm	71.1 µm	

Date: 05-24-2023
Tester: Admin
Program: Hardness Map

Point	Distance	Hardness	Converted	Diagonal X	Diagonal Y	Comments
529	-	188.9 HV 0.5	90.8 HRB	69.6 µm	70.5 µm	
530	-	198.6 HV 0.5	92.7 HRB	67.4 µm	69.2 µm	
531	-	189.5 HV 0.5	90.9 HRB	69.6 µm	70.3 µm	
532	-	191.9 HV 0.5	91.4 HRB	67.6 µm	71.4 µm	
533	-	185.2 HV 0.5	90.0 HRB	70.8 µm	70.7 µm	
534	-	186.7 HV 0.5	90.3 HRB	69.0 µm	72.0 µm	
535	-	190.2 HV 0.5	91.0 HRB	68.6 µm	71.1 µm	
536	-	188.4 HV 0.5	90.7 HRB	69.2 µm	71.1 µm	
537	-	188.1 HV 0.5	90.6 HRB	68.1 µm	72.4 µm	
538	-	183.5 HV 0.5	89.7 HRB	70.7 µm	71.5 µm	
539	-	196.8 HV 0.5	92.4 HRB	68.1 µm	69.2 µm	
540	-	210.5 HV 0.5	95.1 HRB	65.6 µm	67.1 µm	
541	-	184.2 HV 0.5	89.8 HRB	72.7 µm	69.2 µm	
542	-	186.1 HV 0.5	90.2 HRB	70.1 µm	71.1 µm	
543	-	190.0 HV 0.5	91.0 HRB	70.2 µm	69.5 µm	
544	-	183.3 HV 0.5	89.7 HRB	71.0 µm	71.2 µm	
545	-	190.0 HV 0.5	91.0 HRB	68.9 µm	70.8 µm	
546	-	193.3 HV 0.5	91.7 HRB	68.6 µm	69.9 µm	
547	-	185.3 HV 0.5	90.1 HRB	70.4 µm	71.1 µm	
548	-	185.5 HV 0.5	90.1 HRB	70.9 µm	70.5 µm	
549	-	193.9 HV 0.5	91.8 HRB	70.0 µm	68.3 µm	
550	-	188.7 HV 0.5	90.7 HRB	69.8 µm	70.4 µm	
551	-	195.1 HV 0.5	92.0 HRB	68.8 µm	69.0 µm	
552	-	210.8 HV 0.5	95.1 HRB	66.2 µm	66.5 µm	
553	-	199.1 HV 0.5	92.8 HRB	67.7 µm	68.8 µm	
554	-	193.7 HV 0.5	91.7 HRB	68.5 µm	69.8 µm	
555	-	195.6 HV 0.5	92.1 HRB	69.0 µm	68.7 µm	
556	-	192.7 HV 0.5	91.5 HRB	67.4 µm	71.4 µm	
557	-	194.0 HV 0.5	91.8 HRB	67.8 µm	70.5 µm	
558	-	197.8 HV 0.5	92.6 HRB	68.7 µm	68.2 µm	
559	-	191.4 HV 0.5	91.3 HRB	67.7 µm	71.5 µm	
560	-	191.2 HV 0.5	91.2 HRB	68.9 µm	70.4 µm	
561	-	189.3 HV 0.5	90.9 HRB	68.6 µm	71.4 µm	
562	-	199.0 HV 0.5	92.8 HRB	68.2 µm	68.3 µm	
563	-	191.0 HV 0.5	91.2 HRB	70.2 µm	69.1 µm	
564	-	198.2 HV 0.5	92.6 HRB	66.3 µm	70.5 µm	
565	-	189.2 HV 0.5	90.8 HRB	68.9 µm	71.2 µm	
566	-	195.4 HV 0.5	92.1 HRB	66.9 µm	70.9 µm	
567	-	189.9 HV 0.5	91.0 HRB	69.7 µm	70.0 µm	

Date: 05-24-2023
Tester: Admin
Program: Hardness Map

Point	Distance	Hardness	Converted	Diagonal X	Diagonal Y	Comments
568	-	195.8 HV 0.5	92.2 HRB	67.1 µm	70.6 µm	
569	-	196.3 HV 0.5	92.3 HRB	69.0 µm	68.5 µm	
570	-	190.8 HV 0.5	91.2 HRB	69.6 µm	69.8 µm	
571	-	194.9 HV 0.5	92.0 HRB	68.3 µm	69.6 µm	
572	-	190.8 HV 0.5	91.2 HRB	69.6 µm	69.8 µm	
573	-	187.5 HV 0.5	90.5 HRB	68.6 µm	72.1 µm	
574	-	185.6 HV 0.5	90.1 HRB	68.2 µm	73.1 µm	
575	-	194.8 HV 0.5	92.0 HRB	69.8 µm	68.2 µm	
576	-	191.8 HV 0.5	91.4 HRB	68.6 µm	70.5 µm	
577	-	202.9 HV 0.5	93.6 HRB	66.2 µm	69.0 µm	
578	-	194.6 HV 0.5	91.9 HRB	68.3 µm	69.8 µm	
579	-	184.8 HV 0.5	90.0 HRB	69.6 µm	72.1 µm	
580	-	198.3 HV 0.5	92.7 HRB	67.7 µm	69.1 µm	
581	-	198.4 HV 0.5	92.7 HRB	67.3 µm	69.4 µm	
582	-	193.6 HV 0.5	91.7 HRB	67.5 µm	71.0 µm	
583	-	200.3 HV 0.5	93.1 HRB	66.8 µm	69.2 µm	
584	-	222.3 HV 0.5	97.0 HRB	64.3 µm	64.8 µm	
585	-	242.8 HV 0.5	-	62.4 µm	61.2 µm	
586	-	193.5 HV 0.5	91.7 HRB	69.0 µm	69.5 µm	
587	-	187.5 HV 0.5	90.5 HRB	70.2 µm	70.4 µm	
588	-	188.2 HV 0.5	90.6 HRB	69.8 µm	70.6 µm	
589	-	186.1 HV 0.5	90.2 HRB	69.4 µm	71.8 µm	
590	-	197.9 HV 0.5	92.6 HRB	68.3 µm	68.6 µm	
591	-	204.6 HV 0.5	93.9 HRB	67.8 µm	66.8 µm	
592	-	194.5 HV 0.5	91.9 HRB	69.3 µm	68.7 µm	
593	-	195.4 HV 0.5	92.1 HRB	69.7 µm	68.1 µm	
594	-	189.7 HV 0.5	90.9 HRB	69.8 µm	70.0 µm	
595	-	201.1 HV 0.5	93.2 HRB	69.5 µm	66.3 µm	
596	-	207.7 HV 0.5	94.5 HRB	67.6 µm	66.0 µm	
597	-	192.0 HV 0.5	91.4 HRB	67.0 µm	72.0 µm	
598	-	198.5 HV 0.5	92.7 HRB	68.7 µm	67.9 µm	
599	-	201.6 HV 0.5	93.3 HRB	66.0 µm	69.6 µm	
600	-	195.1 HV 0.5	92.0 HRB	67.8 µm	70.0 µm	
601	-	196.9 HV 0.5	92.4 HRB	69.4 µm	67.9 µm	
602	-	190.0 HV 0.5	91.0 HRB	69.6 µm	70.2 µm	
603	-	185.7 HV 0.5	90.1 HRB	68.6 µm	72.8 µm	
604	-	188.9 HV 0.5	90.8 HRB	69.7 µm	70.5 µm	
605	-	186.6 HV 0.5	90.3 HRB	69.6 µm	71.4 µm	
606	-	183.3 HV 0.5	89.7 HRB	68.2 µm	74.0 µm	

Date: 05-24-2023
Tester: Admin
Program: Hardness Map

Point	Distance	Hardness	Converted	Diagonal X	Diagonal Y	Comments
607	-	200.7 HV 0.5	93.1 HRB	67.9 µm	68.0 µm	
608	-	204.9 HV 0.5	94.0 HRB	66.7 µm	67.8 µm	
609	-	199.8 HV 0.5	93.0 HRB	67.1 µm	69.1 µm	
610	-	189.2 HV 0.5	90.8 HRB	68.0 µm	72.0 µm	
611	-	189.1 HV 0.5	90.8 HRB	69.2 µm	70.8 µm	
612	-	195.5 HV 0.5	92.1 HRB	69.4 µm	68.4 µm	
613	-	195.4 HV 0.5	92.1 HRB	68.1 µm	69.7 µm	
614	-	193.9 HV 0.5	91.8 HRB	69.3 µm	69.0 µm	
615	-	187.7 HV 0.5	90.5 HRB	69.8 µm	70.7 µm	
616	-	192.8 HV 0.5	91.6 HRB	68.4 µm	70.2 µm	
617	-	188.1 HV 0.5	90.6 HRB	71.5 µm	68.9 µm	
618	-	199.9 HV 0.5	93.0 HRB	68.2 µm	68.1 µm	
619	-	188.9 HV 0.5	90.8 HRB	70.1 µm	70.0 µm	
620	-	201.8 HV 0.5	93.4 HRB	67.3 µm	68.3 µm	
621	-	198.4 HV 0.5	92.7 HRB	67.6 µm	69.1 µm	
622	-	195.7 HV 0.5	92.1 HRB	68.5 µm	69.2 µm	
623	-	194.4 HV 0.5	91.9 HRB	70.5 µm	67.7 µm	
624	-	194.9 HV 0.5	92.0 HRB	67.9 µm	70.1 µm	
625	-	196.9 HV 0.5	92.4 HRB	68.0 µm	69.2 µm	
626	-	196.6 HV 0.5	92.3 HRB	70.4 µm	67.0 µm	
627	-	183.2 HV 0.5	89.6 HRB	71.4 µm	70.9 µm	
628	-	213.9 HV 0.5	95.6 HRB	64.3 µm	67.3 µm	
629	-	219.1 HV 0.5	96.5 HRB	65.4 µm	64.7 µm	
630	-	238.1 HV 0.5	99.7 HRB	62.2 µm	62.7 µm	
631	-	183.8 HV 0.5	89.8 HRB	73.2 µm	68.9 µm	
632	-	188.7 HV 0.5	90.7 HRB	70.0 µm	70.2 µm	
633	-	181.1 HV 0.5	89.2 HRB	70.4 µm	72.7 µm	
634	-	187.3 HV 0.5	90.5 HRB	70.6 µm	70.1 µm	
635	-	189.9 HV 0.5	91.0 HRB	67.6 µm	72.1 µm	
636	-	194.6 HV 0.5	91.9 HRB	68.7 µm	69.3 µm	
637	-	197.3 HV 0.5	92.5 HRB	68.7 µm	68.4 µm	
638	-	197.9 HV 0.5	92.6 HRB	69.3 µm	67.6 µm	
639	-	204.6 HV 0.5	93.9 HRB	69.3 µm	65.3 µm	
640	-	236.2 HV 0.5	99.4 HRB	62.7 µm	62.6 µm	
641	-	215.1 HV 0.5	95.9 HRB	65.2 µm	66.1 µm	
642	-	202.2 HV 0.5	93.4 HRB	65.8 µm	69.6 µm	
643	-	210.0 HV 0.5	95.0 HRB	66.4 µm	66.5 µm	
644	-	202.9 HV 0.5	93.6 HRB	66.5 µm	68.7 µm	
645	-	217.9 HV 0.5	96.3 HRB	64.4 µm	66.0 µm	

Date: 05-24-2023
Tester: Admin
Program: Hardness Map

Point	Distance	Hardness	Converted	Diagonal X	Diagonal Y	Comments
646	-	211.7 HV 0.5	95.3 HRB	65.7 µm	66.7 µm	
647	-	210.9 HV 0.5	95.1 HRB	67.4 µm	65.2 µm	
648	-	205.3 HV 0.5	94.1 HRB	66.1 µm	68.3 µm	
649	-	208.7 HV 0.5	94.7 HRB	66.0 µm	67.3 µm	
650	-	221.6 HV 0.5	96.9 HRB	63.9 µm	65.5 µm	
651	-	211.6 HV 0.5	95.3 HRB	65.3 µm	67.1 µm	
652	-	207.6 HV 0.5	94.5 HRB	67.9 µm	65.7 µm	
653	-	214.6 HV 0.5	95.8 HRB	67.4 µm	64.1 µm	
654	-	201.6 HV 0.5	93.3 HRB	65.8 µm	69.8 µm	
655	-	214.1 HV 0.5	95.7 HRB	63.8 µm	67.8 µm	
656	-	220.2 HV 0.5	96.7 HRB	63.3 µm	66.5 µm	
657	-	217.8 HV 0.5	96.3 HRB	63.7 µm	66.8 µm	
658	-	220.6 HV 0.5	96.8 HRB	64.9 µm	64.8 µm	
659	-	210.1 HV 0.5	95.0 HRB	66.4 µm	66.4 µm	
660	-	233.4 HV 0.5	98.9 HRB	65.1 µm	60.9 µm	
661	-	215.8 HV 0.5	96.0 HRB	65.4 µm	65.6 µm	
662	-	201.9 HV 0.5	93.4 HRB	70.4 µm	65.1 µm	
663	-	217.4 HV 0.5	96.2 HRB	64.7 µm	65.9 µm	
664	-	217.5 HV 0.5	96.3 HRB	64.8 µm	65.7 µm	
665	-	210.6 HV 0.5	95.1 HRB	65.7 µm	67.0 µm	
666	-	218.7 HV 0.5	96.4 HRB	64.5 µm	65.7 µm	
667	-	218.1 HV 0.5	96.3 HRB	64.6 µm	65.8 µm	
668	-	212.5 HV 0.5	95.4 HRB	65.5 µm	66.6 µm	
669	-	219.7 HV 0.5	96.6 HRB	64.4 µm	65.5 µm	
670	-	217.2 HV 0.5	96.2 HRB	65.2 µm	65.5 µm	
671	-	212.2 HV 0.5	95.4 HRB	64.1 µm	68.1 µm	
672	-	223.2 HV 0.5	97.2 HRB	63.4 µm	65.5 µm	
673	-	242.7 HV 0.5	-	61.3 µm	62.3 µm	
674	-	255.7 HV 0.5	-	60.3 µm	60.1 µm	
675	-	268.3 HV 0.5	-	58.9 µm	58.7 µm	
676	-	206.2 HV 0.5	94.2 HRB	66.6 µm	67.5 µm	
677	-	192.3 HV 0.5	91.5 HRB	69.2 µm	69.7 µm	
678	-	192.2 HV 0.5	91.4 HRB	69.4 µm	69.5 µm	
679	-	186.9 HV 0.5	90.4 HRB	70.3 µm	70.5 µm	
680	-	190.4 HV 0.5	91.1 HRB	70.0 µm	69.5 µm	
681	-	192.5 HV 0.5	91.5 HRB	69.9 µm	68.9 µm	
682	-	213.1 HV 0.5	95.5 HRB	65.5 µm	66.4 µm	
683	-	216.1 HV 0.5	96.0 HRB	65.4 µm	65.6 µm	
684	-	218.2 HV 0.5	96.4 HRB	65.4 µm	65.0 µm	

Date: 05-24-2023
Tester: Admin
Program: Hardness Map

Point	Distance	Hardness	Converted	Diagonal X	Diagonal Y	Comments
685	-	209.5 HV 0.5	94.9 HRB	65.5 µm	67.6 µm	
686	-	206.3 HV 0.5	94.3 HRB	66.1 µm	68.0 µm	
687	-	206.2 HV 0.5	94.2 HRB	66.1 µm	68.0 µm	
688	-	199.2 HV 0.5	92.8 HRB	66.5 µm	70.0 µm	
689	-	207.7 HV 0.5	94.5 HRB	68.1 µm	65.5 µm	
690	-	208.5 HV 0.5	94.7 HRB	65.6 µm	67.8 µm	
691	-	207.9 HV 0.5	94.6 HRB	65.6 µm	67.9 µm	
692	-	226.8 HV 0.5	97.8 HRB	65.0 µm	62.9 µm	
693	-	207.1 HV 0.5	94.4 HRB	67.2 µm	66.6 µm	
694	-	204.6 HV 0.5	93.9 HRB	66.1 µm	68.5 µm	
695	-	188.0 HV 0.5	90.6 HRB	70.5 µm	70.0 µm	
696	-	207.8 HV 0.5	94.6 HRB	67.4 µm	66.2 µm	
697	-	198.8 HV 0.5	92.8 HRB	66.6 µm	70.0 µm	
698	-	217.6 HV 0.5	96.3 HRB	64.4 µm	66.1 µm	
699	-	212.8 HV 0.5	95.5 HRB	66.4 µm	65.6 µm	
700	-	205.4 HV 0.5	94.1 HRB	67.5 µm	66.8 µm	
701	-	194.5 HV 0.5	91.9 HRB	69.3 µm	68.8 µm	
702	-	208.0 HV 0.5	94.6 HRB	66.7 µm	66.8 µm	
703	-	208.8 HV 0.5	94.8 HRB	65.5 µm	67.8 µm	
704	-	209.4 HV 0.5	94.9 HRB	65.5 µm	67.5 µm	
705	-	208.3 HV 0.5	94.7 HRB	66.5 µm	67.0 µm	
706	-	205.9 HV 0.5	94.2 HRB	66.0 µm	68.2 µm	
707	-	207.5 HV 0.5	94.5 HRB	66.3 µm	67.4 µm	
708	-	200.2 HV 0.5	93.0 HRB	68.0 µm	68.1 µm	
709	-	198.8 HV 0.5	92.8 HRB	69.9 µm	66.7 µm	
710	-	199.4 HV 0.5	92.9 HRB	68.2 µm	68.1 µm	
711	-	199.2 HV 0.5	92.8 HRB	68.3 µm	68.2 µm	
712	-	211.3 HV 0.5	95.2 HRB	65.6 µm	66.8 µm	
713	-	209.9 HV 0.5	95.0 HRB	66.0 µm	66.9 µm	
714	-	207.1 HV 0.5	94.4 HRB	64.8 µm	69.0 µm	
715	-	204.9 HV 0.5	94.0 HRB	66.9 µm	67.7 µm	
716	-	215.9 HV 0.5	96.0 HRB	66.5 µm	64.6 µm	
717	-	211.2 HV 0.5	95.2 HRB	67.3 µm	65.2 µm	
718	-	229.7 HV 0.5	98.3 HRB	62.4 µm	64.7 µm	
719	-	242.1 HV 0.5	-	61.9 µm	61.9 µm	
720	-	246.2 HV 0.5	-	61.9 µm	60.9 µm	
721	-	215.7 HV 0.5	95.9 HRB	65.7 µm	65.4 µm	
722	-	214.5 HV 0.5	95.7 HRB	65.1 µm	66.4 µm	
723	-	192.7 HV 0.5	91.5 HRB	69.3 µm	69.5 µm	

Date: 05-24-2023
Tester: Admin
Program: Hardness Map

Point	Distance	Hardness	Converted	Diagonal X	Diagonal Y	Comments
724	-	195.2 HV 0.5	92.0 HRB	68.5 µm	69.3 µm	
725	-	208.8 HV 0.5	94.8 HRB	66.6 µm	66.7 µm	
726	-	210.5 HV 0.5	95.1 HRB	65.9 µm	66.9 µm	
727	-	208.9 HV 0.5	94.8 HRB	66.5 µm	66.8 µm	
728	-	203.2 HV 0.5	93.6 HRB	67.6 µm	67.5 µm	
729	-	196.2 HV 0.5	92.2 HRB	67.1 µm	70.4 µm	
730	-	210.0 HV 0.5	95.0 HRB	67.0 µm	65.8 µm	
731	-	206.9 HV 0.5	94.4 HRB	67.8 µm	66.1 µm	
732	-	201.5 HV 0.5	93.3 HRB	68.0 µm	67.6 µm	
733	-	204.5 HV 0.5	93.9 HRB	66.7 µm	67.9 µm	
734	-	210.2 HV 0.5	95.0 HRB	66.9 µm	65.9 µm	
735	-	205.4 HV 0.5	94.1 HRB	67.3 µm	67.1 µm	
736	-	200.6 HV 0.5	93.1 HRB	69.2 µm	66.8 µm	
737	-	207.1 HV 0.5	94.4 HRB	67.1 µm	66.7 µm	
738	-	217.7 HV 0.5	96.3 HRB	65.5 µm	65.1 µm	
739	-	201.0 HV 0.5	93.2 HRB	68.3 µm	67.5 µm	
740	-	199.3 HV 0.5	92.9 HRB	67.5 µm	69.0 µm	
741	-	203.4 HV 0.5	93.7 HRB	66.8 µm	68.3 µm	
742	-	210.7 HV 0.5	95.1 HRB	64.7 µm	68.0 µm	
743	-	208.6 HV 0.5	94.7 HRB	65.9 µm	67.5 µm	
744	-	210.2 HV 0.5	95.0 HRB	67.4 µm	65.4 µm	
745	-	199.6 HV 0.5	92.9 HRB	65.8 µm	70.5 µm	
746	-	216.9 HV 0.5	96.2 HRB	66.0 µm	64.7 µm	
747	-	200.1 HV 0.5	93.0 HRB	66.1 µm	70.0 µm	
748	-	203.4 HV 0.5	93.7 HRB	65.3 µm	69.7 µm	
749	-	206.7 HV 0.5	94.3 HRB	66.5 µm	67.4 µm	
750	-	218.1 HV 0.5	96.4 HRB	64.9 µm	65.5 µm	
751	-	219.7 HV 0.5	96.6 HRB	64.4 µm	65.5 µm	
752	-	244.7 HV 0.5	-	60.5 µm	62.6 µm	
753	-	234.7 HV 0.5	99.1 HRB	63.8 µm	61.9 µm	
754	-	234.8 HV 0.5	99.1 HRB	62.5 µm	63.2 µm	
755	-	213.6 HV 0.5	95.6 HRB	66.5 µm	65.3 µm	
756	-	207.5 HV 0.5	94.5 HRB	65.4 µm	68.3 µm	
757	-	214.4 HV 0.5	95.7 HRB	65.4 µm	66.1 µm	
758	-	214.4 HV 0.5	95.7 HRB	66.4 µm	65.1 µm	
759	-	215.6 HV 0.5	95.9 HRB	64.9 µm	66.3 µm	
760	-	209.5 HV 0.5	94.9 HRB	66.5 µm	66.5 µm	
761	-	207.9 HV 0.5	94.6 HRB	66.0 µm	67.5 µm	
762	-	211.1 HV 0.5	95.2 HRB	65.6 µm	67.0 µm	

Date: 05-24-2023
Tester: Admin
Program: Hardness Map

Point	Distance	Hardness	Converted	Diagonal X	Diagonal Y	Comments
763	-	212.9 HV 0.5	95.5 HRB	65.3 µm	66.6 µm	
764	-	211.2 HV 0.5	95.2 HRB	65.8 µm	66.7 µm	
765	-	214.6 HV 0.5	95.8 HRB	65.2 µm	66.3 µm	
766	-	221.0 HV 0.5	96.8 HRB	64.5 µm	65.1 µm	
767	-	204.9 HV 0.5	94.0 HRB	67.3 µm	67.2 µm	
768	-	211.8 HV 0.5	95.3 HRB	66.5 µm	65.8 µm	
769	-	211.9 HV 0.5	95.3 HRB	66.0 µm	66.3 µm	
770	-	213.7 HV 0.5	95.6 HRB	65.5 µm	66.2 µm	
771	-	218.2 HV 0.5	96.4 HRB	65.5 µm	64.9 µm	
772	-	213.5 HV 0.5	95.6 HRB	65.5 µm	66.3 µm	
773	-	214.8 HV 0.5	95.8 HRB	66.1 µm	65.3 µm	
774	-	214.6 HV 0.5	95.8 HRB	64.8 µm	66.7 µm	
775	-	203.1 HV 0.5	93.6 HRB	68.0 µm	67.2 µm	
776	-	219.8 HV 0.5	96.6 HRB	65.3 µm	64.6 µm	
777	-	221.3 HV 0.5	96.9 HRB	63.9 µm	65.5 µm	
778	-	212.6 HV 0.5	95.4 HRB	63.8 µm	68.3 µm	
779	-	236.7 HV 0.5	99.4 HRB	62.3 µm	62.8 µm	
780	-	227.4 HV 0.5	97.9 HRB	63.3 µm	64.4 µm	
781	-	249.1 HV 0.5	-	61.6 µm	60.4 µm	